2019 Fall

"Advanced Physical Metallurgy"

- Non-equilibrium Solidification -

12.05.2019

Eun Soo Park

Office: 33-313
Telephone: 880-7221
Email: espark@snu.ac.kr
Office hours: by appointment

Deformation behavior: crystalline VS. amorphous

Crystalline

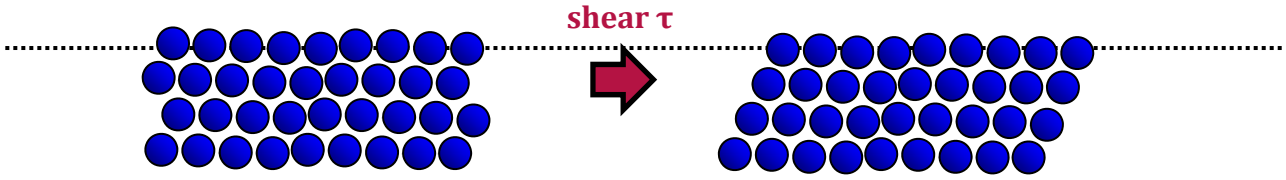

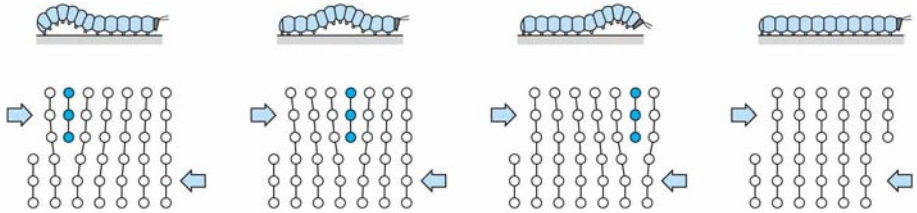

Dislocation motion in crystalline metal

Dislocations

- "Incrementally breaking bonds"
- Has relatively low strength, performs work hardening
- Slip plane + Slip direction = Slip system
  (preferred crystallographic planes and directions)

Amorphous metal do not have slip system.

How to deform ?

Amorphous

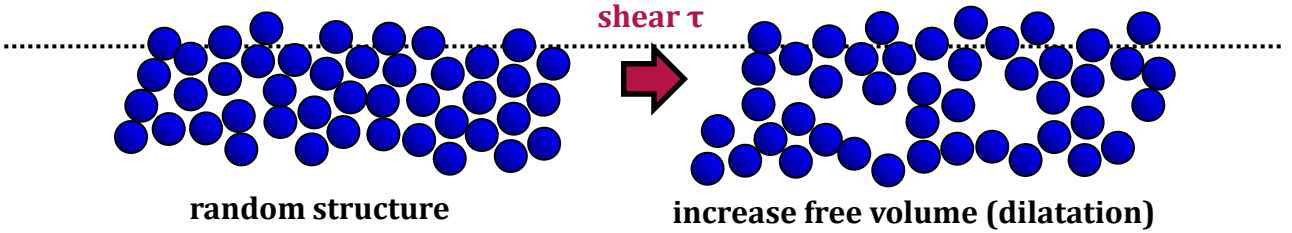

Atomistic models for plastic deformation in metallic glasses

Free volume theory ⟺ STZ model

F. Spaepen

Free volume theory

Homogeneous flow @ steady state

Inhomogeneous flow @ steady state

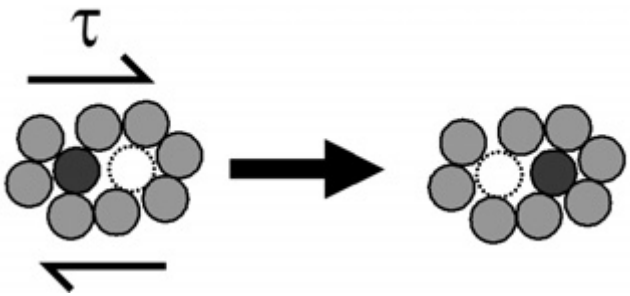

Single-atom/ Diffusion-like model/
Internal volume creation

Steady state inhomogeneous flow :
dynamic equilibrium between shear-induced disordering (creation of free volume) & diffusional annihilation of structural disorder

Forward – backward process
Thermally activated, similar energy scales
Dilatational mechanism

A. S. Argon

Shear transformation zone (STZ)

Homogeneous plastic flow Steady / Non-steady

Inhomogeneous plastic flow

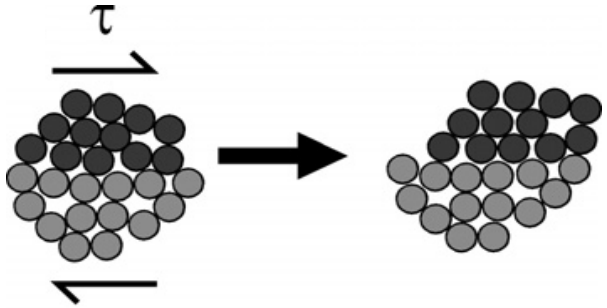

Spontaneous & cooperative reorganization of a small cluster of randomly close-packed atoms

STZ motion = local shear transformation
STZ pushes apart the atoms around free volume site along activation path

Plastic flow in metallic glass in which strain is produced by local shear transformations nucleated under the applied stress & the assistance of thermal fluctuations in regions around free volume sites (adiabatic heating)

Atomic bond topology

Free volume theory ⟺ STZ model

F. Spaepen

Free volume theory

Homogeneous flow @ steady state

Inhomogeneous flow @ steady state

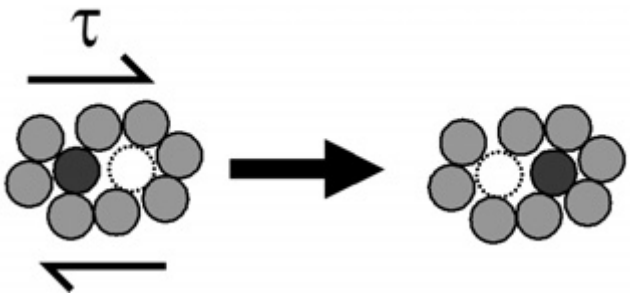

T. Egami

Atomic bond topology

A. S. Argon

Shear transformation zone (STZ)

Homogeneous plastic flow Steady / Non-steady

Inhomogeneous plastic flow

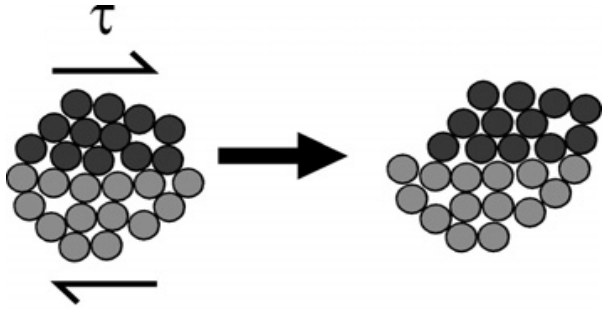

STZ: basic shear unit
(a few to perhaps up to 100 atoms)

- **Free volume approach**
  (1) dense random packing of hard spheres
  (2) free volume cannot be described by the volume alone, and we have to consider the shape
- **Network of atomic connectivity / topology of the atomic structure**

Atomistic theory of metallic liquids and glasses – T. Egami

- Structure of liquids and glasses is usually described in terms of the atomic pair-density correlation function (PDF; $\rho_0 g(r)$) or the radial distribution function (RDF; $4\pi r^2 \rho_0 g(r)$)
- PDF : distribution of the distances between pairs of atoms, averaged over the volume and angle.

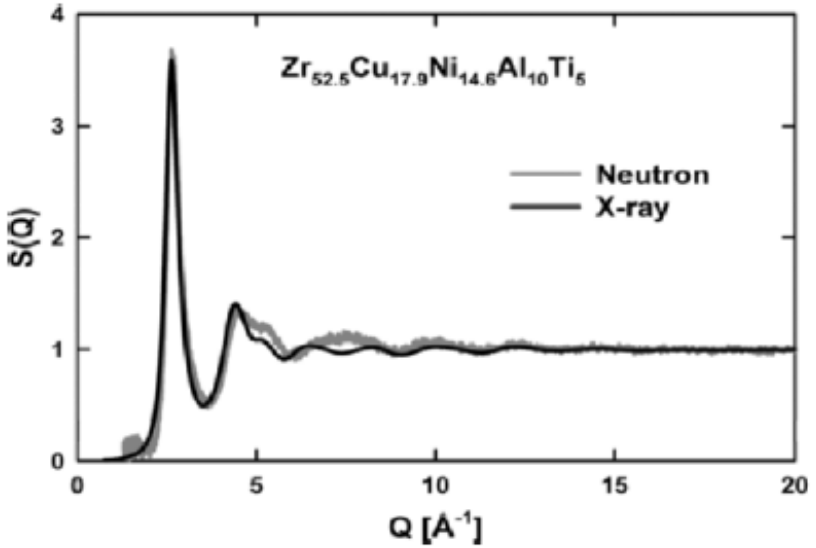

Structure function S(Q) of BMG $Zr_{52.5}Cu_{17.9}Ni_{14.6}Al_{10}Ti_5$

fourier transformation

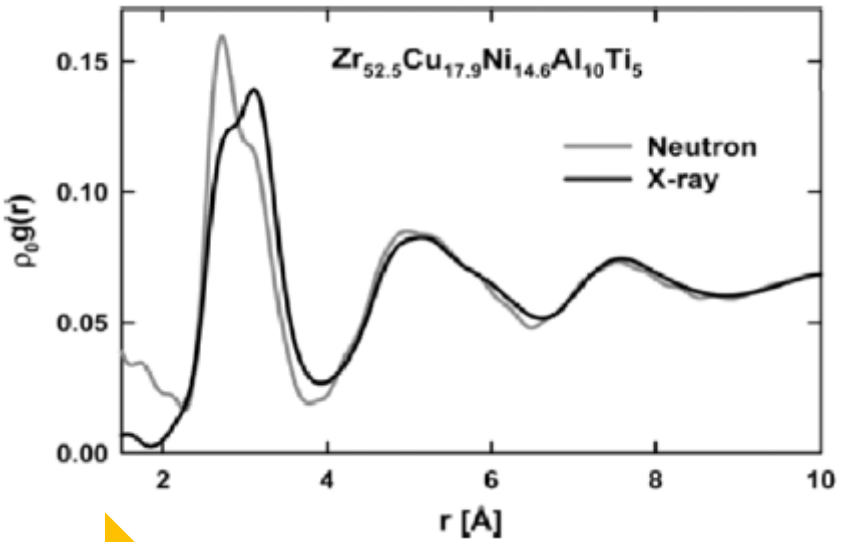

PDF of BMG $Zr_{52.5}Cu_{17.9}Ni_{14.6}Al_{10}Ti_5$

- The idea most frequently used in discussing atomic transport and deformation is free volume.
- Free volume is a space between atoms, and it is intuitively reasonable to assume that atoms need some space for moving around.

Bond-exchange mechanism of shear deformation

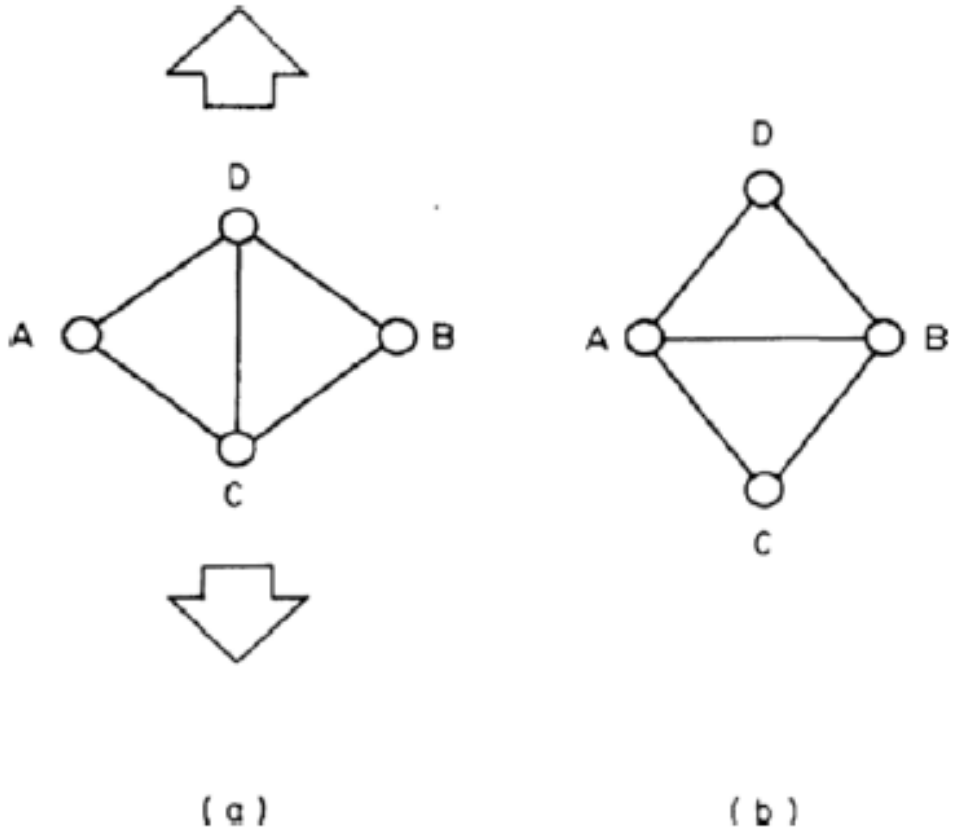

Fig. 2.17. The bond-exchange mechanism of shear deformation.[44] When a vertical tensile stress is applied the bond C–D is cut, and the new bond A–B is formed. The total number of bonds remains unchanged, but the distribution of orientation becomes anisotropic. Bond orientational anisotropy (BOA) is formed as a result of such a bond-exchange process (reprinted from reference [44] with permission from the American Physical Society)

T. Egami: Local topological instability

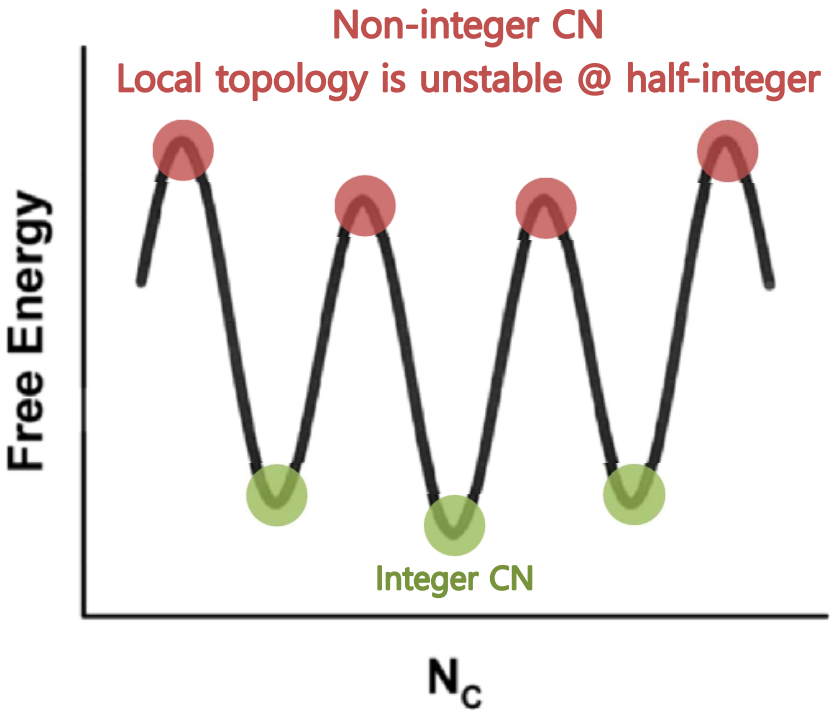

The energy landscape of an atom as a function of $x=r_A/r_B$

$$\Delta x = \frac{1/2}{\partial N_c(x)/\partial x},$$

$$\frac{\partial N_c(x)}{\partial x} = 8\pi\left(1-\frac{\sqrt{3}}{2}\right)\left[1+x+\sqrt{x(x+2)}+\frac{1}{2\sqrt{x(x+2)}}\right]$$

Δx caused by : local volume strain / uniform expansion

Homogeneous volume strain $\langle \varepsilon_v \rangle = (3/2)\Delta x/x,$

x=1, $\varepsilon_v^{crit}(H) = \frac{3}{2}\Delta x\big|_{x=1} = \frac{6\sqrt{3}-9}{8\pi} = 0.0554.$

Local volume strain $\varepsilon_v = 3\Delta x/x,$

x=1, $\varepsilon_v^{crit}(L) = 3\Delta x\big|_{x=1} = \frac{6\sqrt{3}-9}{4\pi} = 0.111.$

Total volume expands more than 6 %: unstable structure

Local volume strain is larger than 11 %: the site is topologically unstable; local CN may change

This leads to the definition of the free-volume in terms of the critical local volume strain.

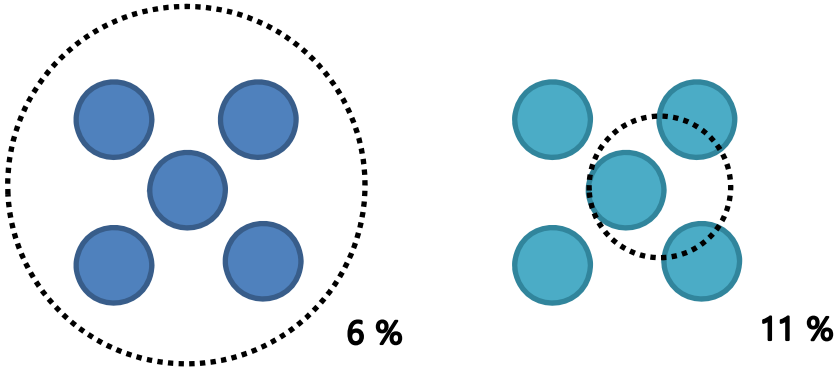

T. Egami: Local topological fluctuation

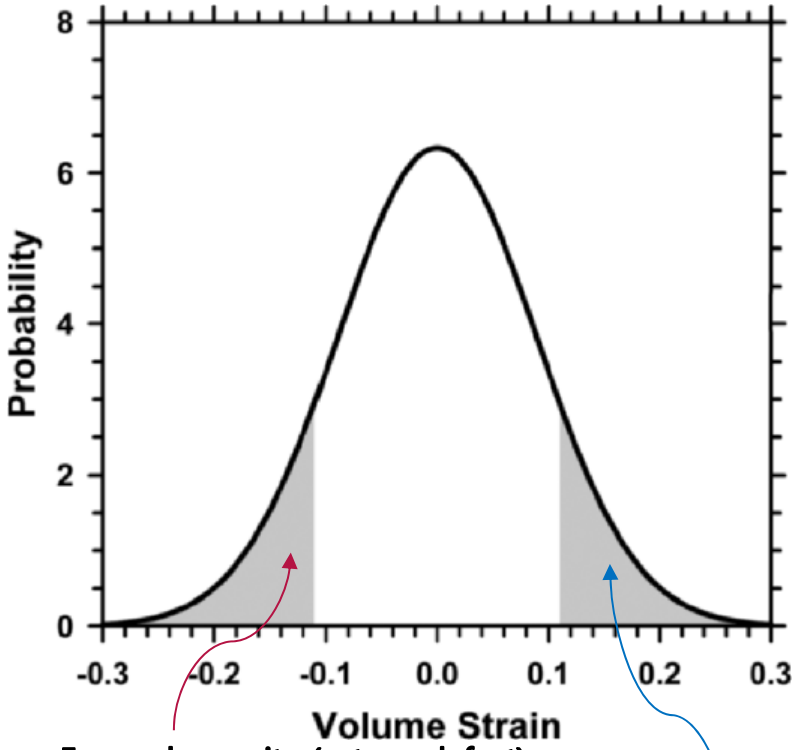

Free volume site (n-type defect)

Negative (dilatational) volume strain > 11 %

$\varepsilon_V < -\varepsilon_V^{crit}(L)$

Antifree volume site / p-type defect

Positive (compressive) volume strain > 11 %

$\varepsilon_V^{crit}(L) < \varepsilon_V$

> **Defect sites are *liquid-like* / topologically unstable**
> ***Solid-like* / topologically stable sites (ε_V < 11 %)**

여기에서 제안된 critical local volume strain은 free-volume theory에서 정의된 v*와 같은 order of magnitude를 가진다. 즉, free-volume은 원자 크기만큼의 부피가 아니라, 11 % 정도의 local dilatation이 원자 topology를 불안정하게 하여 CN을 1 정도 바꿈

> **Deformation of metallic glasses**

본 조건에서 정의된 defect는 negative와 positive 양 방향의 strain이 가능하기 때문에, 기존의 hard sphere model에서처럼 소성변형에 반드시 free volume이 필요한 것은 아니다. Free volume은 주로 소성변형의 결과로 생겨나는 것이지 꼭 pre-existing할 필요는 없다.

Microscopic bases for the mode-coupling theory

$$m = \left.\frac{\partial \log \eta(T)}{\partial (T_g/T)}\right|_{T=T_g} = \frac{13}{1-(T_g/T_s)} = 13K_\alpha = \frac{39(1-\nu)}{2(1-2\nu)}.$$

Atomic processes and deformation mechanisms

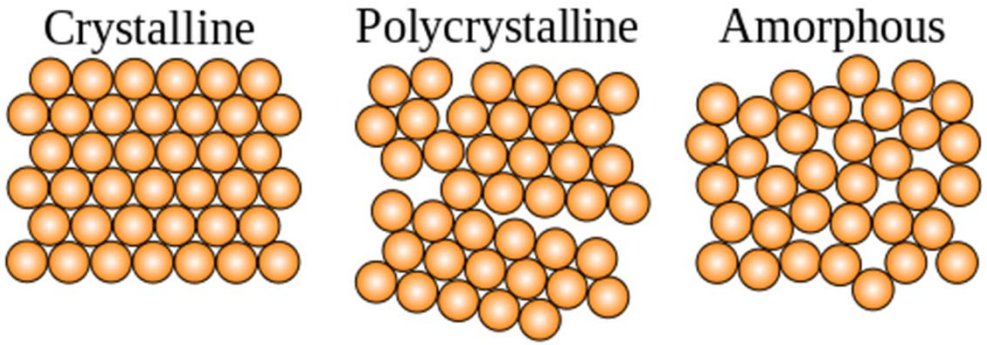

- Plastic flow is **a *kinetic process.***
- At absolute zero, **polycrystalline solid** as having a well defined **yield strength**, below which it does not flow and above which flow is rapid.
- Variables that solid strength depends on : **strain, strain-rate, and temperature**. (atomistic processes : glide-motion of dislocation lines, their coupled glide and climb, the diffusive flow of individual atoms, the relative displacement of grains by grain boundary sliding, mechanical twinning etc.)
- **Deformation mechanisms** were considered to describe polycrystal plasticity (or flow); they divided into five groups.

1. **Collapse at the ideal strength**
2. **Low-temperature plasticity by dislocation glide**
3. **Low-temperature plasticity by twinning**
4. **Power-law creep by dislocation glide, or glide-plus-climb**
5. **Diffusional flow**

- It's possible to superimpose upper mechanisms. (superplastic flow etc.)

Deformation modes

Plastic deformation

(γ', τ, T)

F. Spaepen : Free volume theory

Homogeneous flow @ steady state

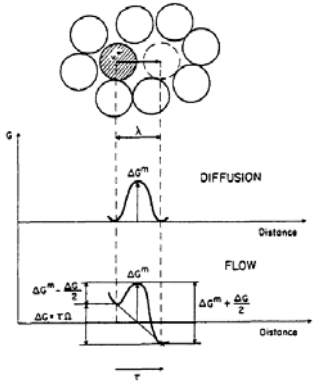

Inhomogeneous flow @ steady state

Competition of shear-induced disordering and a diffusion controlled reordering;

creation of FV vs. relaxation

$\Delta v_f^+ = \Delta v_f^-$

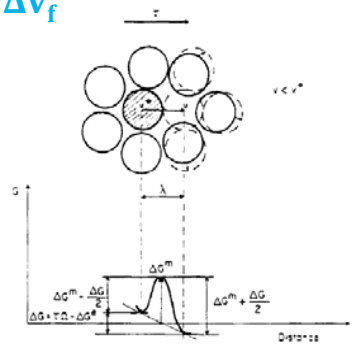

A. S. Argon / C. A. Schuh: STZ model

Homogeneous plastic flow

Viscous flow of a SCL

Steady-state flow

Structural disordering과 ordering,
즉 free volume creation과 annihilation 사이의 균형.
$\Delta v_f^+ = \Delta v_f^-$
Local diffusive jump 또는 STZ operation이 stress를 분산시키고, dilatation을 통해 free volume을 만들지만 동시에 relaxation이 진행되어 free volume을 없앤다.
Structural maintanance

Non-steady-state flow

Structural transience가 일어남.
균형이 이루어지지 않아 net gain / loss of free volume이 일어날 수 있다.
"overshoot" "undershoot"

Inhomogeneous plastic flow

Localization → Shear band formation
local production of FV (dilatation)
local evolution of structural order due to STZ operation
redistribution of internal stresses

8.2 Deformation Behavior

Deformation behavior of Metallic glass

8.2.2 Homogeneous Deformation

- high temp. (>0.7T_g) and in the SCLR/ high strain rate
- Viscous flow → significant plasticity
  : achieve net-shape forming capability
- Newtonian (high temp. & low stress) vs non-Newtonian (high temp. & applied stress) : associated with the precipitation of nanocrystals

⇩

Homogeneous deformation

8.2.1 Inhomogeneous Deformation

- Low temp. (<0.5T_g)/ high stress
- Localized shear band/ 45° to the loading axis
- Strain softening: deformed at lower stress and higher rate

⇩

Catastrophically Failure

Ashby deformation maps for crystalline materials

Delineating the different modes and mechanism of plastic deformation of a material as a function of stress, temperature, and structure

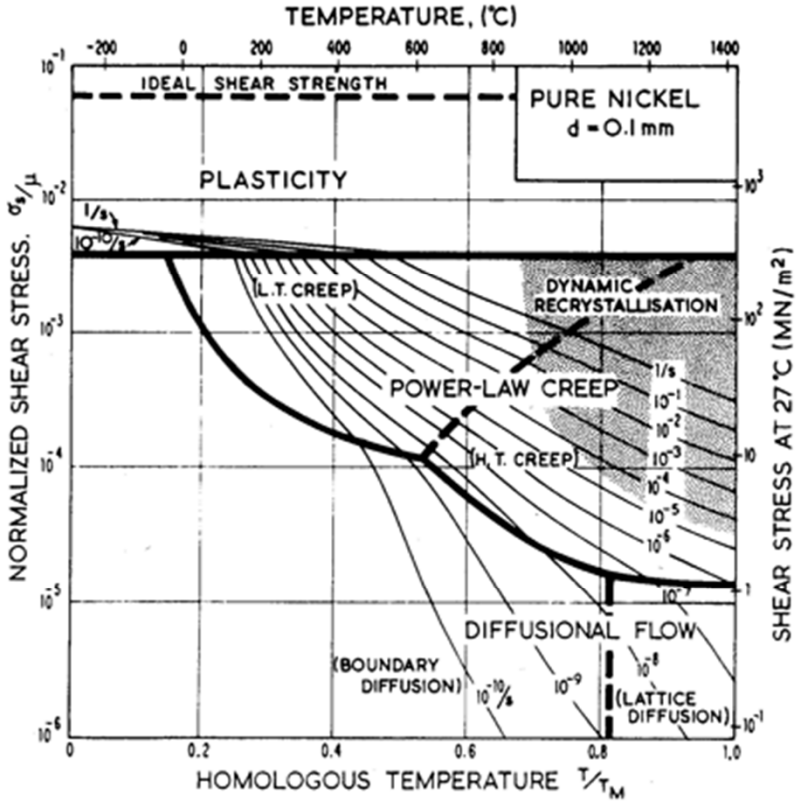

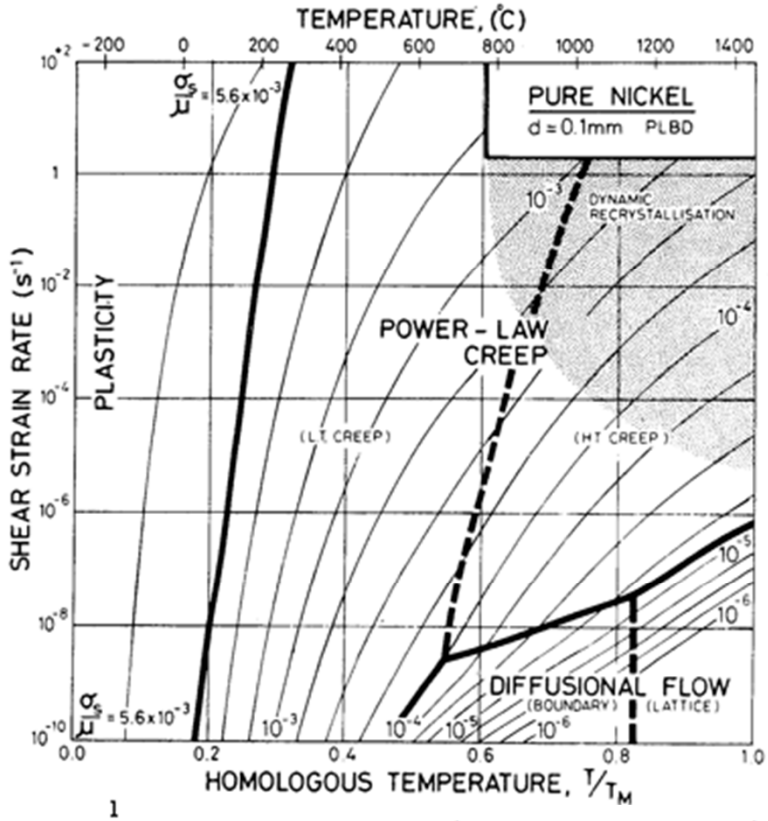

- **Rate equations** $\dot{\gamma} = \left(\frac{2}{3}\left((\dot{\varepsilon}_1 - \dot{\varepsilon}_2)^2 + (\dot{\varepsilon}_2 - \dot{\varepsilon}_3)^2 + (\dot{\varepsilon}_3 - \dot{\varepsilon}_1)^2\right)\right)^{\frac{1}{2}}$ ⇒ $\dot{\gamma} = f(\tau, T, \text{structure})$

  steady-state constitutive flow law

- **Deformation-mechanism map shows how to combine each plastic deformation mechanisms.**
- normalized stress σ_s/μ
  homologous temperature, T/T_M (where μ is the shear modulus and T_M the melting temperature)
  shear strain γ'

Empirical deformation mechanism maps for metallic glasses

Developed by Spaepen using the results for melt-spun metallic glasses,
Explained by using the concept of free volume model

Flow Mechanisms

❖ Basic Modes of Deformation

- Homogeneous Flow
  - Each volume element undergoes the same strain.

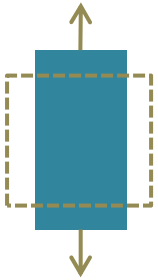

- Inhomogeneous Flow
  - Strain is concentrated in a few thin shear bands.

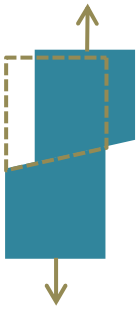

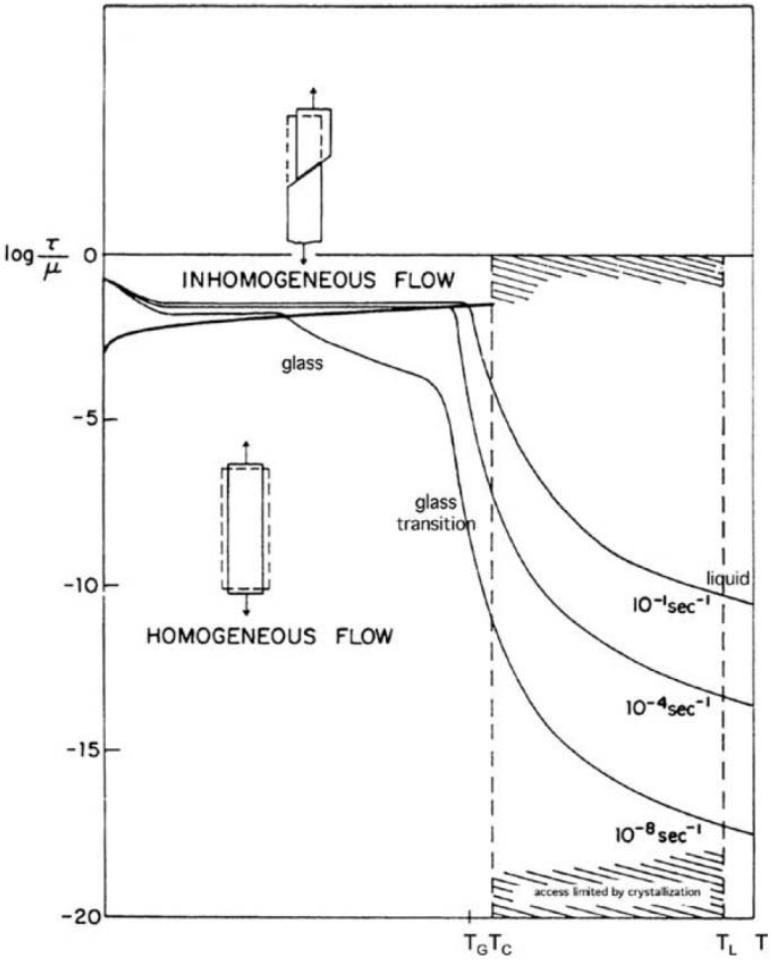

Fig. 1. Deformation mechanism map for a metallic glass.

Homogeneous Deformation

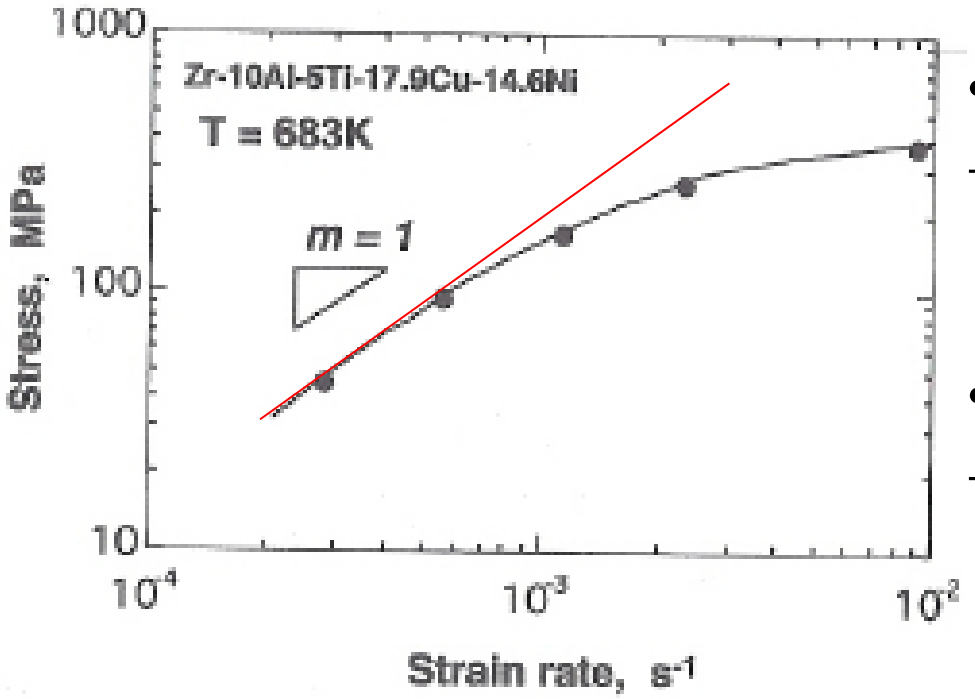

• Under low strain rate
→ Homogeneous deformation
(= Newtonian fluid)

• Under high strain rate
→ Inhomogneous deformation
(= non-Newtonian fluid)

• Newtonian to non-Newtonian transition is dependent on the test temperature.

Liquid Flow

❖ Liquid Region (above and near T_g)

- Homogeneous Flow
- Low stress in liquid region
- Strain rate is proportional to the stress
- Viscosity is not dependent on stress, but temperature.

$$\sinh\left[\frac{\varepsilon_0 \nu_0 \sigma}{2kT}\right] \approx \frac{\varepsilon_0 \nu_0 \sigma}{2kT} \quad @ \text{ low stress}$$

- Newtonian Viscous Flow

$$\tau = \eta \cdot \dot{\gamma}$$

Shear stress | Viscosity | Strain rate

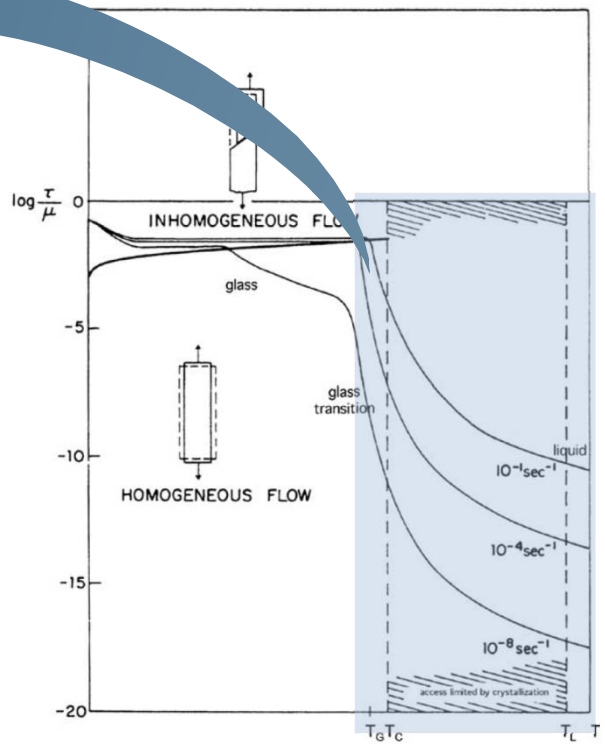

Fig. 1. Deformation mechanism map for a metallic glass.

Homogeneous deformation near glass transition temperature (High T)

Homogeneous operation of flow defects in a dilatated state

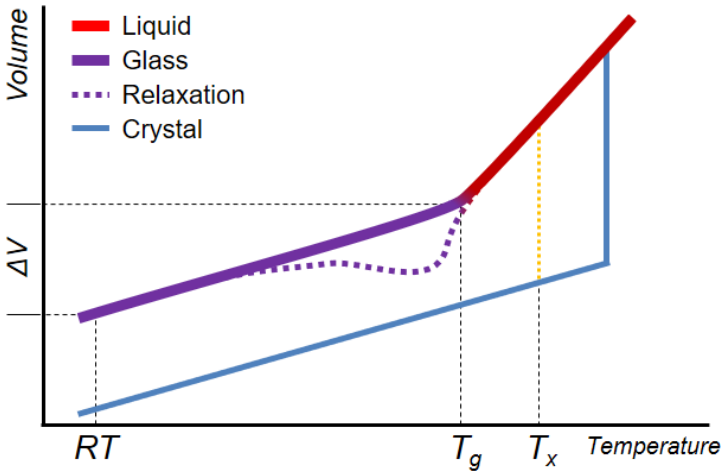

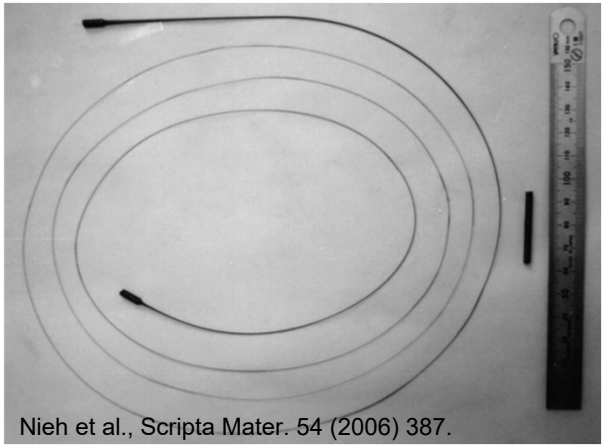

$La_{55}Al_{25}Ni_{20}$ alloy deformed to 20,000% in the supercooled liquid region.

Lu et al., Acta Mater. 51 (2003) 3429.
Schuh et al., Acta Mater. 55 (2007) 4067.

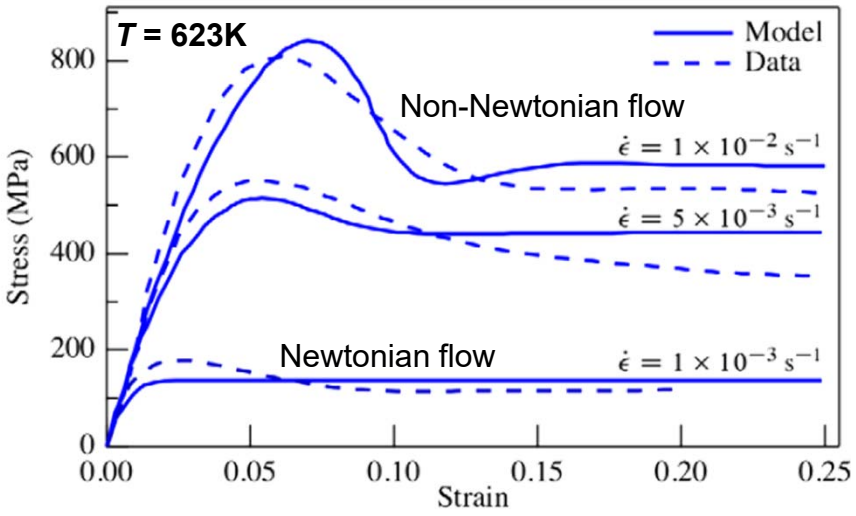

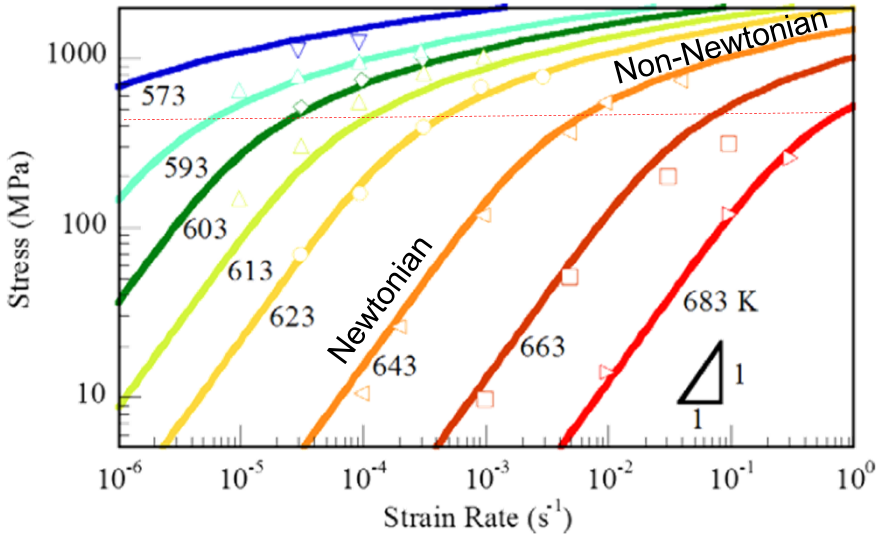

Deformation-induced Softening

- Softening : Lowering of viscosity in the shear bands

- Structural Change : Creation of free volume due to high stress level

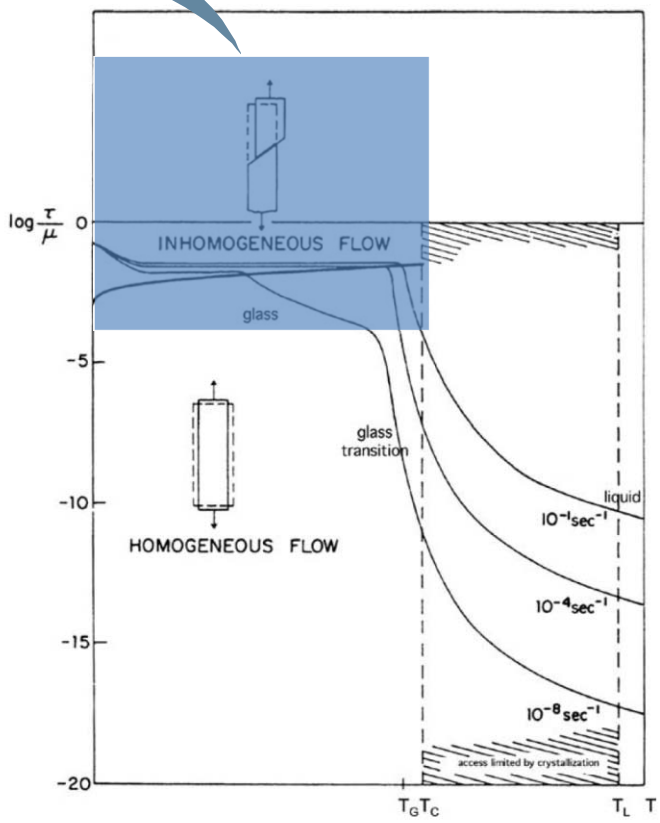

Fig. 1. Deformation mechanism map for a metallic glass.

Plastic deformation of metallic glass near RT : Viscous flow →"Shear bands"

Scattered operation of STZ

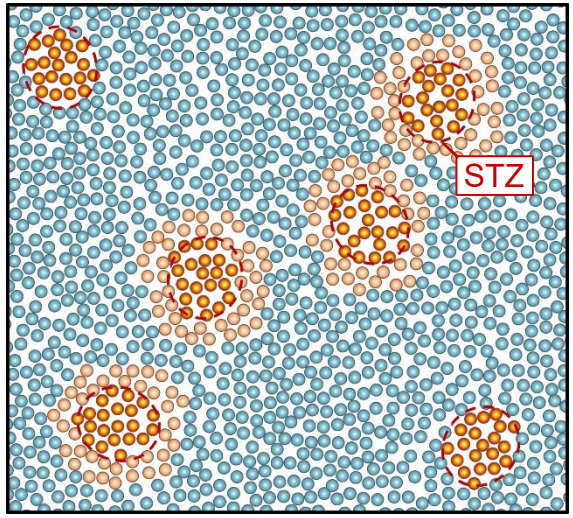

Percolation of STZ to nucleate **SBs**

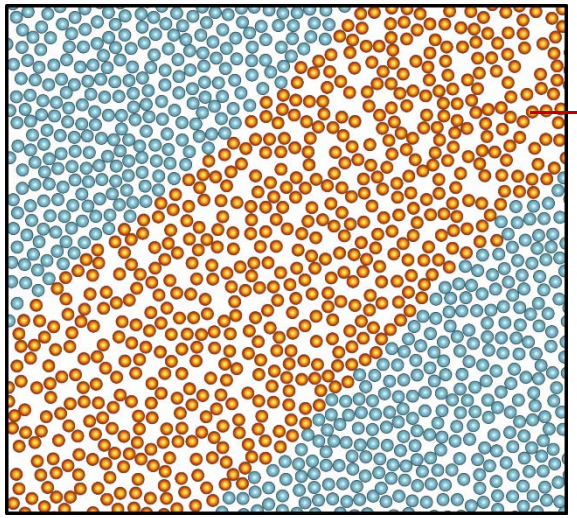

Shear band (SB) : Plastic instability that localizes large shear strains in a relatively thin band

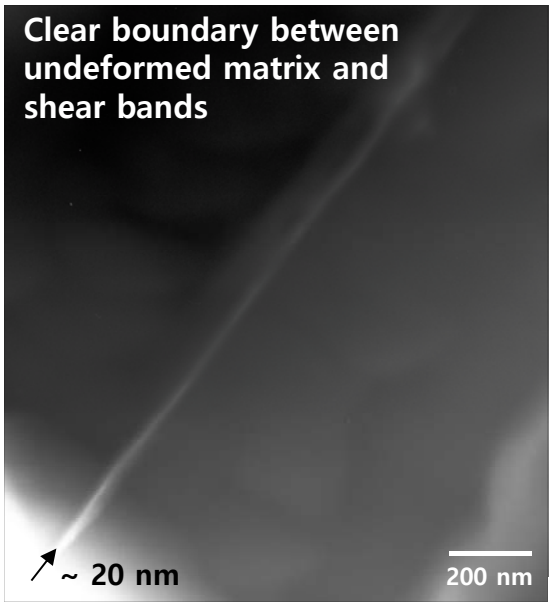

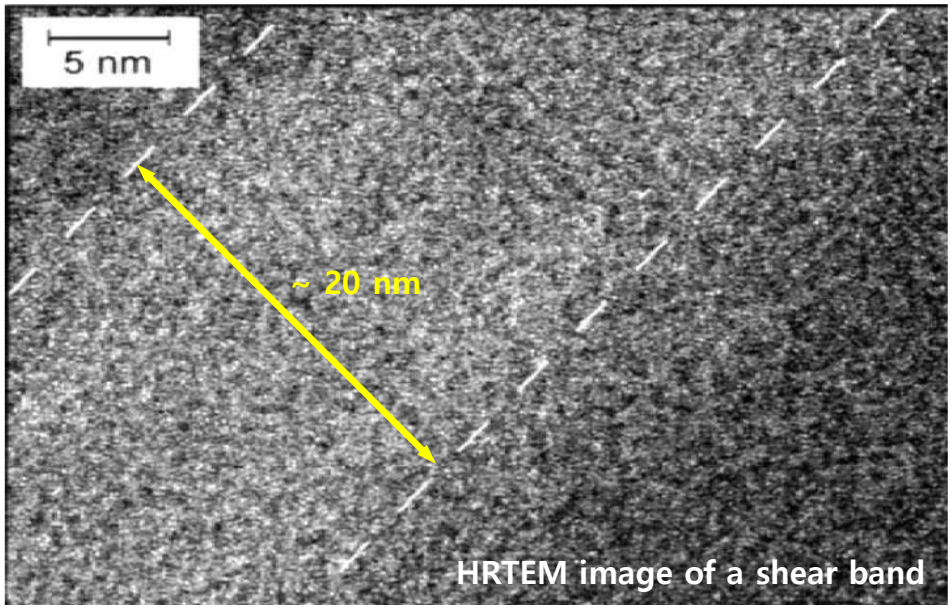

Empirical deformation mechanism maps for metallic glasses

Developed by Spaepen using the results for melt-spun metallic glasses,
Explained by using the concept of free volume model

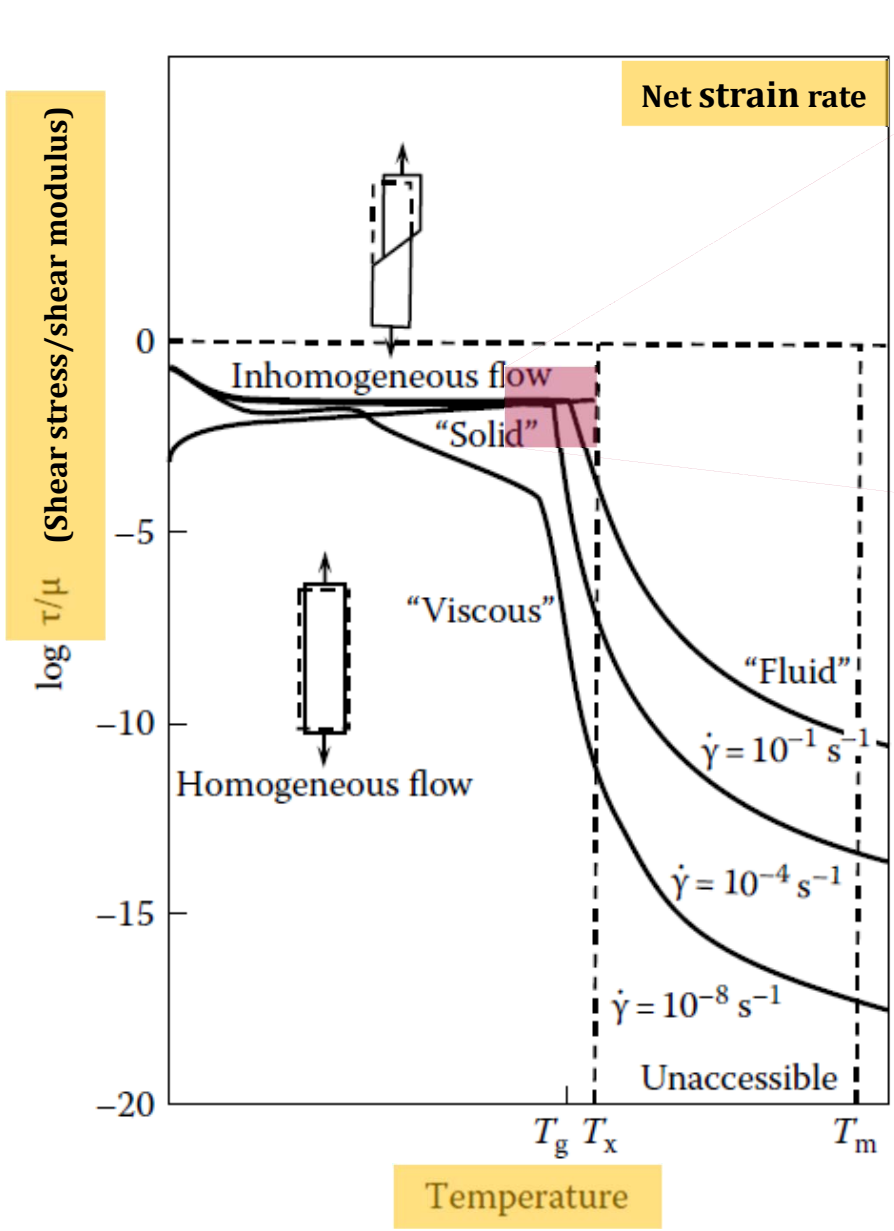

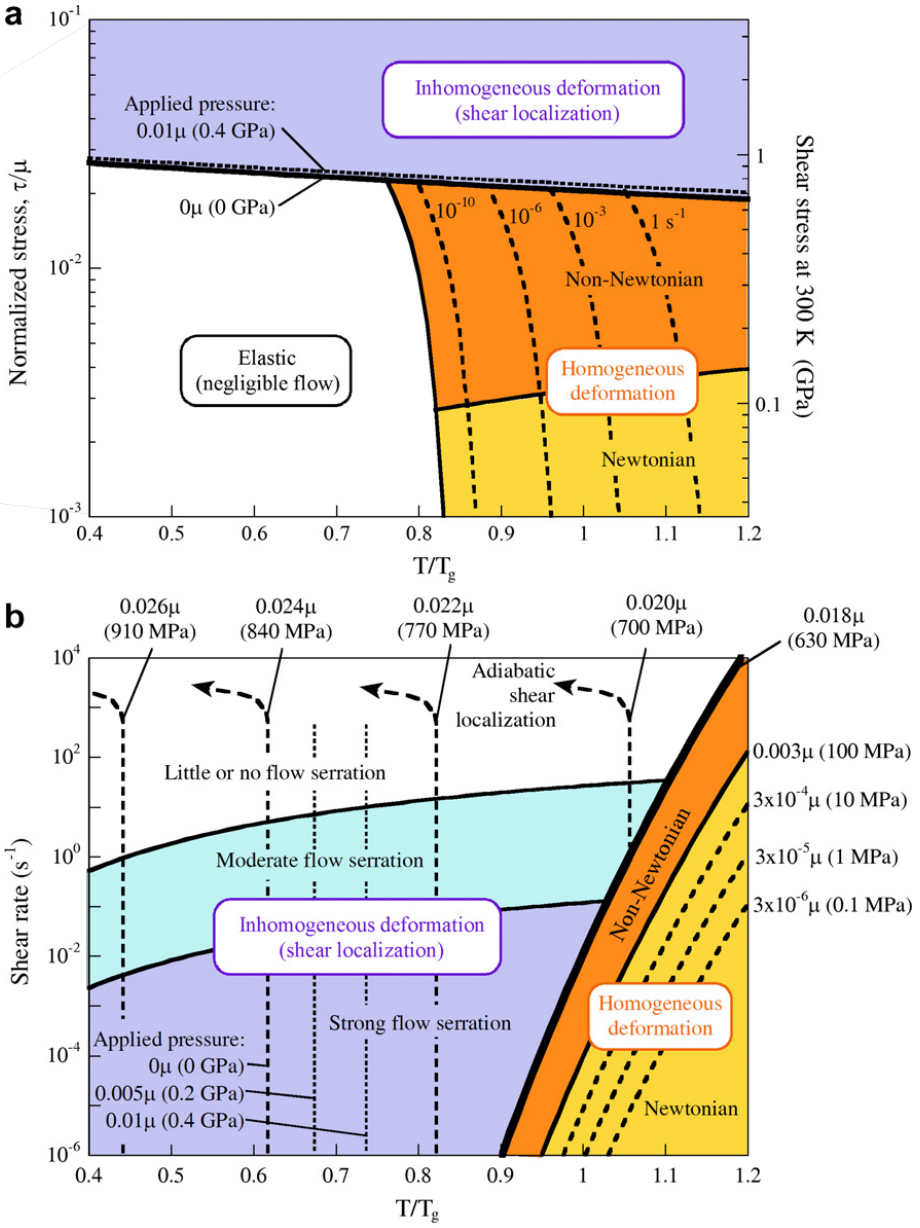

Deformation map drawn by C.A. Schuh

Explained by using the concept of STZ, strain rates are represented as a series of contours.

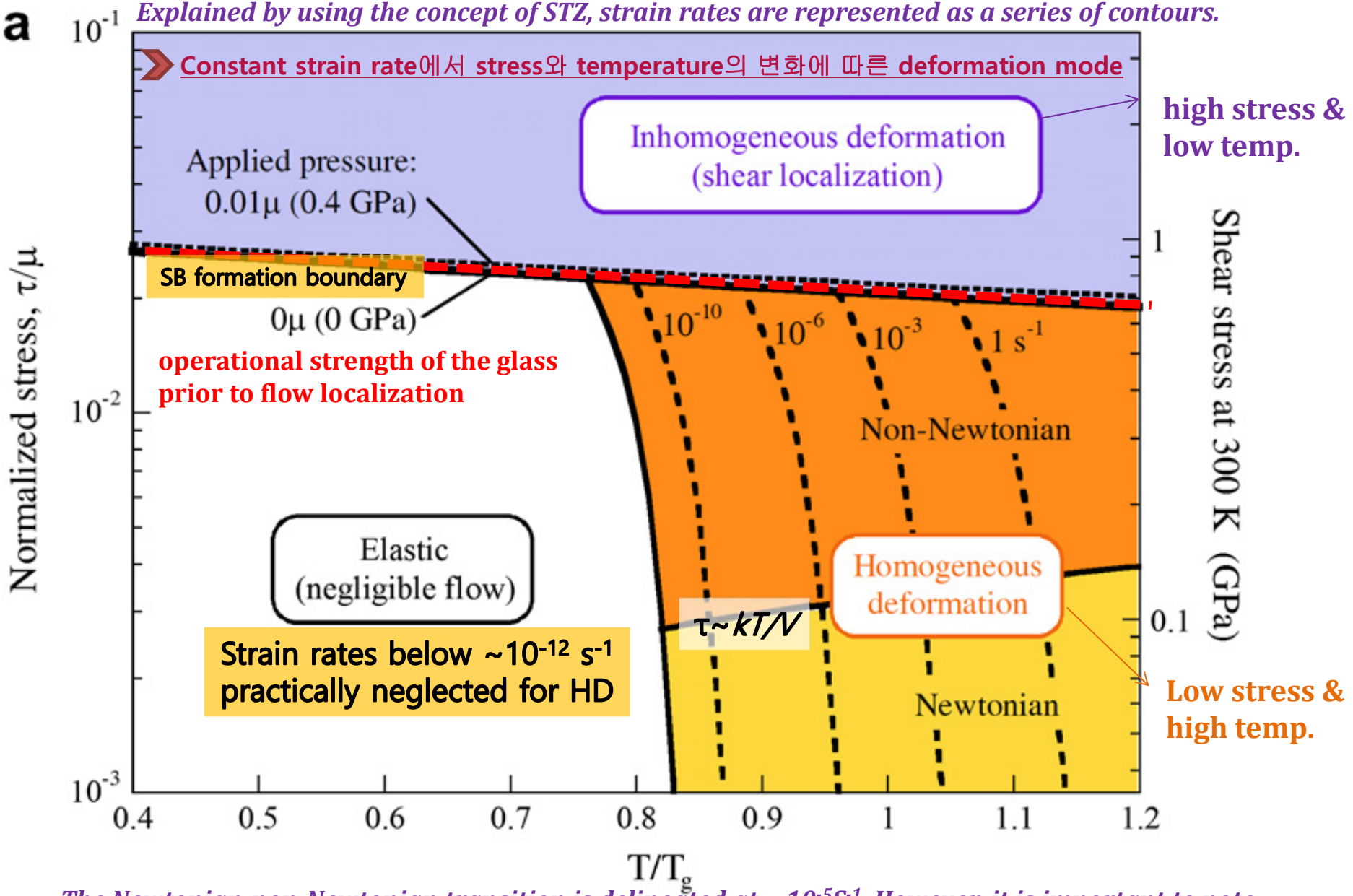

The Newtonian-non-Newtonian transition is delineated at ~ $10^{-5}S^{-1}$. However, it is important to note that at high enough shear rates, non-Newtonian flow as well as shear localization can occur at high temperature – even in the supercooled liquid region.

Deformation map drawn by C.A. Schuh

Explained by using the concept of STZ, stress is represented as a series of contours.

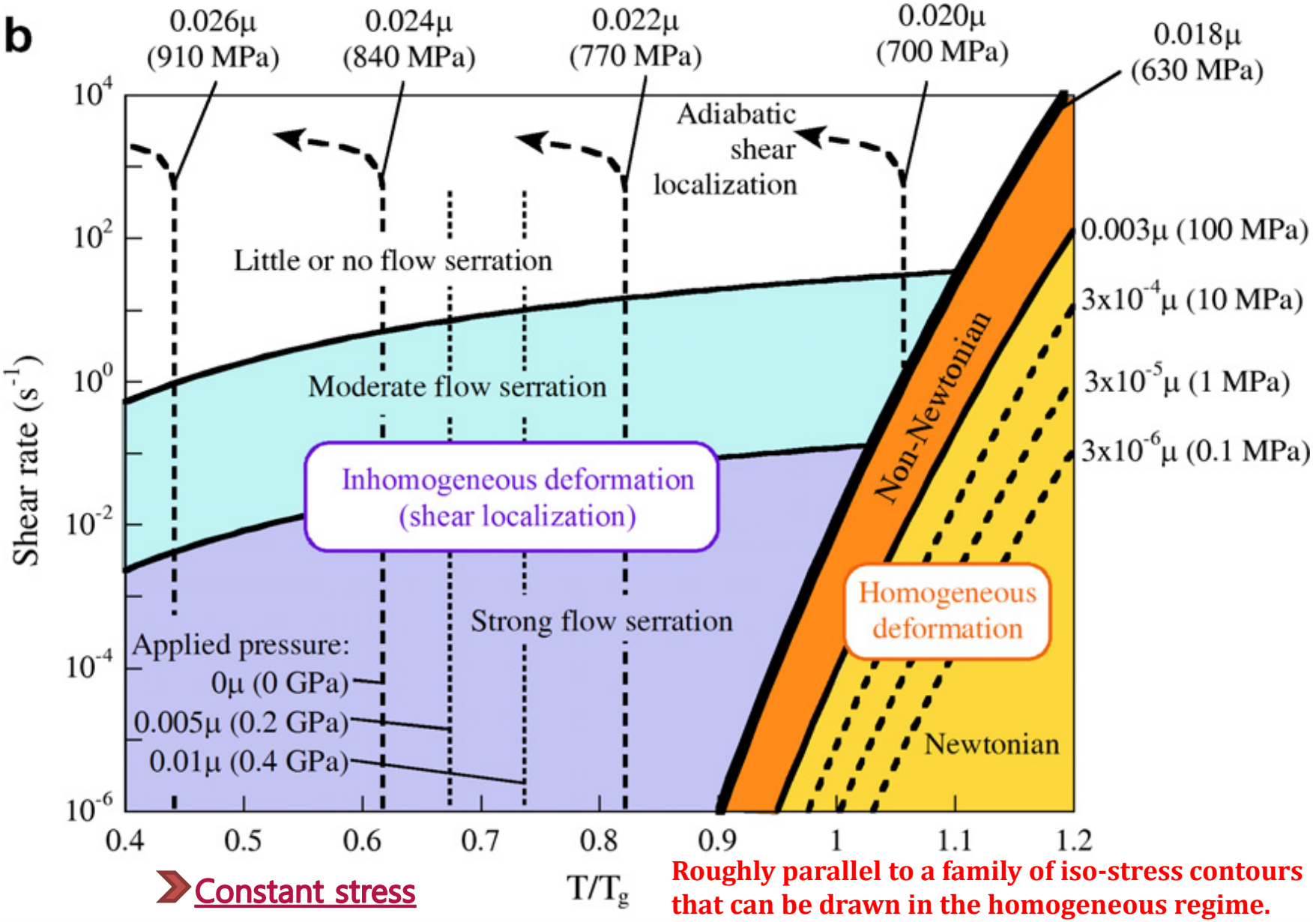

Constant stress

Roughly parallel to a family of iso-stress contours that can be drawn in the homogeneous regime.

Deformation mode of bulk metallic glasses

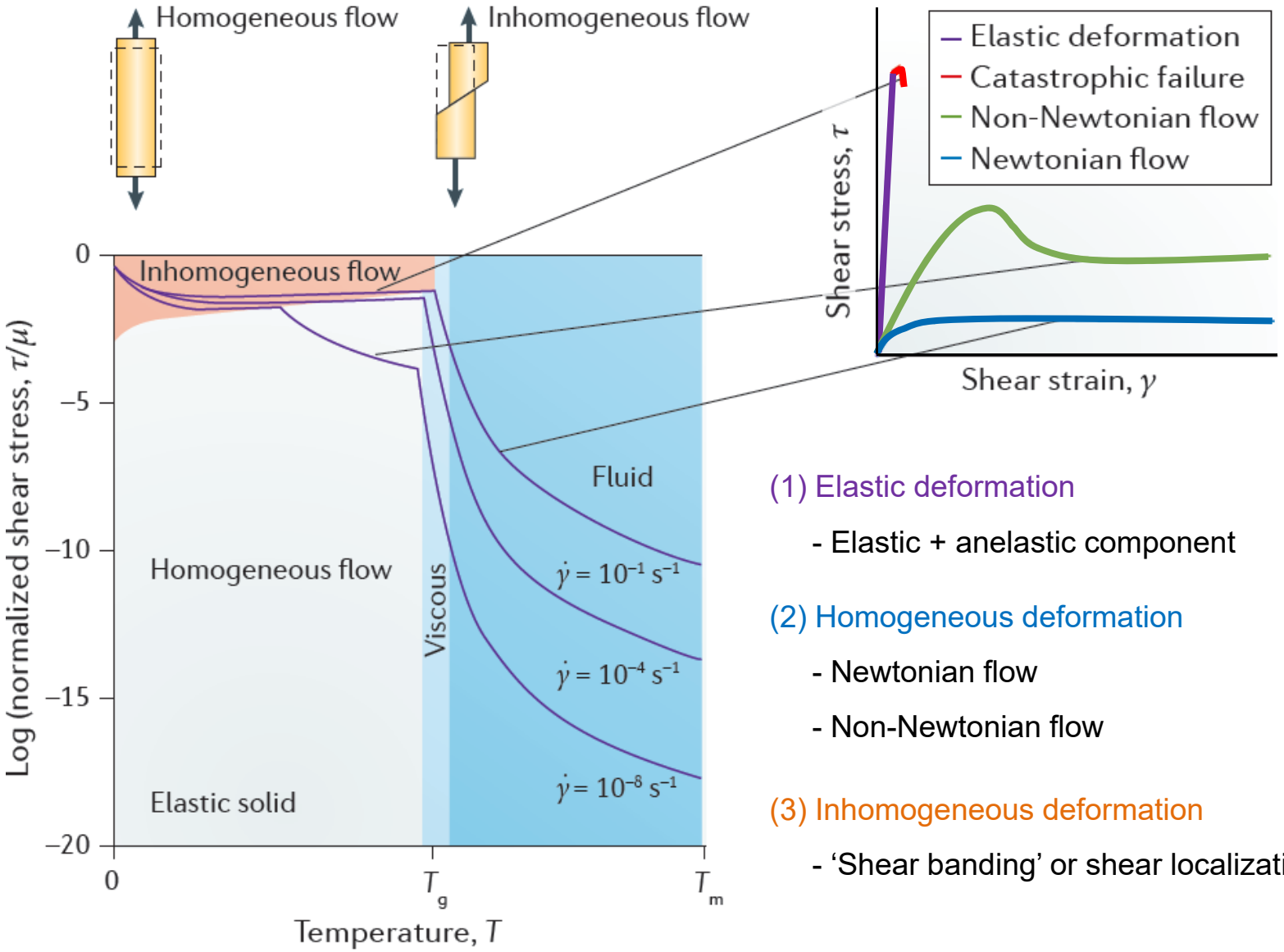

(1) Elastic deformation

- Elastic + anelastic component

(2) Homogeneous deformation

- Newtonian flow
- Non-Newtonian flow

(3) Inhomogeneous deformation

- 'Shear banding' or shear localization

Spaepen, Acta Metall. 25 (1977) 407.
Sun et al., Nature Rev. Mater. 1 (2016) 16039.

Summary of BMG deformation behavior

- **Plastic deformation in metallic glasses controlled by shear band nucleation and propagation.**

- **Atomistic views of deformation of metallic glasses**

  F. Spaepen: Free volume theory
  A.S. Argon: Shear transformation zone theory
  T. Egami: Atomic bond topology

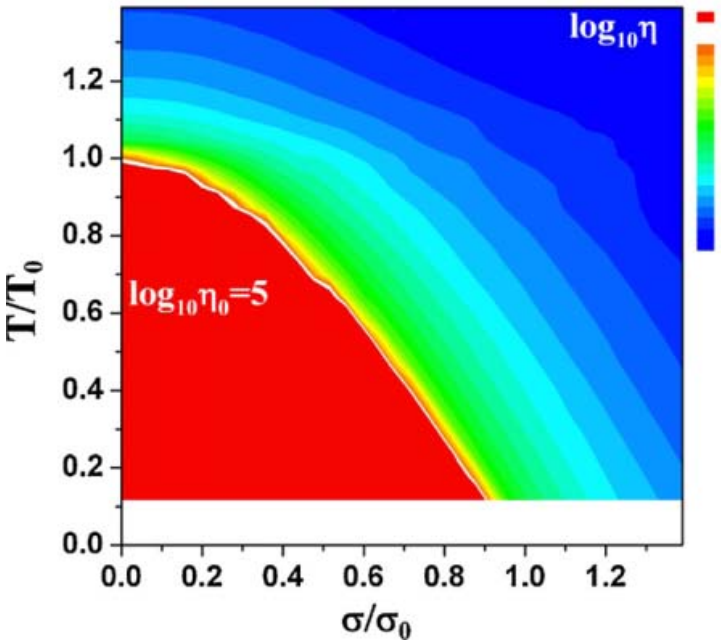

- Free volume theory: liquid 상에서의 free volume 개념이 모호, MD simulation 결과와는 맞지 않음
- Free volume theory는 현상을 설명하기에 매우 적합하지만 그 자체로 microscopic theory가 될 수는 없다. (free volume이 없어도 변형 가능)
- Local topological fluctuation은 원자 수준의 stress를 온도에 따라 재배열함에 따라 thermal property를 설명할 수 있다.

- **Deformation map predicts the deformation modes of metallic glasses**

  normalized stress σ_s/μ, homologous temperature T/T_M, shear strain γ'

Deformation behavior of nanoscale metallic glass

Bulk metallic glass

(Brittleness, Strength ~*0.02E*)

Nanoscale metallic glass

(The smaller is the stronger,
and be also more ductile!)

- **Sample size effect on the strength and elastic limit of metallic glasses**

Wang et al., Acta. Mater. 60 (2012) 5370.

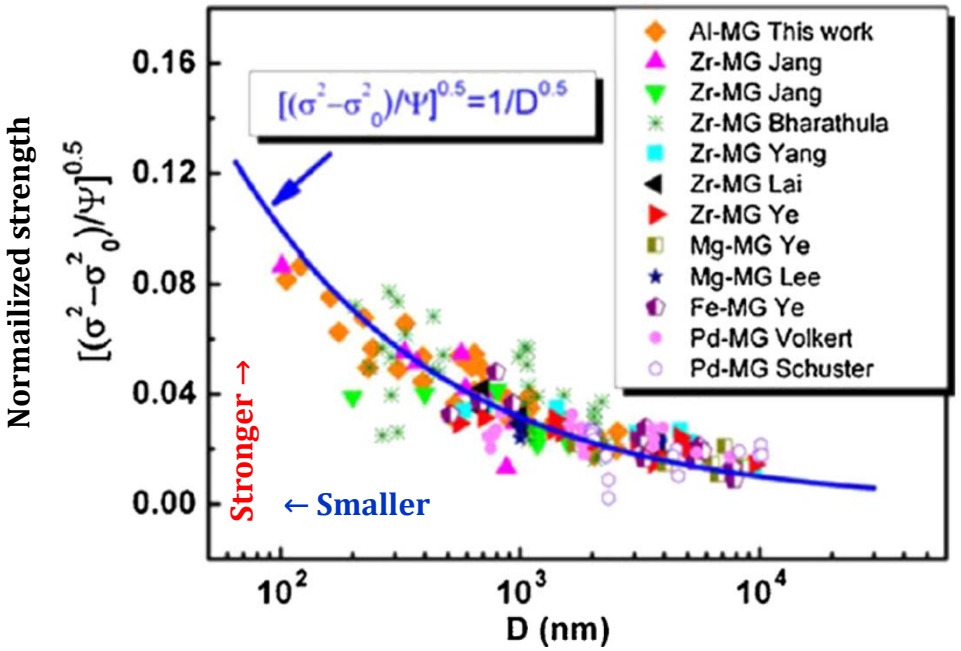

Tian et al., Nature Comm. 3 (2012) 609.

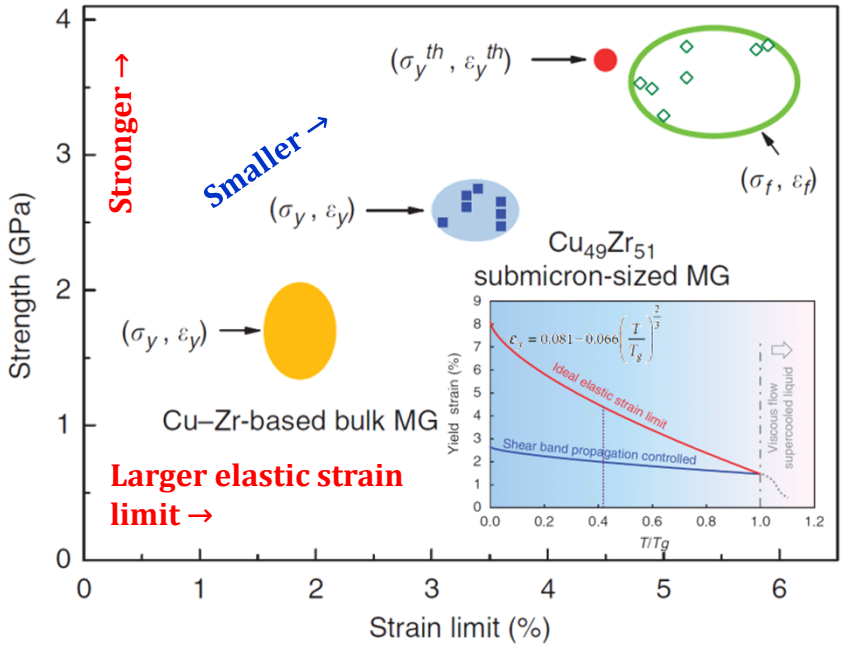

Plastic deformation in metallic glasses: Homogeneous deformation in nanoscale

- **Deformation mode transition in compression mode**

Volkert et al., J. Appl. Phys. 103 (2008) 083539.

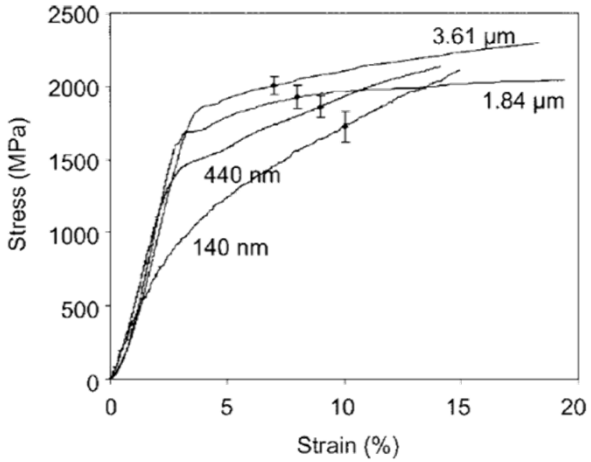

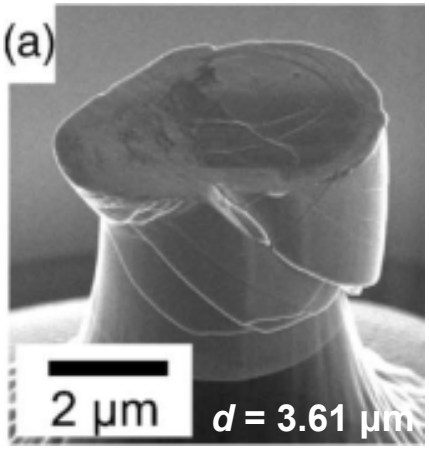

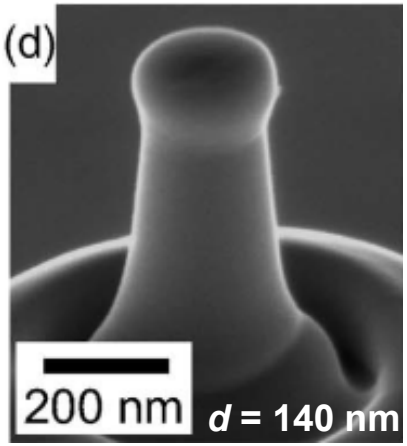

Bulk / microscale **inhomogeneous** → Nanoscale **homogeneous**

- **Deformation mode transition (necking) in tensile mode**

Jang et al., Nature Mater. 9 (2010) 215.

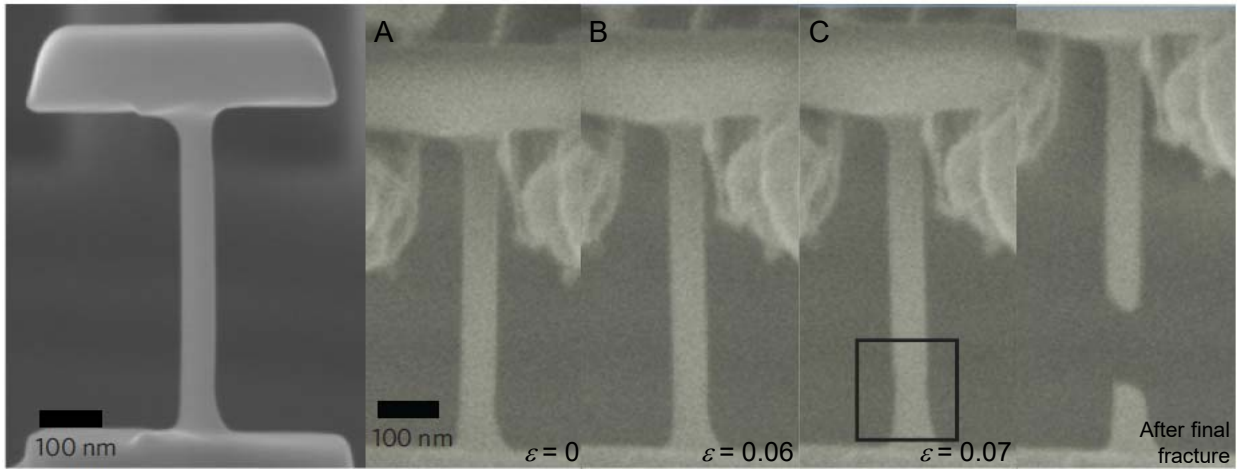

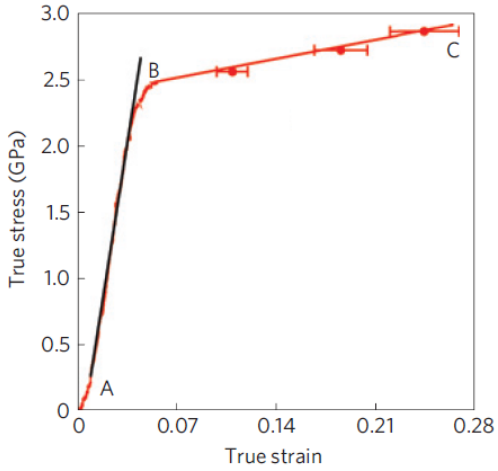

Suppression of shear banding and homogeneous deformation

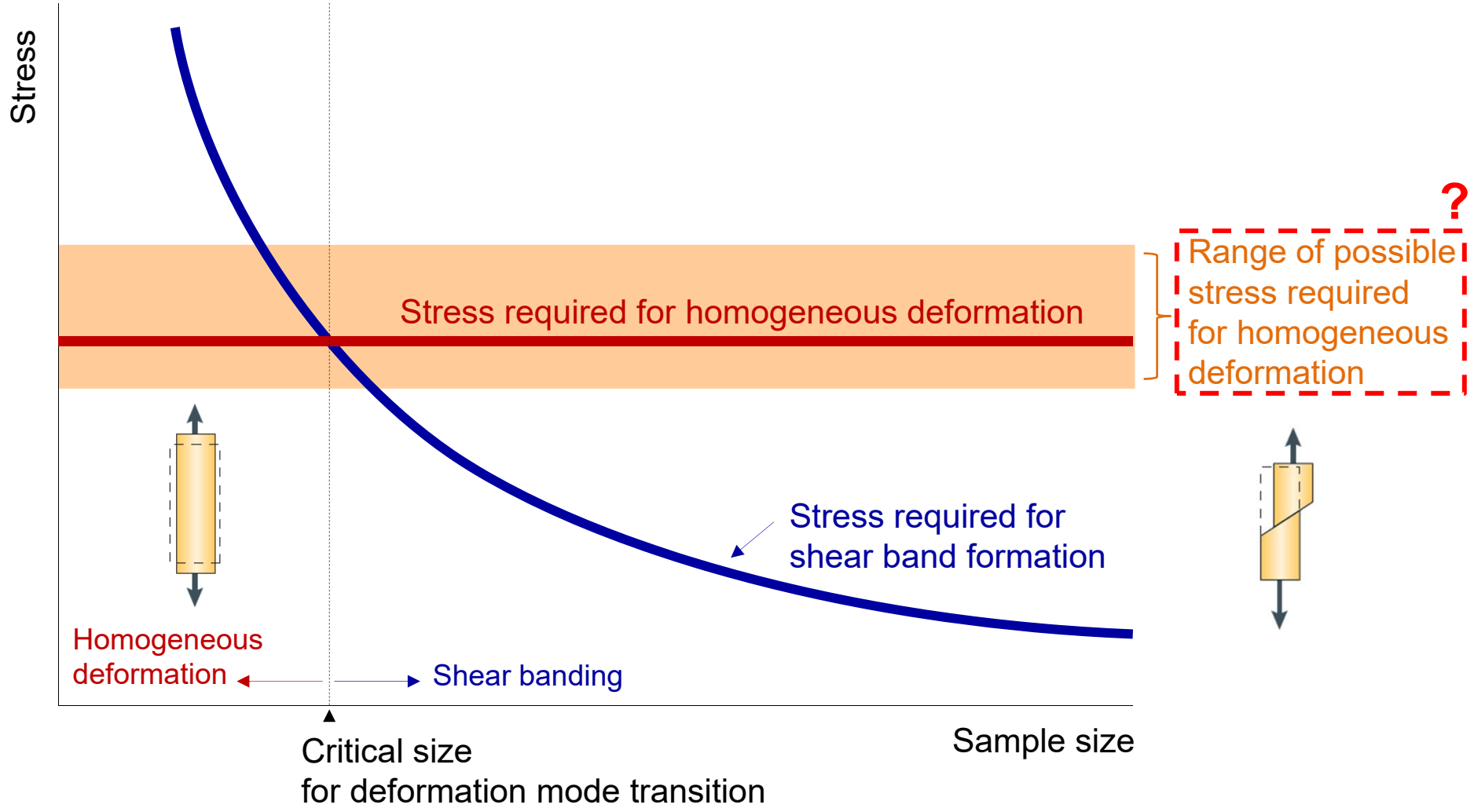

Volkert et al., J. Appl. Phys. 103 (2008) 083539.
Jang et al., Nature Mater. 9 (2010) 215.

Effect of Ga+ (FIB) irradiation on mechanical behavior of nanoscale metallic glass

Ductility dependence on irradiation

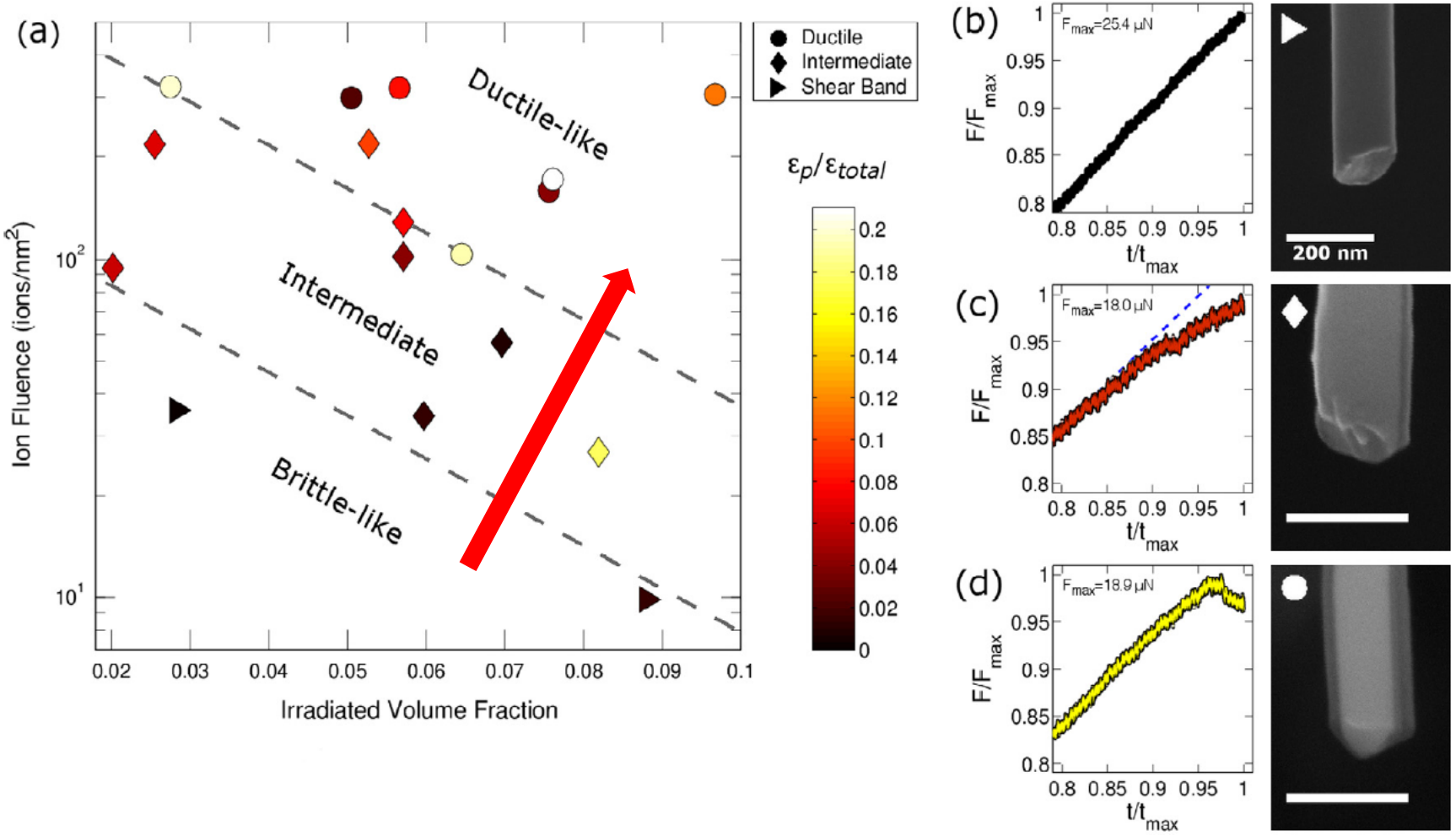

Magagnosc et al., Acta Mater. 74 (2014) 165.

MG Nanoparticle preparation: Compositional effects on PS microstructures

▼ Y-Ti-Al-Co system

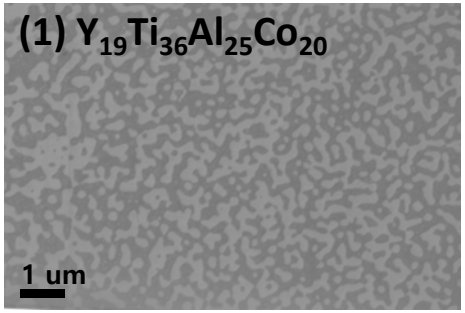

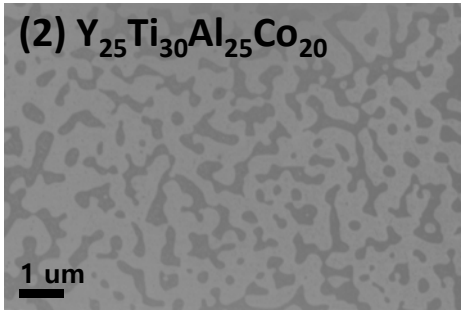

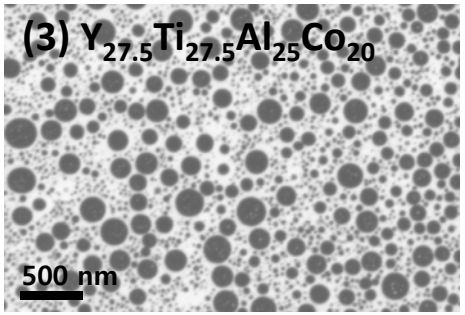

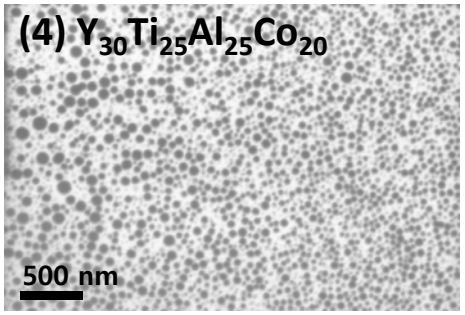

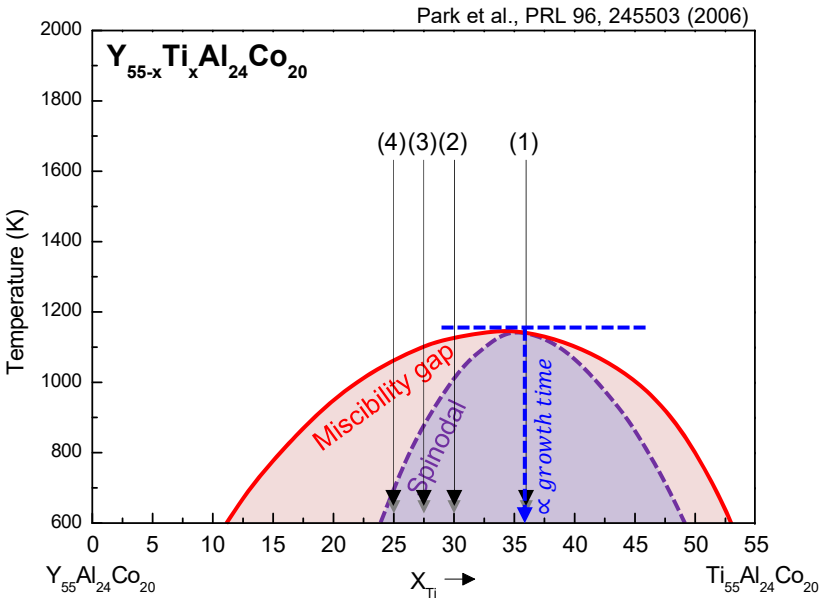

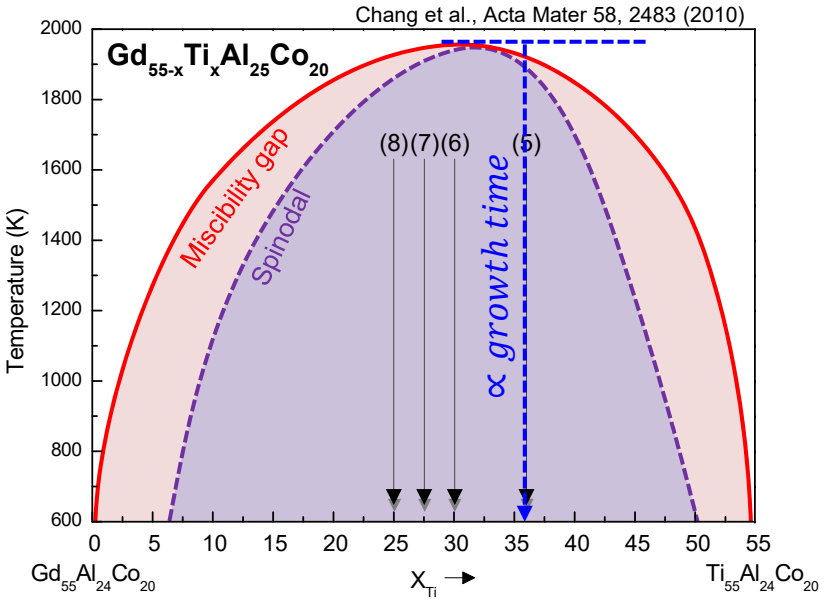

▼ Gd-Ti-Al-Co system

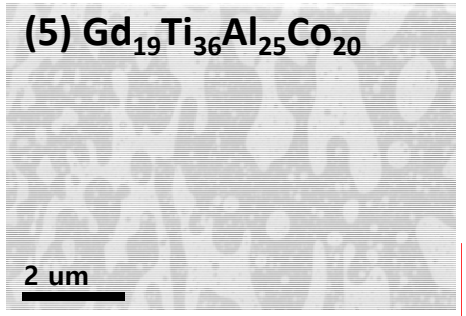

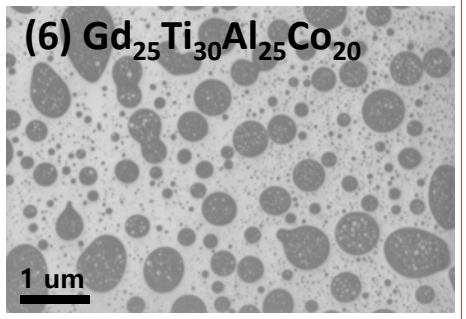

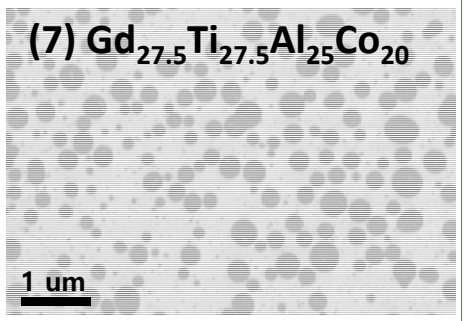

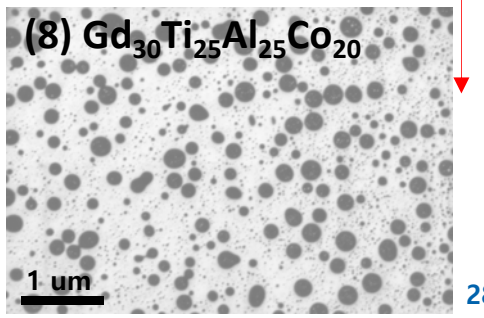

Increase of (Y,Gd) composition

MG Nanoparticle preparation: Cooling rate effect on PS microstructures

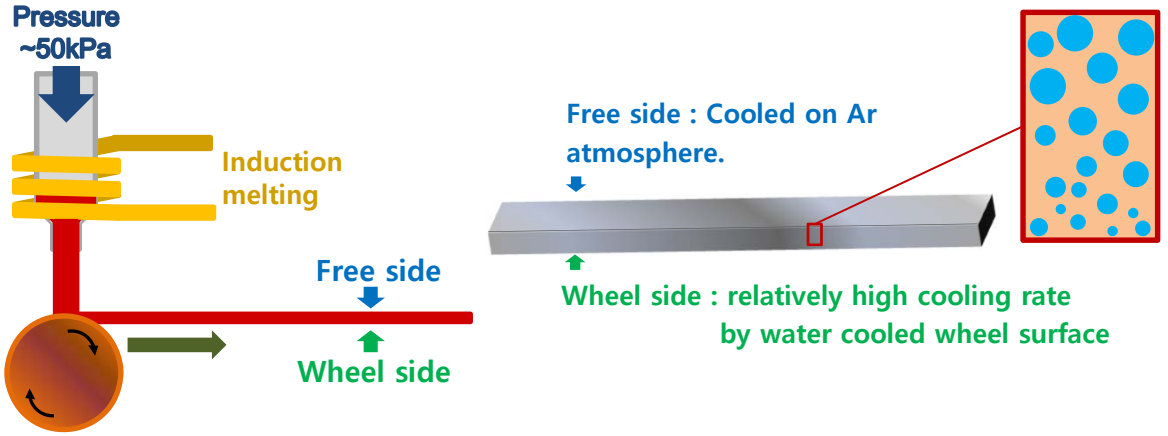

- SEM images of $Y_{27.5}Ti_{27.5}Al_{25}Co_{20}$ ribbon sample

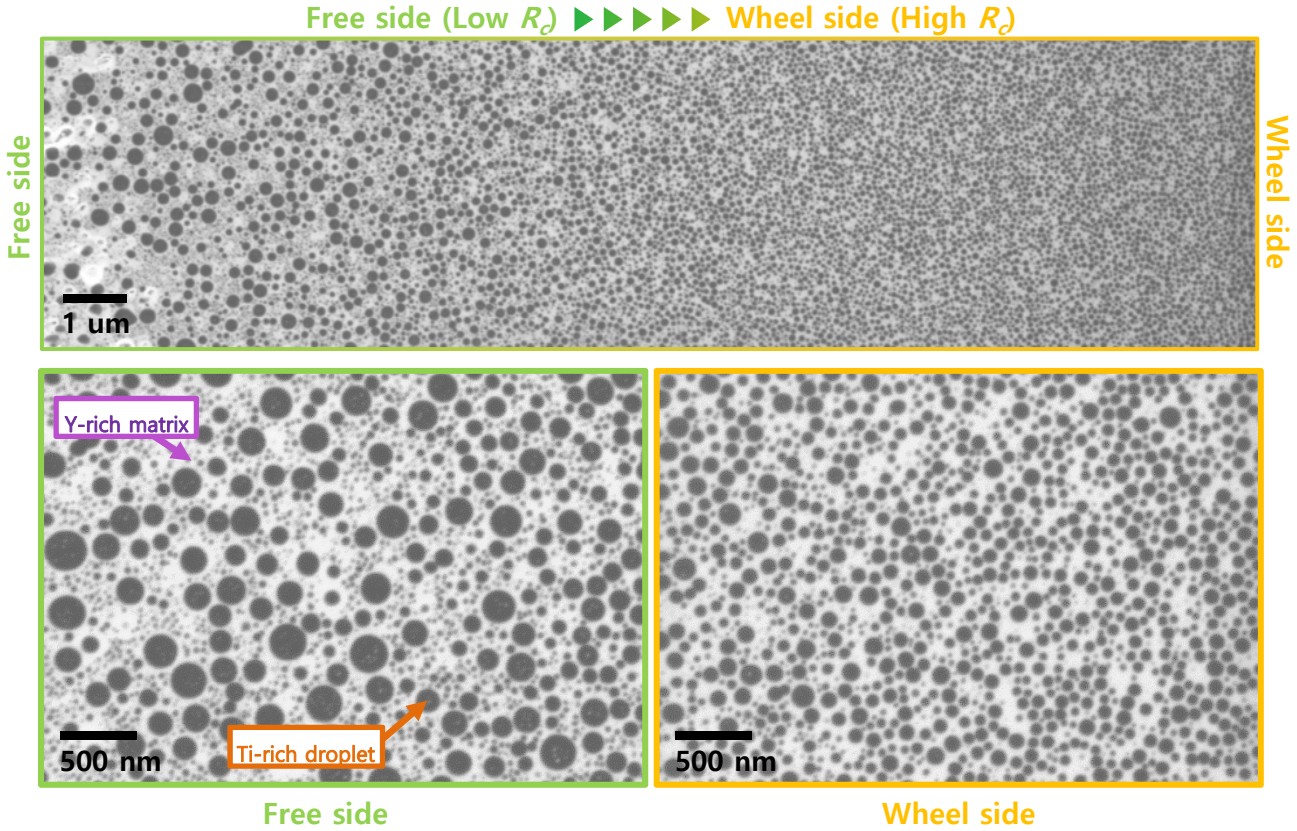

Nanoparticle preparation : Dealloying of phase separating metallic glass

Dealloying process

J. Jayaraj et al., Scripta Mat., 55 (2006) 1063.

Y, Gd : intensively reactive to HNO_3 soln.
Ti : strong resistance to corrosion by HNO_3 soln.

Immersion of the alloy in etchant solution.

➡ **Selective dissolution of Y, Gd-rich phase**

➡ **Formation of Ti-rich spherical nanoparticles**

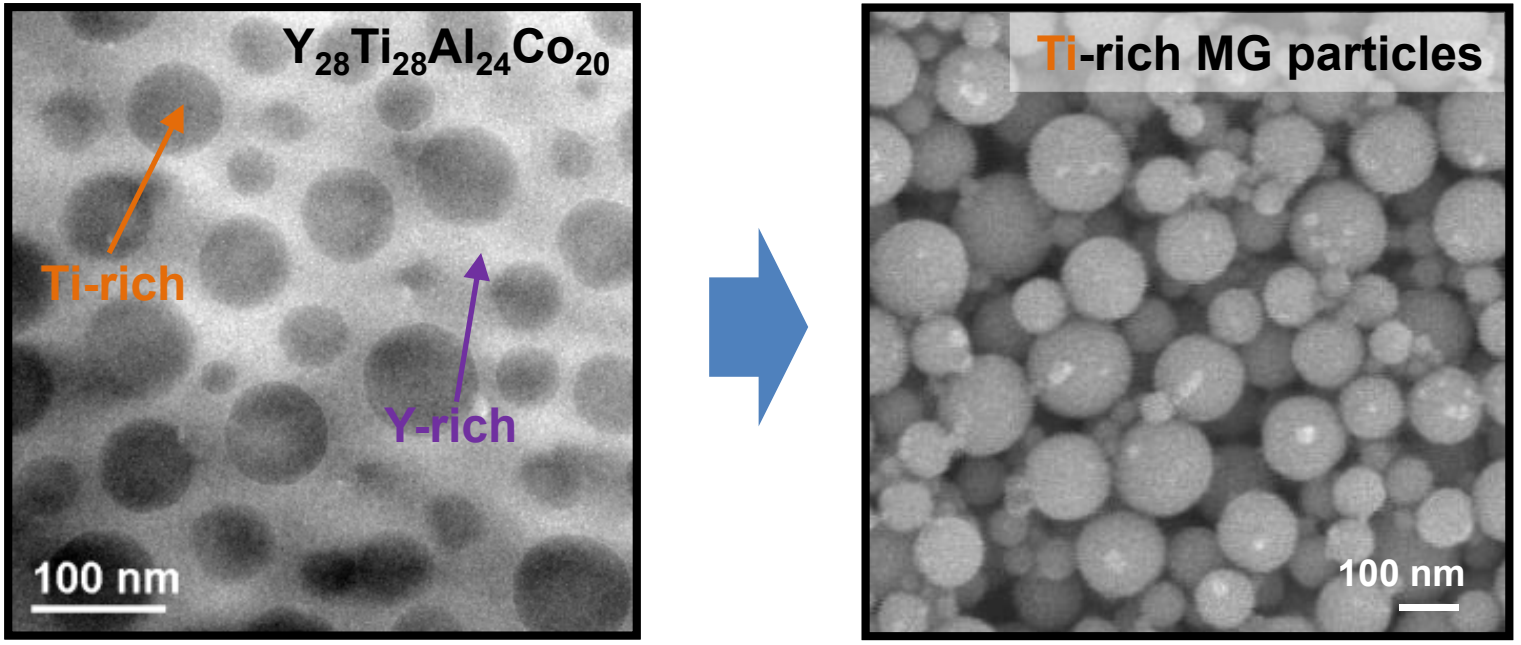

⇨ **Various diameters / same spherical geometry / without FIB process / relatively short preparation time**

Dispersion of dissolved TiAlCo MG nanoparticles by spin coating technique

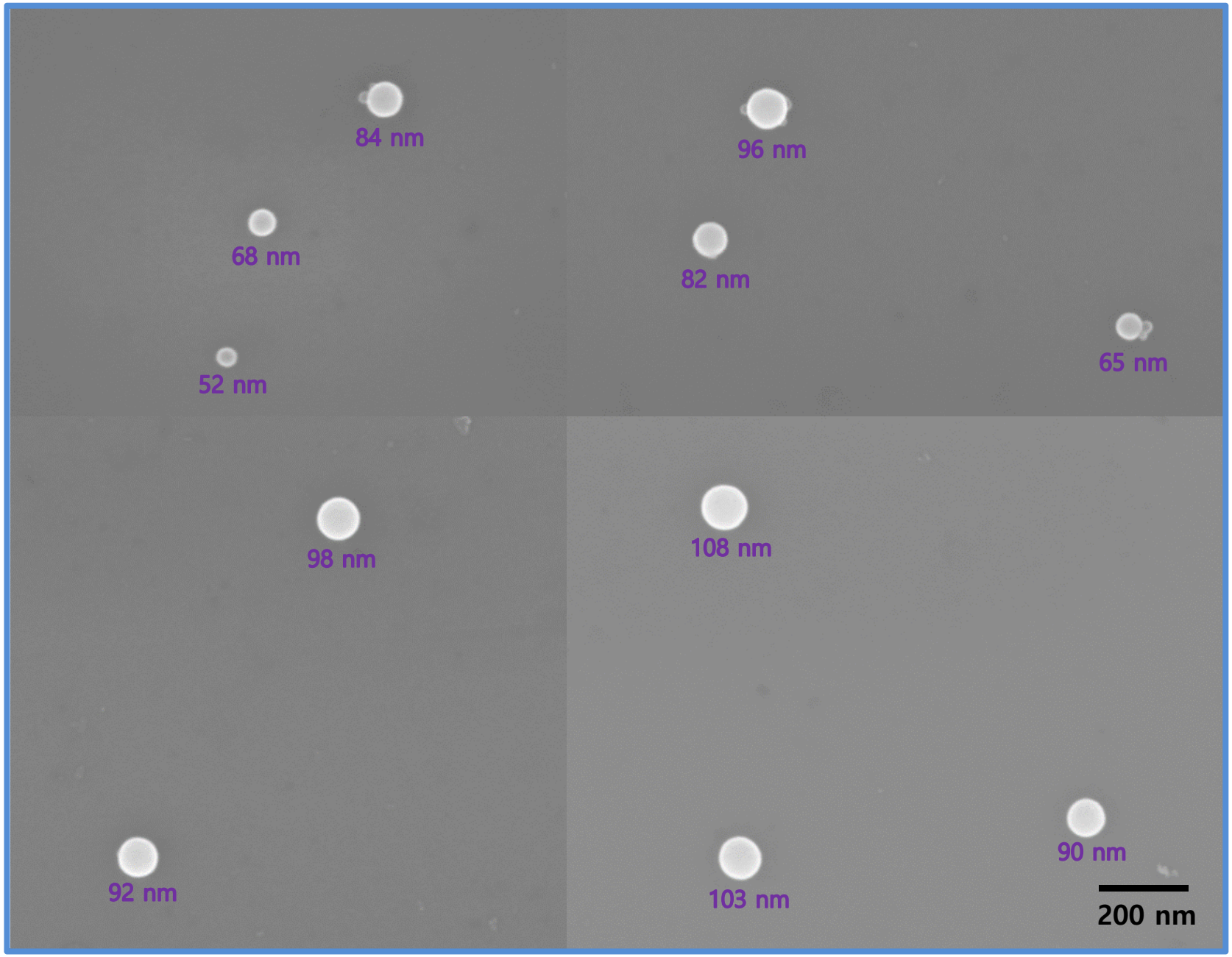

Surface morphology and microstructure of the metallic glass nanoparticle

- **Particles prepared by dealloying $Gd_{27.5}Ti_{27.5}Al_{25}Co_{20}$ ribbon sample**

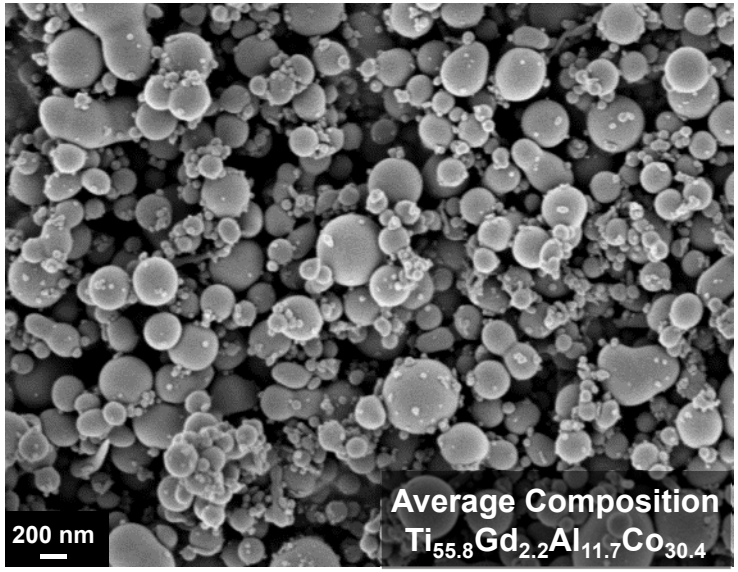

SEM image : Dealloyed Ti-Co-based MG nanoparticles

Ultrasonication

Spin-coating, Spraying

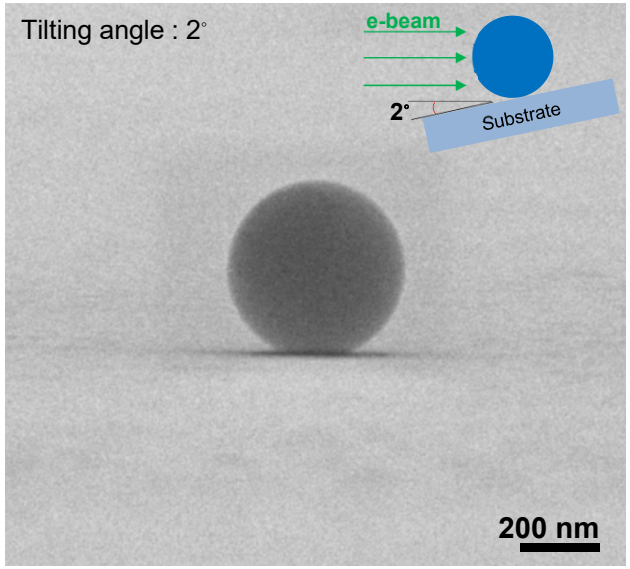

SEM image : Single nanoparticle on flat substrate

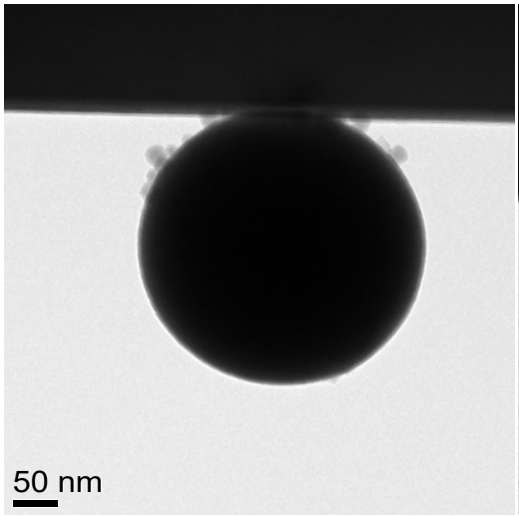

BF-TEM image : a particle (d>300nm)

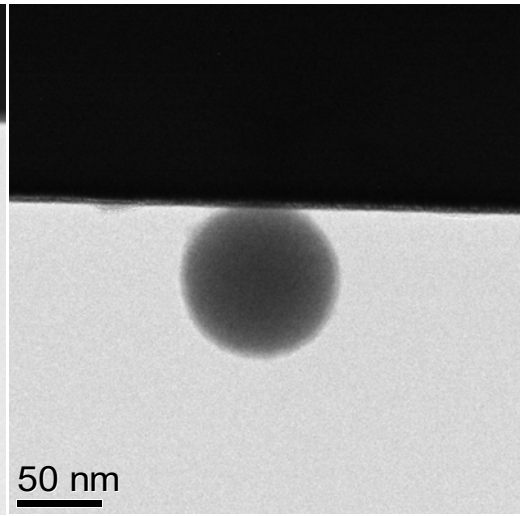

BF-TEM image : a particle (d<100nm)

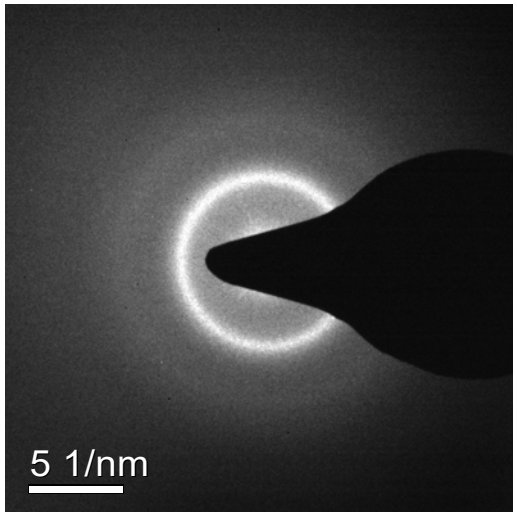

SADP of a single particle

Overview of Hysitron Picoindenter PI-85 with FEI FE-SEM

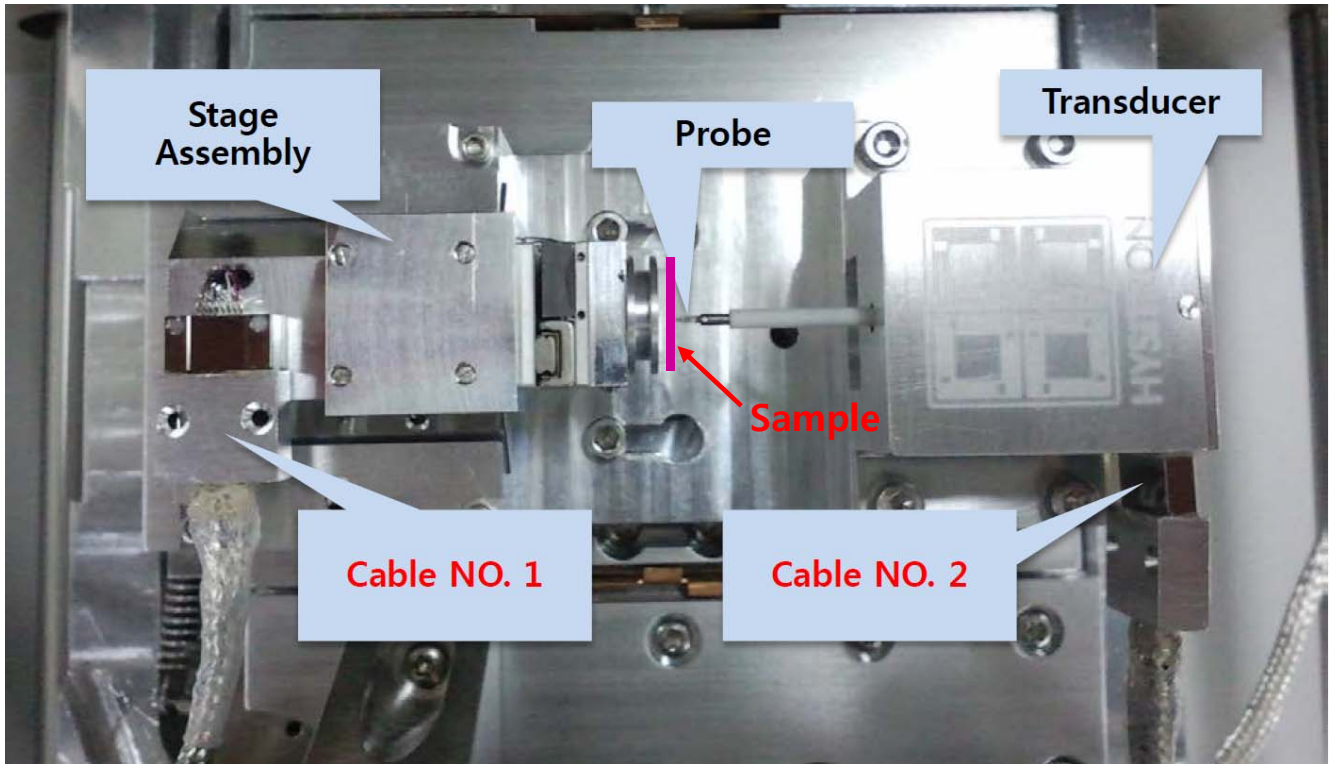

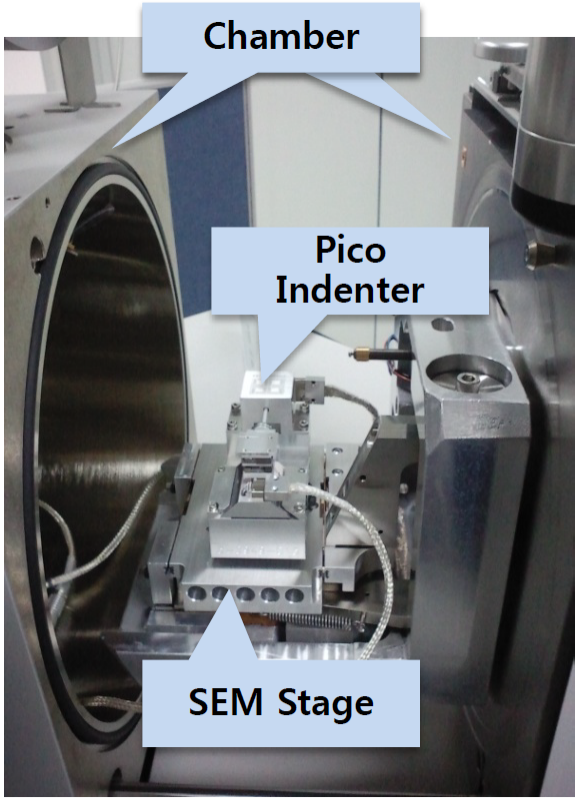

□ Pico Indenter + SEM Chamber

Compression test of MG nanoparticles using in-situ SEM indentation holder

- Particles prepared by dealloying $Gd_{27.5}Ti_{27.5}Al_{25}Co_{20}$ ribbon sample
  - Particle diameter, d_1 = 410 nm
  - Depth control mode, compression rate : 1 nm/s (strain rate: 2.4 x 10^{-3} s^{-1})
  - Indenting probe : Flat punch diamond tip (diameter ~ 1.2um)

20x speed video from SEM imaging (15kV, Tilt angle : 2°)

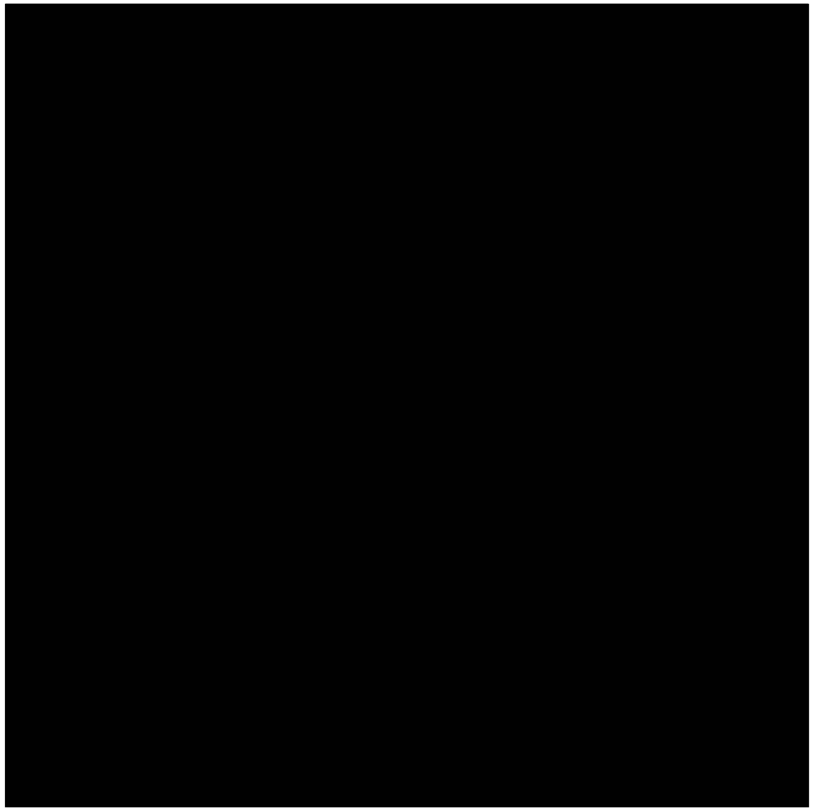

Load-depth plot from in-situ compression test

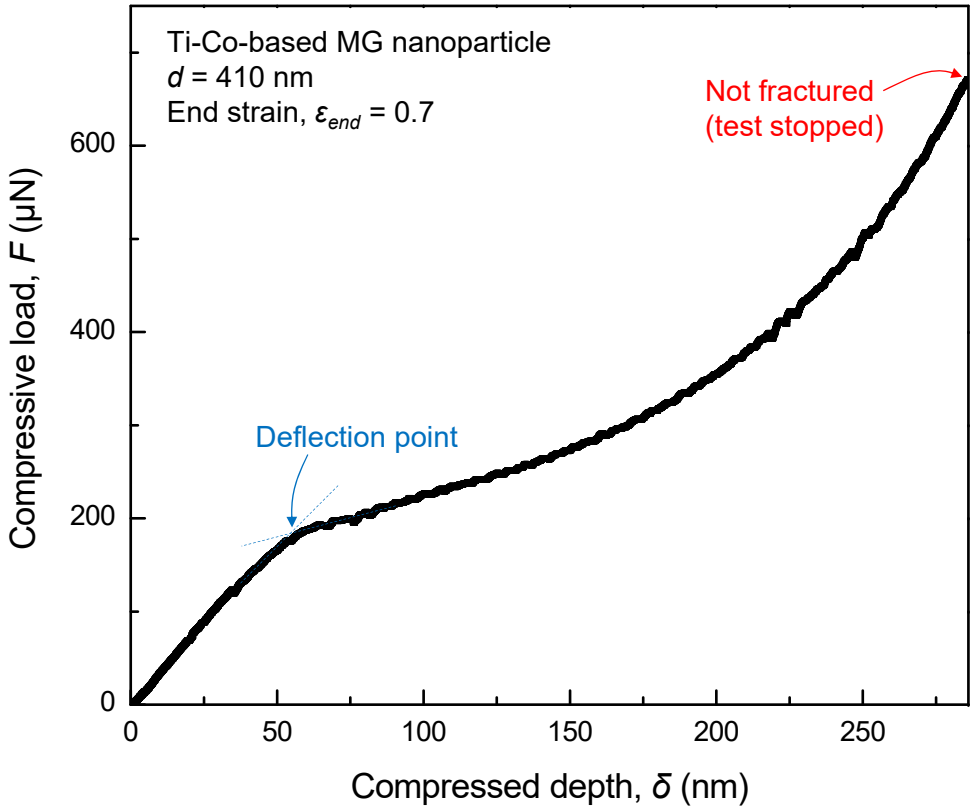

Contact diameter measurement and fitting with contact models

a. Hertzian contact

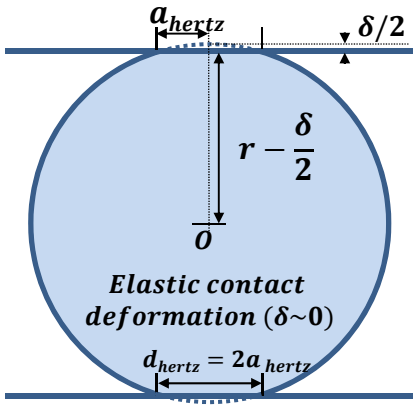

$$d_{hertz}=\sqrt{\varepsilon d^2}$$

b. Geometric contact

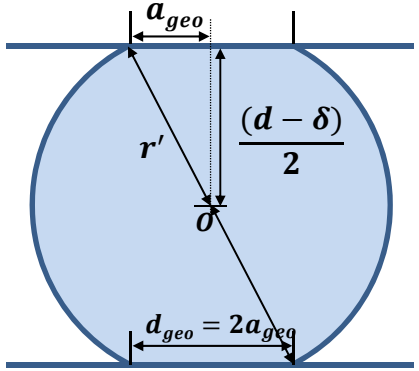

$$d_{geo}=d\sqrt{2\varepsilon-\varepsilon^2}$$

c. Cylindrical contact

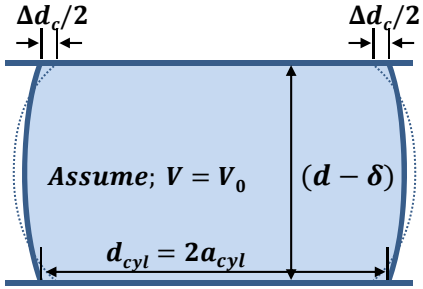

$$d_{cyl}=\sqrt{\frac{2d^2}{3(1-\varepsilon)}}$$

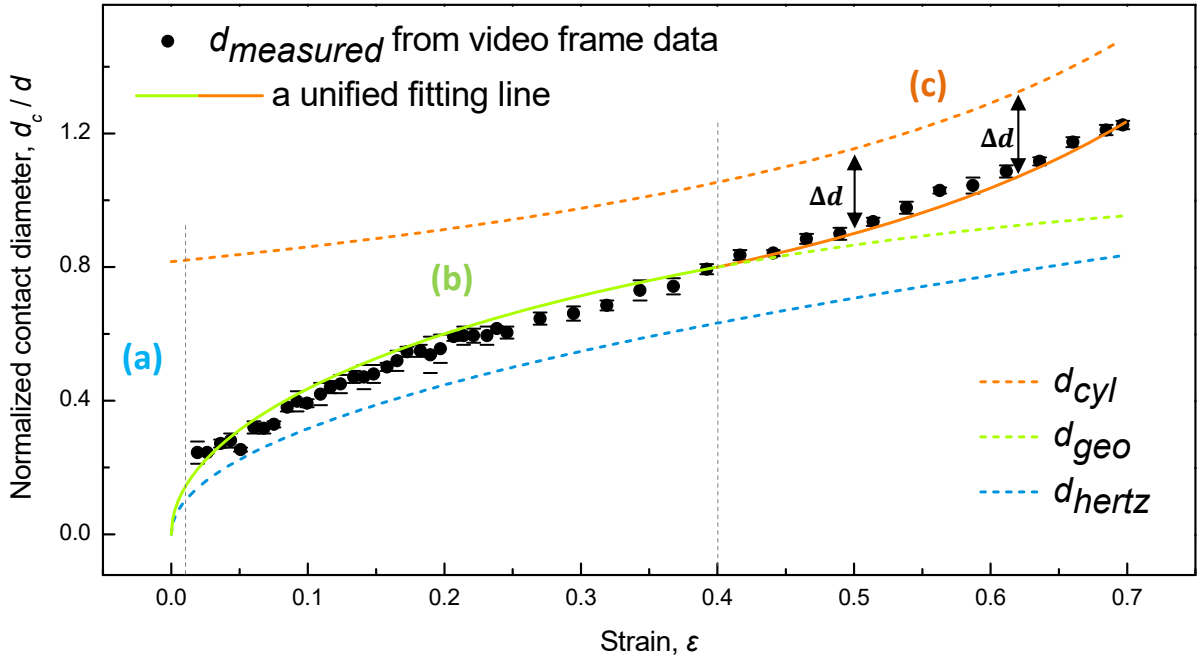

Elastic-plastic deformation stages in compression of MG nanoparticle

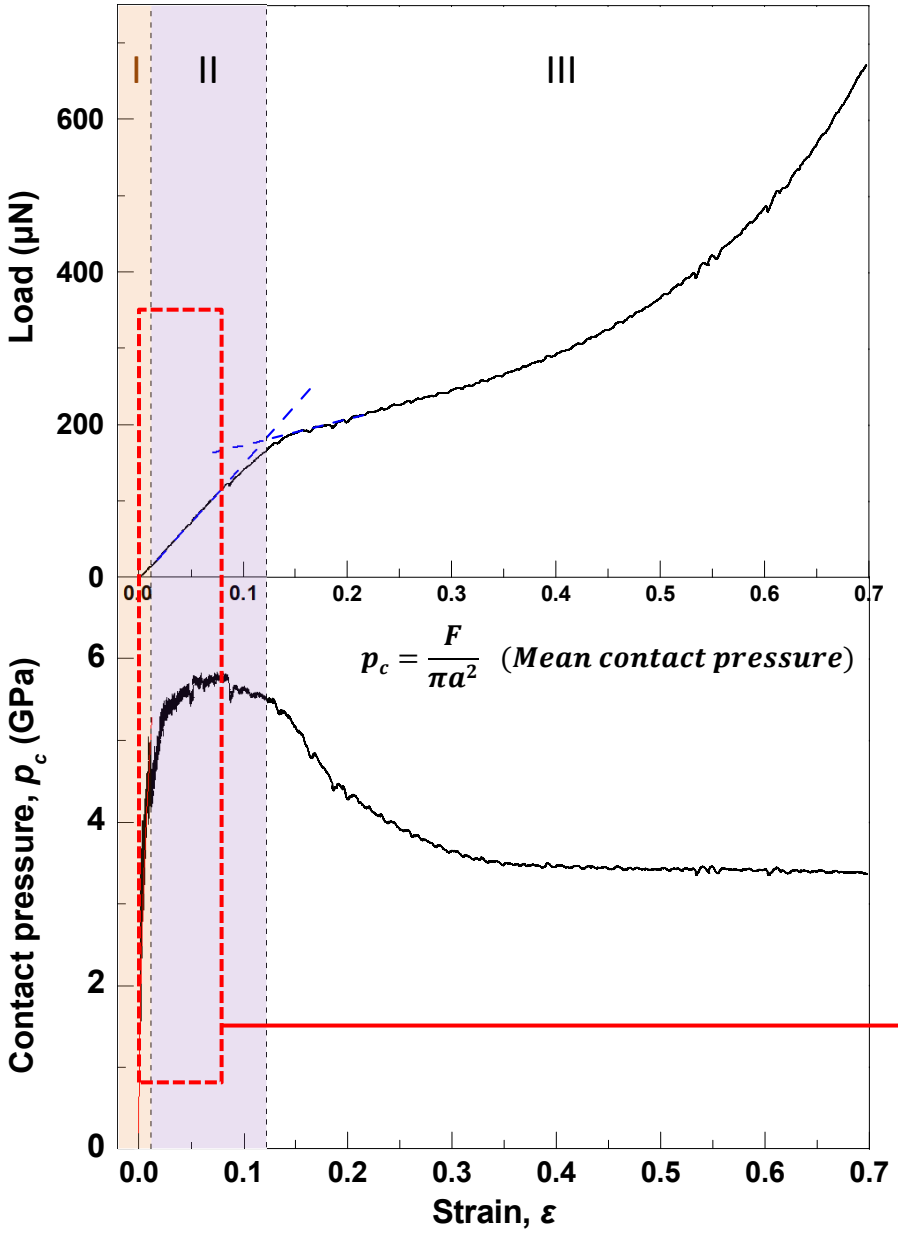

- **I. Elastic-dominant deformation**
  - Before first pop-in behavior
  - follows Hertzian contact theory
  - Non-uniform stress distribution

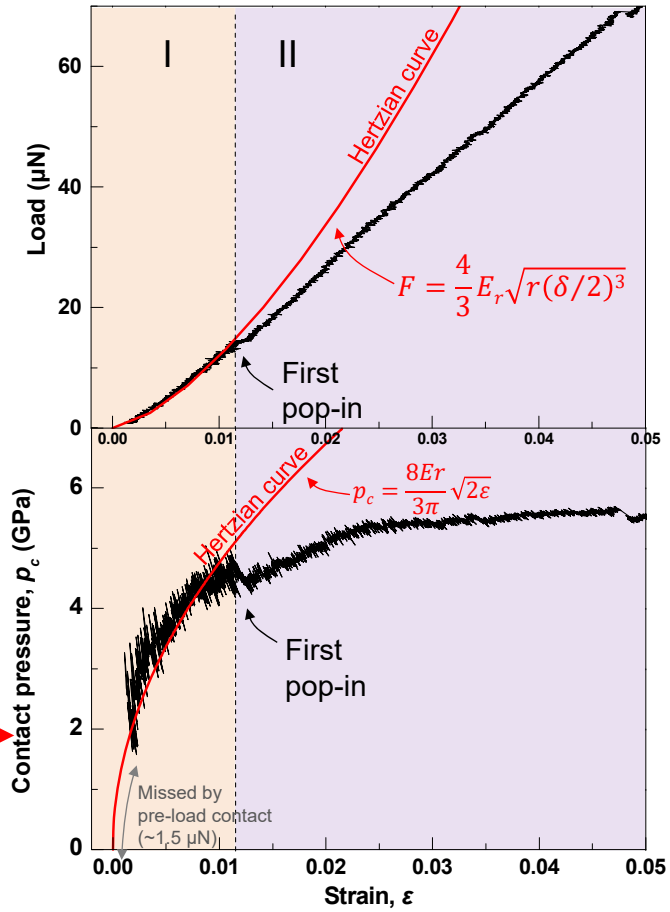

Elastic-plastic deformation stages in compression of MG nanoparticle

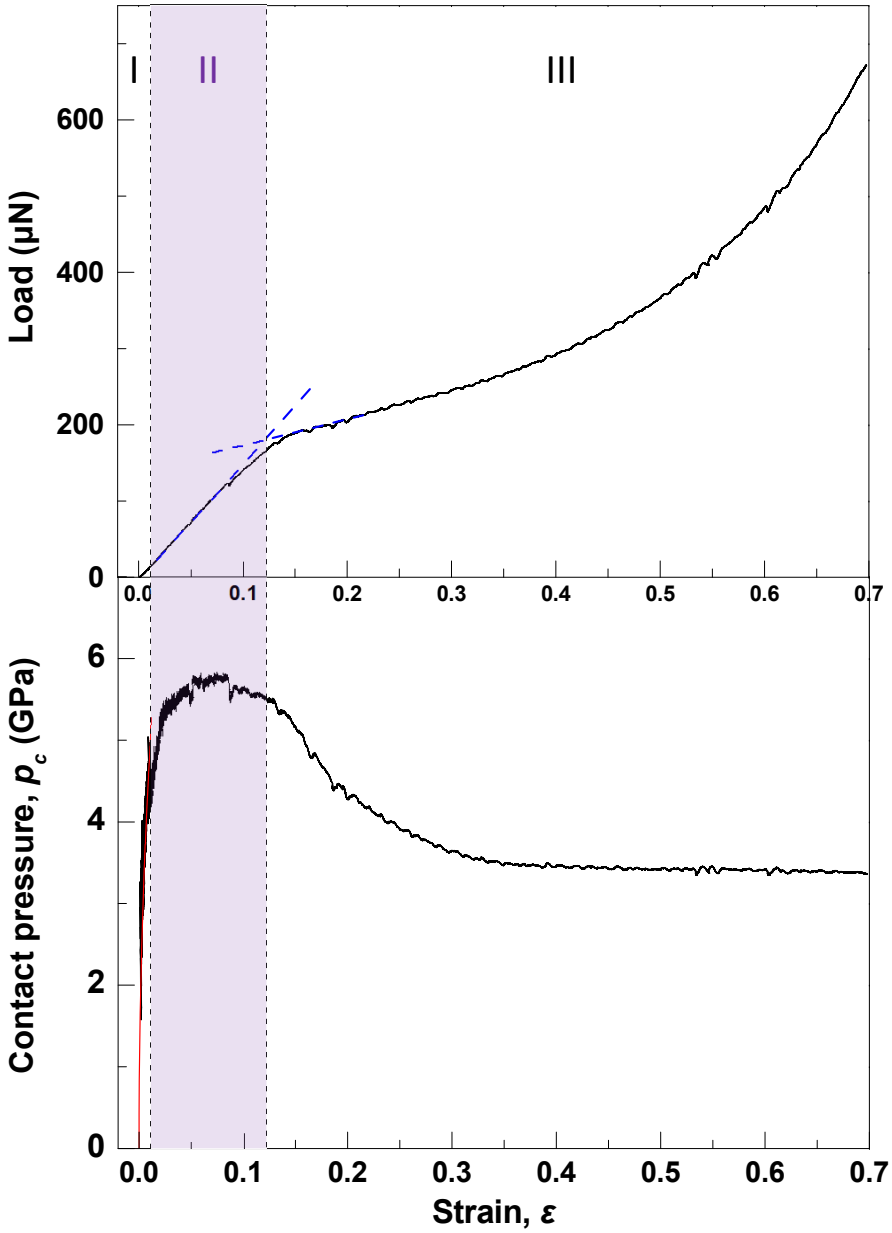

- **II. Elastic-plastic deformation**

  - Due to the inhomogeneous stress distribution, the plastic deformed zone is formed near the origin of contact circle, while near edge the elastic deformed zone is still remaining.

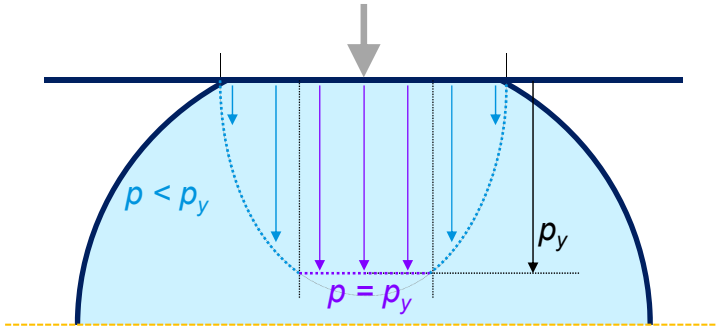

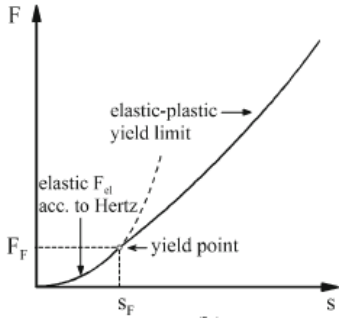

$$F_{el\_pl} = \pi r_1^2 p_F \kappa_A \varepsilon$$

p_F : *micro yield stress*
κ_A : *elastic − plastic contact ratio coefficient*

➡ Close to linear relation in load-depth plot

Antonyuk et al., Granular Matter 12 (2010) 15.

Elastic-plastic deformation stages in compression of MG nanoparticle

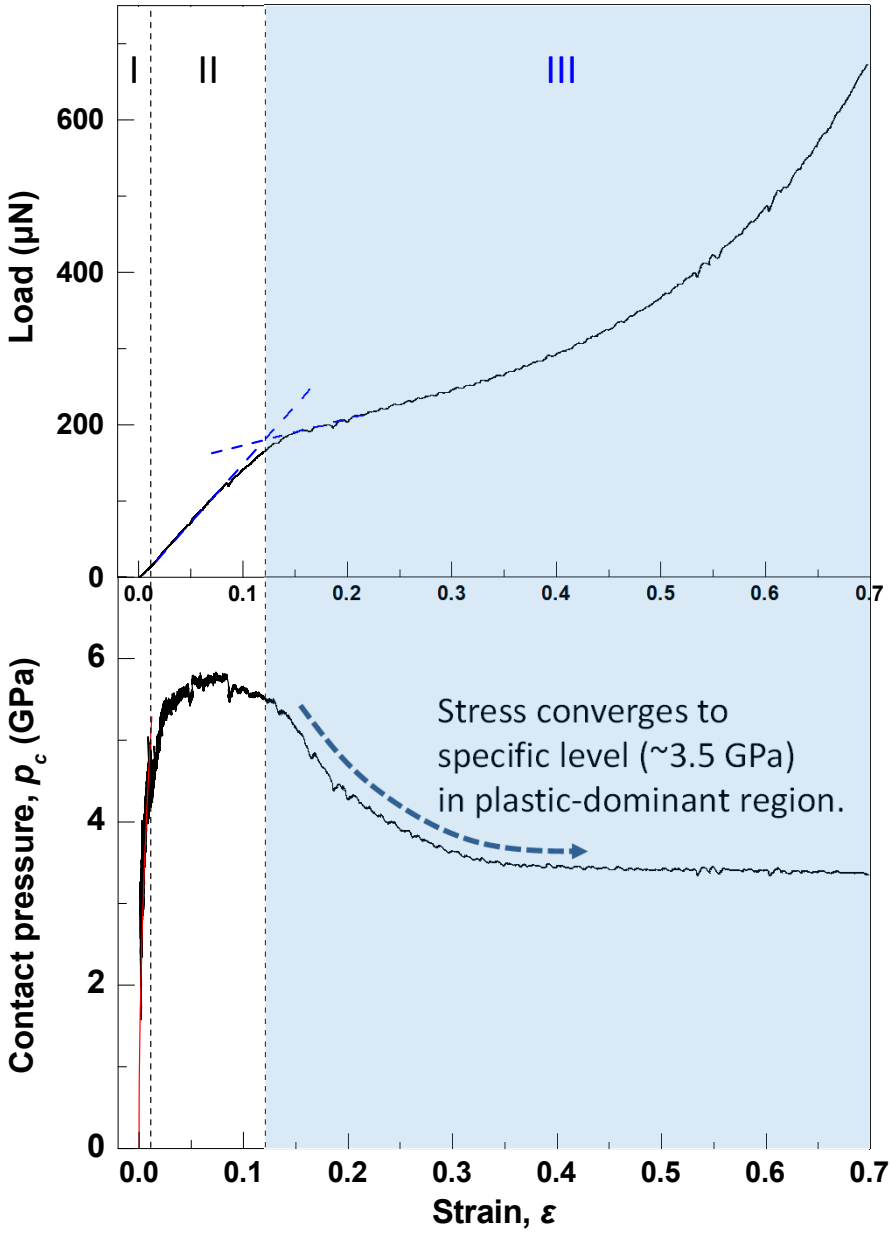

▸ III. Dominantly plastic deformation

- As compressed depth increases, the elastic range is much smaller in comparison with the plastic displacement. Finally, it can be assumed that the whole contact area deforms plastically, and stress distribution near contact becomes uniform.

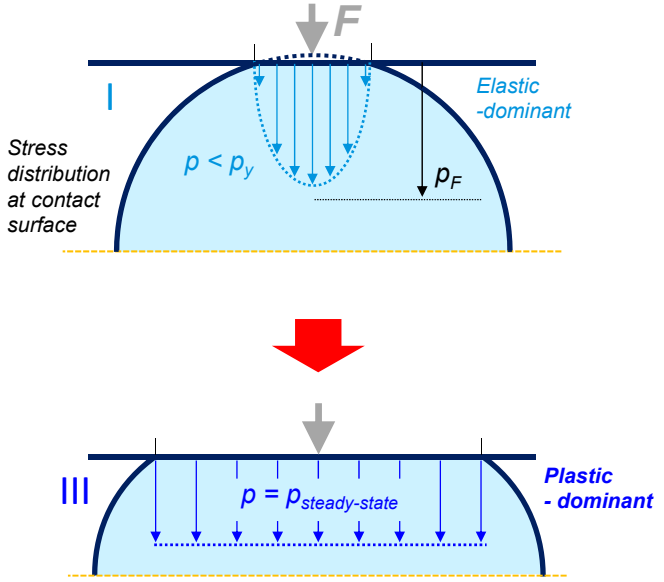

Griffith energy balance criterion for shear band formation in spherical particle

Released elastic strain energy by shear band formation

$$\Rightarrow \quad \left(\frac{{\sigma_I}^2}{2E} - \frac{{\sigma_f}^2}{2E}\right) \times V = A \cdot \Gamma$$

Wang et al., Acta Mater. 60 (2012) 5370.
Yabari et al., Phys. Rev. B 82 (2010) 172202.

V : sample volume
A : Area of a shear band
Γ : Shear band energy per unit area

$\Gamma \approx t\mu\gamma_c$, where t = shear band thickness
μ = shear modulus
γ_c = characteristic shear strain ~ 0.037

- **For spherical particle-type sample, compressed depth dependence of σ_c**

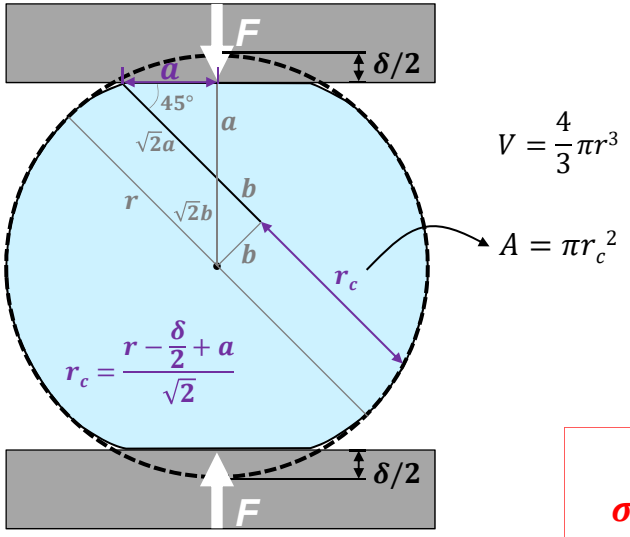

$$V = \frac{4}{3}\pi r^3$$

$$A = \pi {r_c}^2$$

$$\left(\frac{\sigma_{SB}^2(r)}{2E} - \frac{\sigma_0^2}{2E}\right) \times \frac{4}{3}\pi r^3 = \pi r_c^2 \Gamma$$

$$r_c = \frac{1}{\sqrt{2}}\left(r - \frac{\delta}{2} + a\right) = \frac{r}{\sqrt{2}}\varepsilon' \qquad (\varepsilon' = 1 - \varepsilon + a/r)$$

$$Contact\ radius, \qquad a = \begin{cases} a_{geo} \ at \ \varepsilon \le 0.4 \\ a_{cyl} \ at \ \varepsilon \ge 0.4 \end{cases}$$

$$\boldsymbol{\sigma_{SB}(d,\varepsilon) = \sqrt{\sigma_0^2 + \frac{3E}{2d}(\varepsilon')^2 \cdot \Gamma}}$$

(critical stress for shear band formation)

** for uniform-stress state in plastic-dominant region

I. Homogeneous flow in plastic-dominant deformation stage

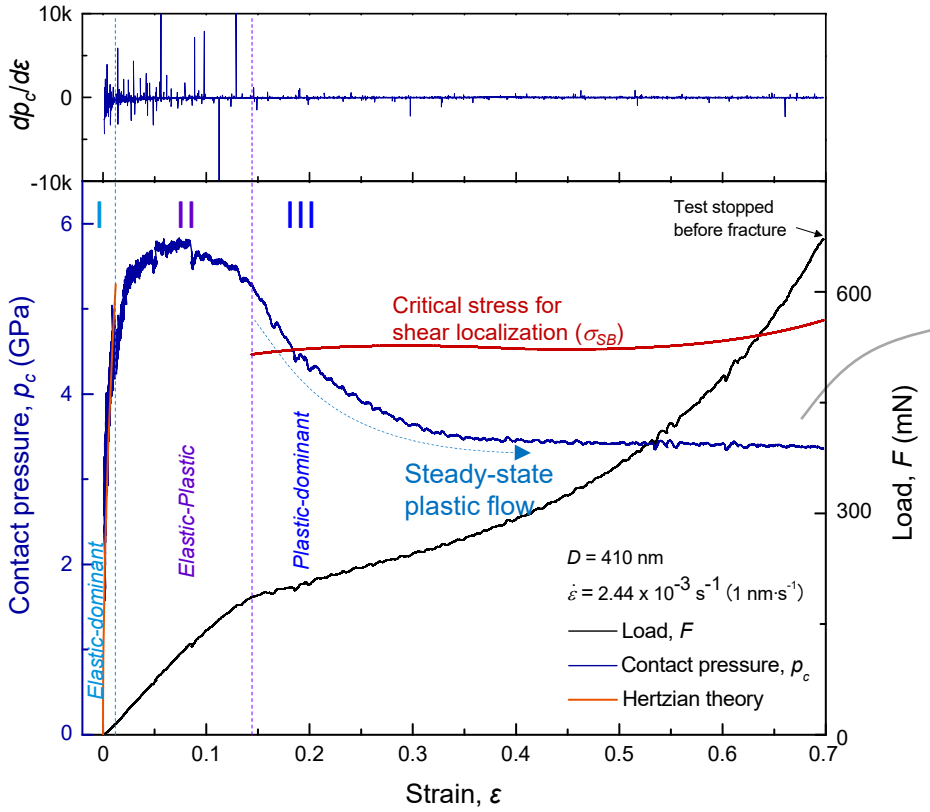

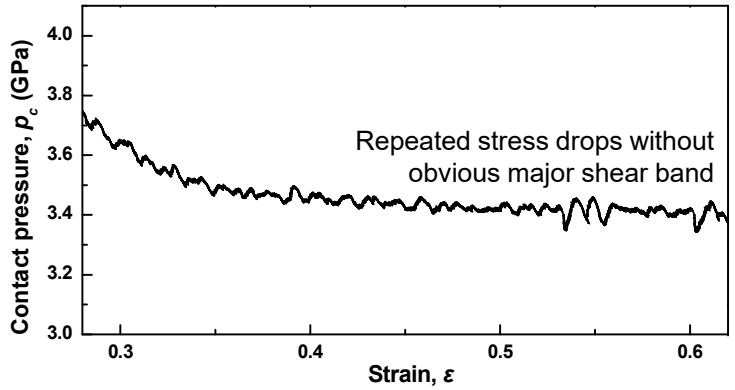

(1) Friction effect between particle and diamond tip

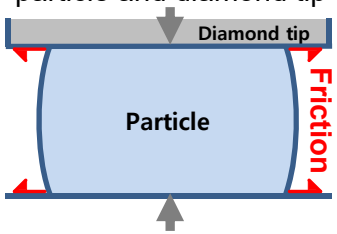

(2) Formation of multiple infinitesimal shear transformation

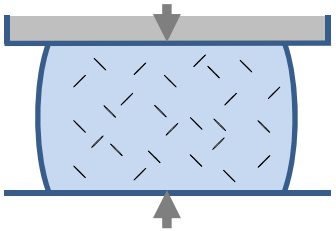

- At $\varepsilon > 0.3$, homogeneous plastic flow occurs with constant pressure level

  (1) The steady-state stress level is lower than theoretical critical stress for shear band propagation.

  (2) The amount of each abrupt stress drop decreases with being close to plastic-dominant deformation region.

  (3) The particle was compressed without fracture up to $\varepsilon = 0.7$ *through the homogeneous plastic deformation*.

Molecular dynamics (MD) simulation of MG nanoparticle compression

- $Cu_{64}Zr_{36}$ binary metallic glass : a simple model metallic glass system
- Periodic boundary conditions : non-periodic
- Particle size : 20 nm / Strain rate: 10^8 s^{-1}

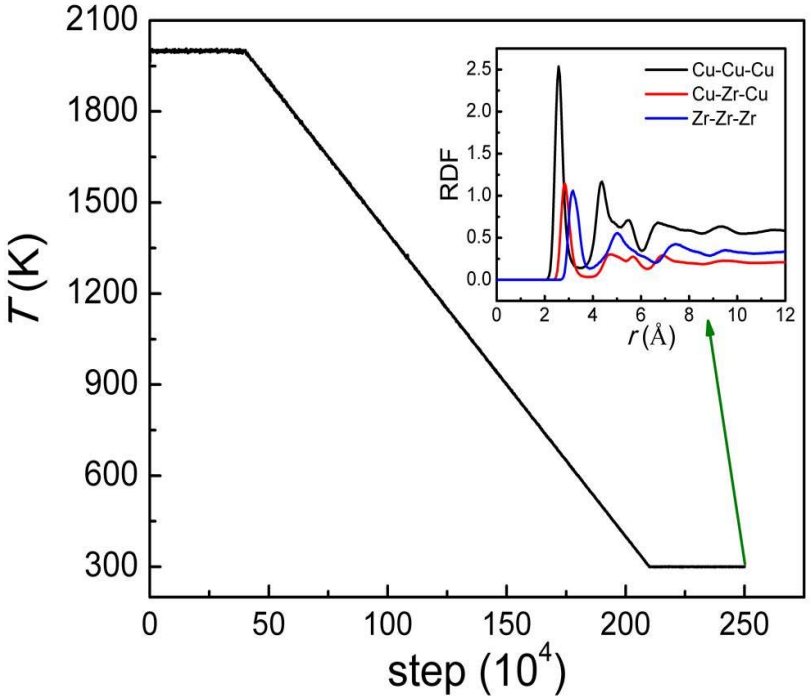

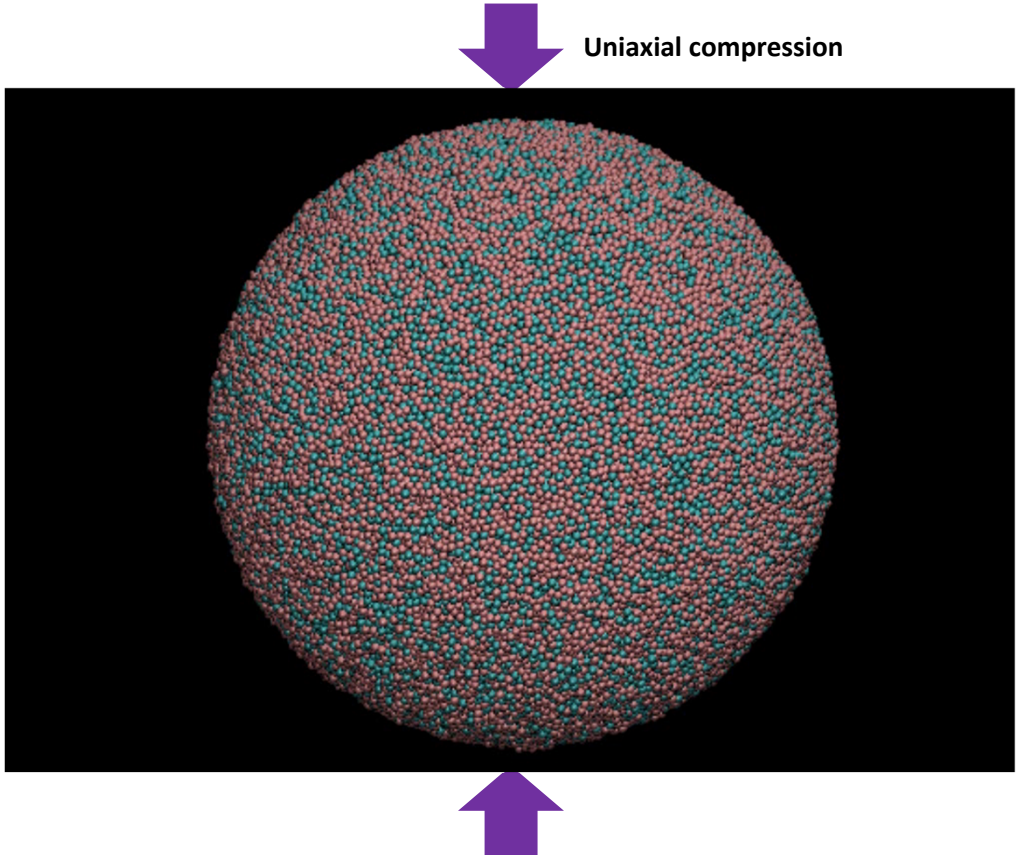

Atomic local shear strain distribution during MG nanoparticle compression

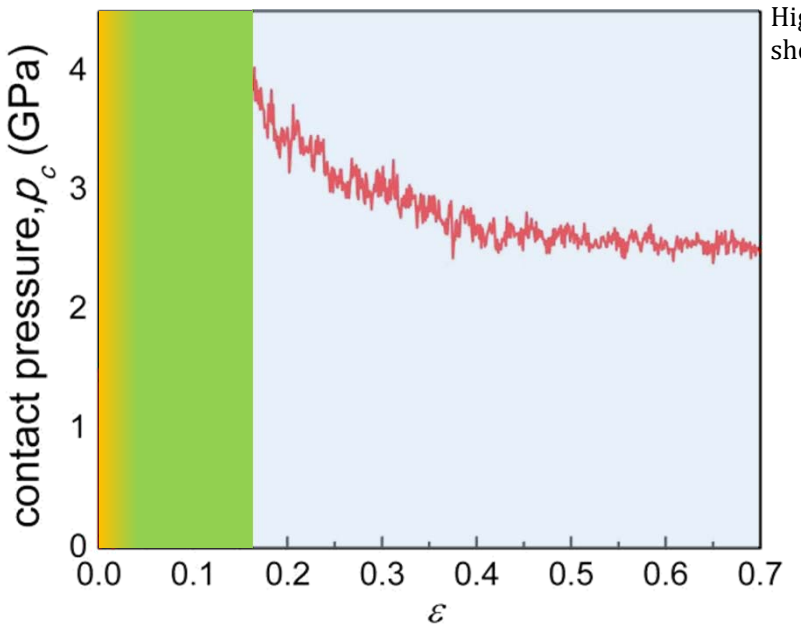

High local atomic shear strain zone

$\eta^{Mises} > 0.6$

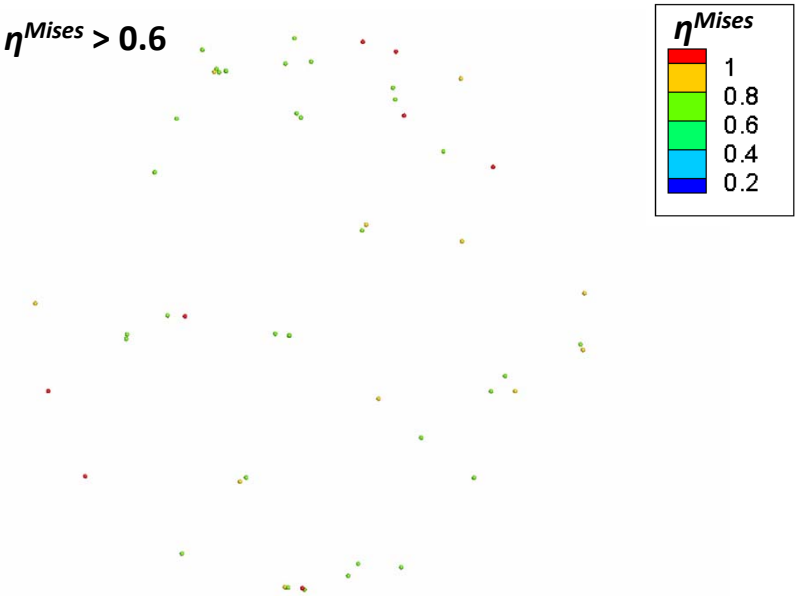

Surface view

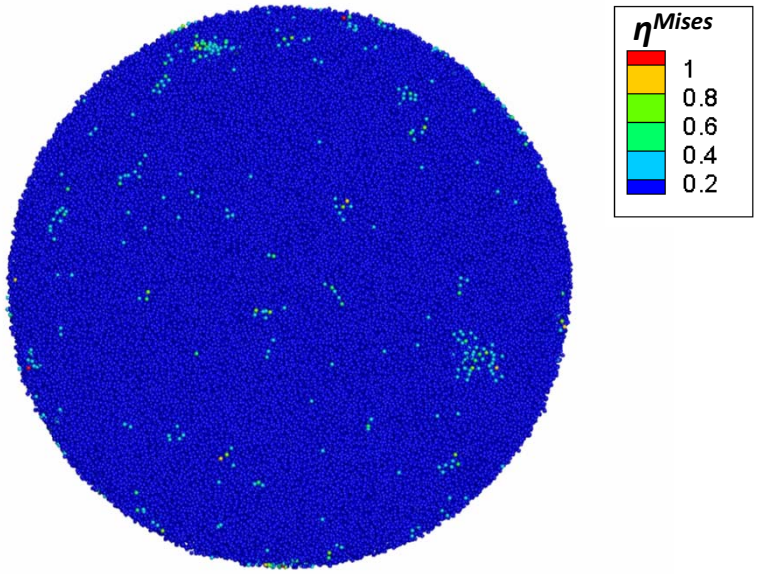

Cross-section view

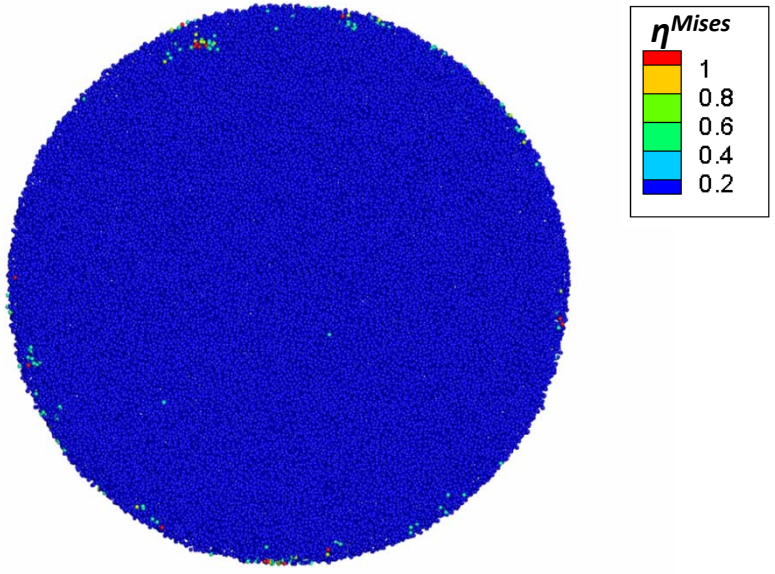

Atomic local shear strain distribution depending on strain

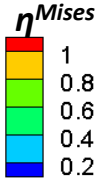

The transition of strain distribution <u>from localization to "uniform state"</u> is well described from atomic shear strain analysis.

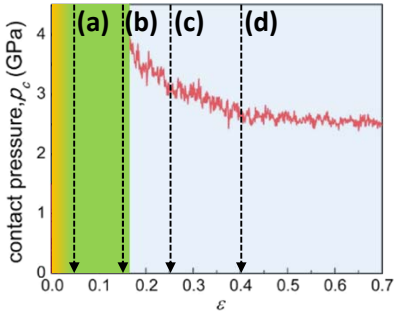

(a) ε = 0.05 **(b) ε = 0.15** **(c) ε = 0.25** **(d) ε = 0.40**

η^{Mises} > 0.6
High local atomic shear strain zone

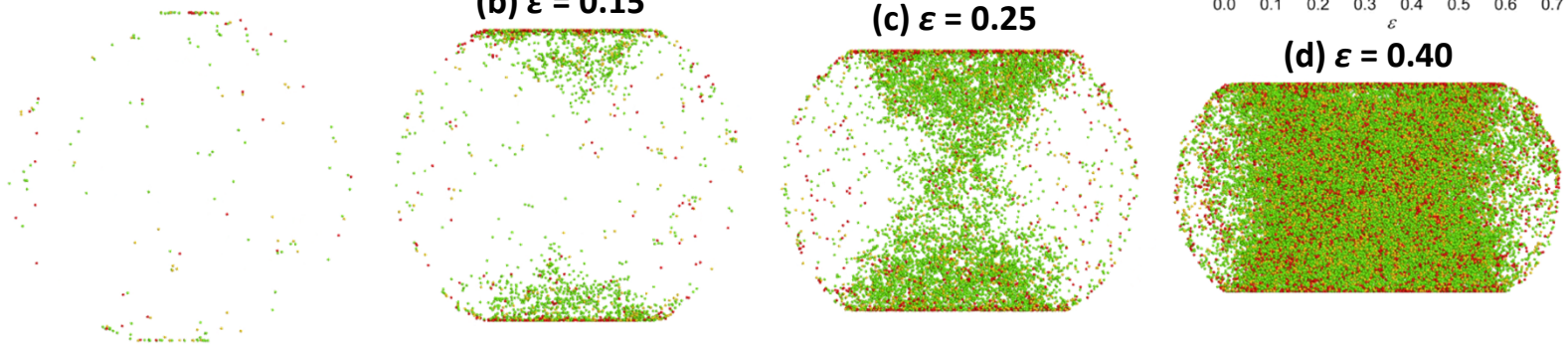

Surface view

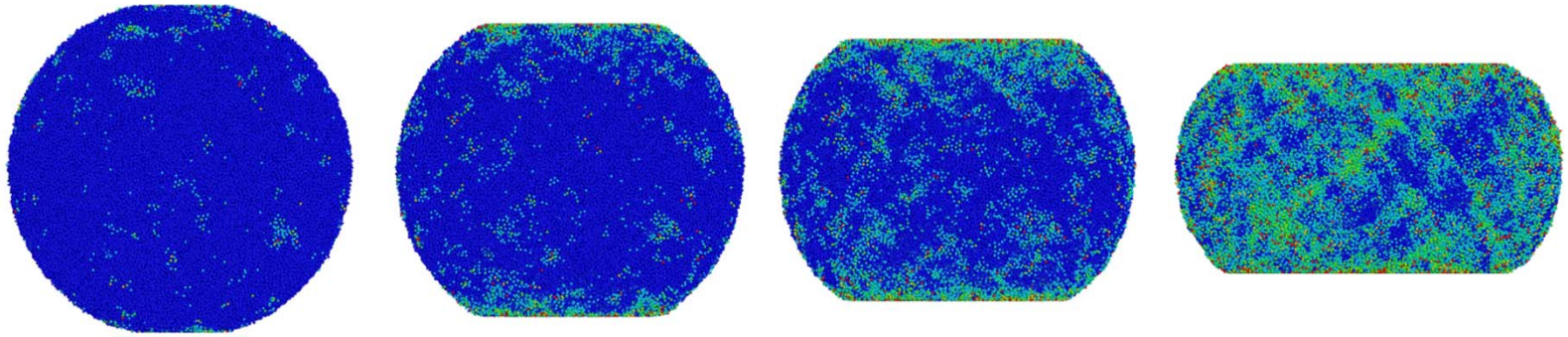

Cross-section view

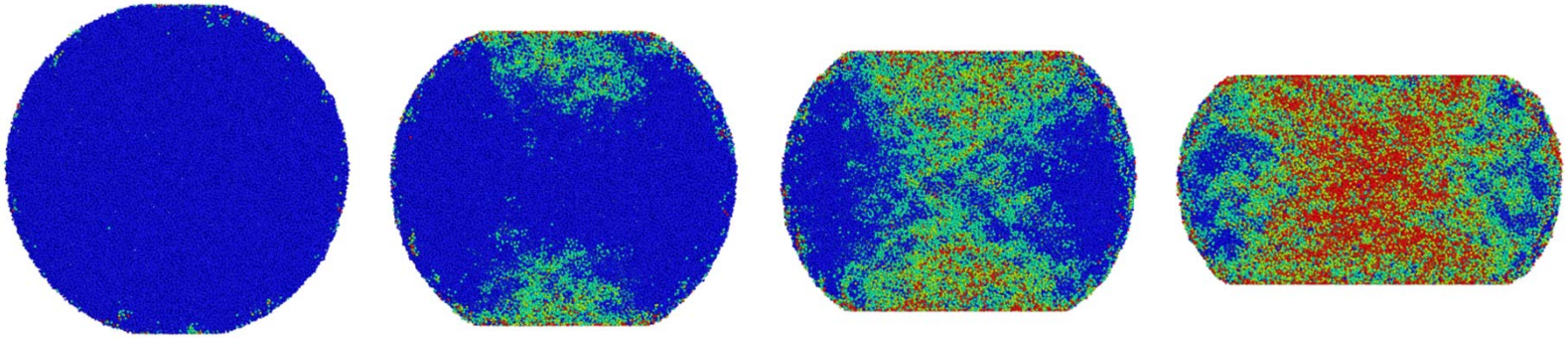

Flow behavior classification : Newtonian flow v.s. Non-Newtonian flow

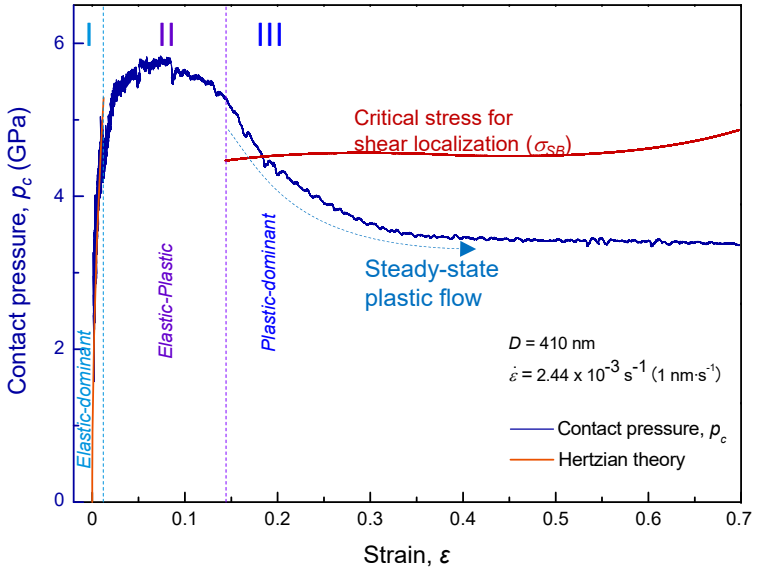

← $\sigma_{steady\text{-}state}$

(Flow stress of steady-state homogeneous flow)

➡

Flow stress dependence on strain rate decides characteristics of viscous behavior.

- Classification of viscous behavior

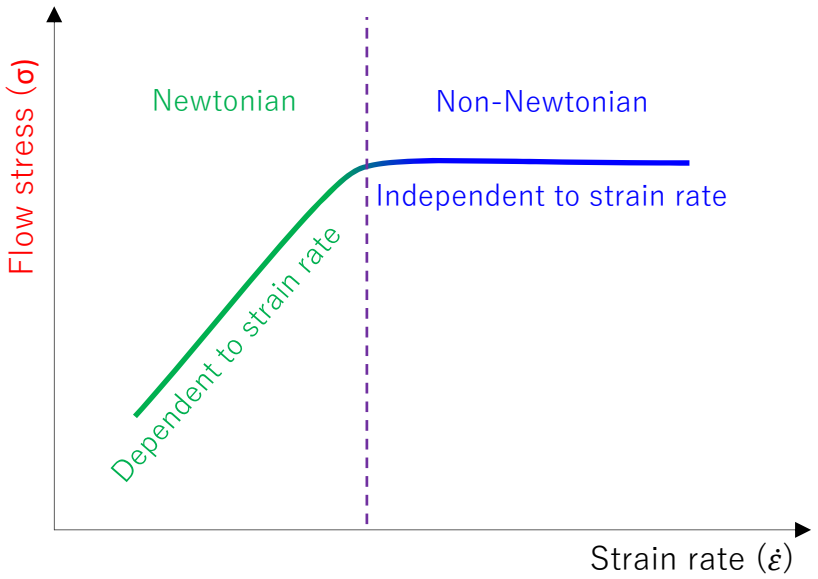

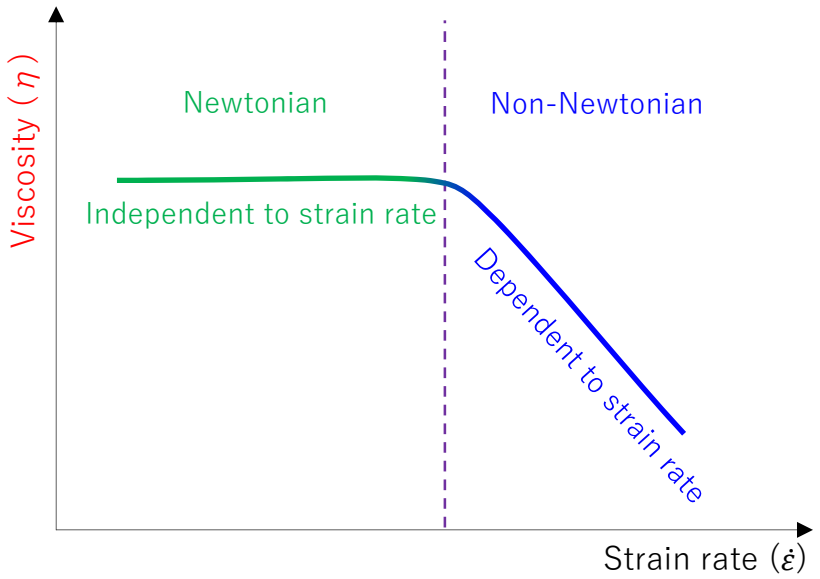

Independency of steady-state flow stress on particle size and strain rate

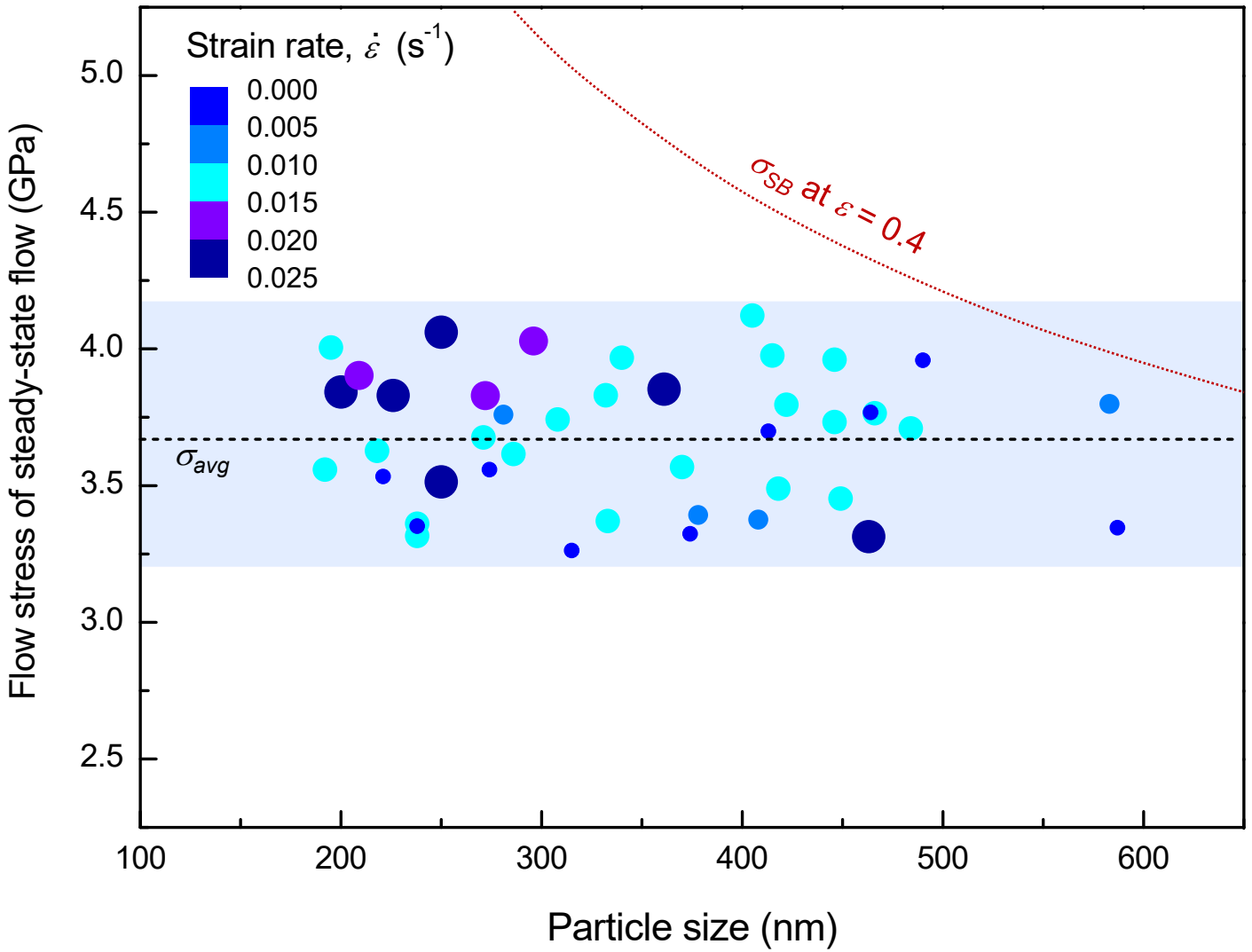

Flow stress of steady-state flow → independent from particle size and strain rate

Effect of particle size and strain rate on steady-state stress: Non-Newtonian flow

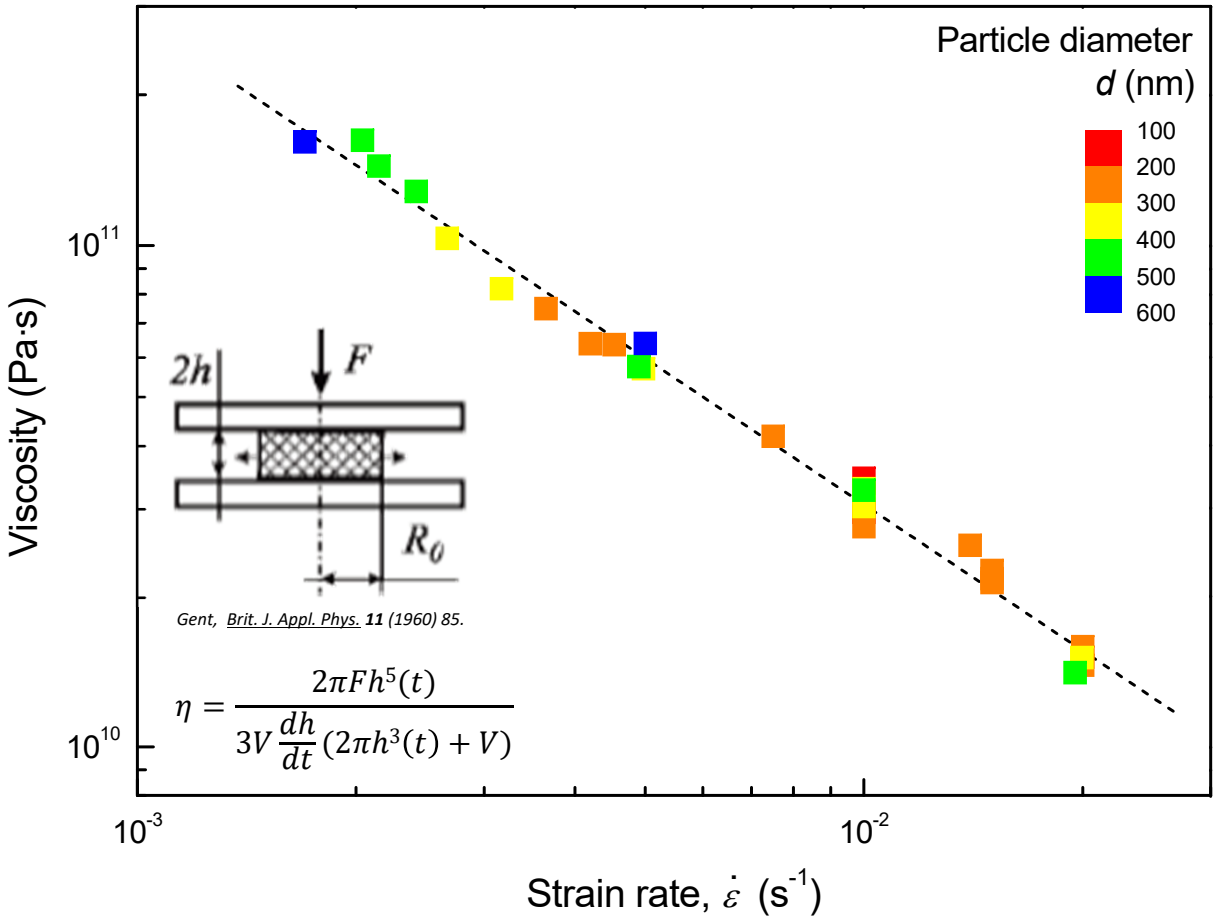

Viscosity of steady-state flow → Decreased with increasing strain rate, independent from particle size

➡ **Homogeneous deformation of nanoscale metallic glass : II. Non-Newtonian viscous flow**

(Metallic glass near glass transition temperature (T_g) : Newtonian flow behavior)

Non-Newtonian homogeneous flow of nanoscale metallic glasses

Can the nanoscale metallic glasses **flow as the high-T supercooled liquid state** ?

Nanoscale metallic glass at RT

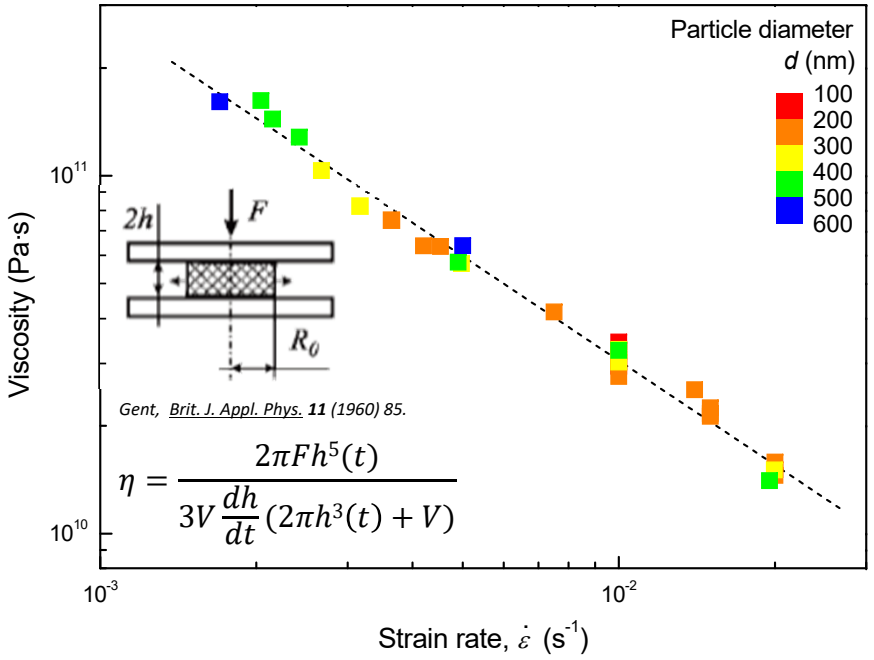

Non-Newtonian homogeneous flow

of nanoscale metallic glass

Bulk MG at near supercooled liquid region

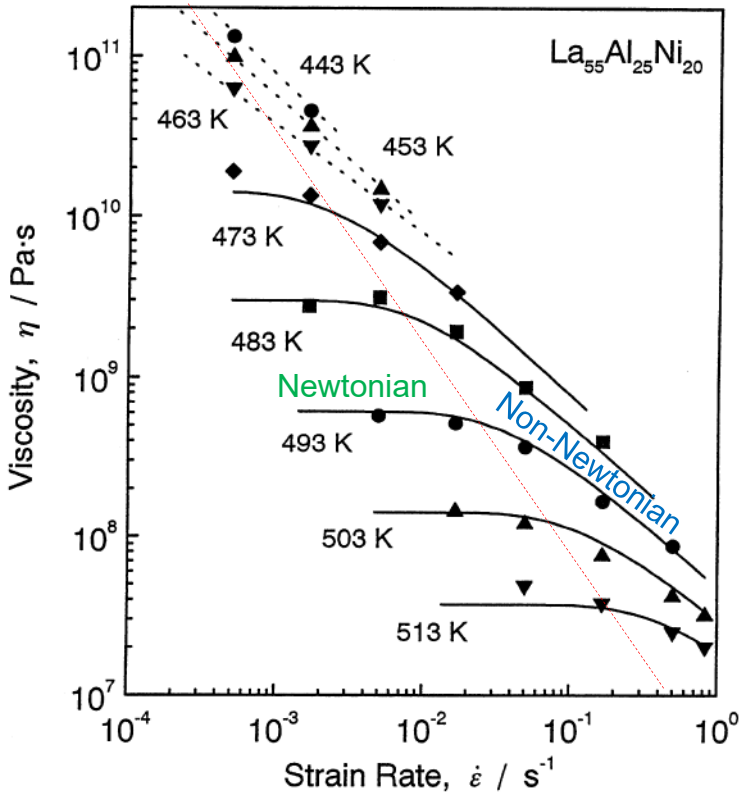

Strain rate-dependent flow behavior

(Transition between Newtonian and Non-Newtonian homogeneous flow)

Deformation-mechanism maps for materials

Diagrams displaying the dominant deformation mechanisms of materials under extrinsic conditions as stress, temperature, or strain rate

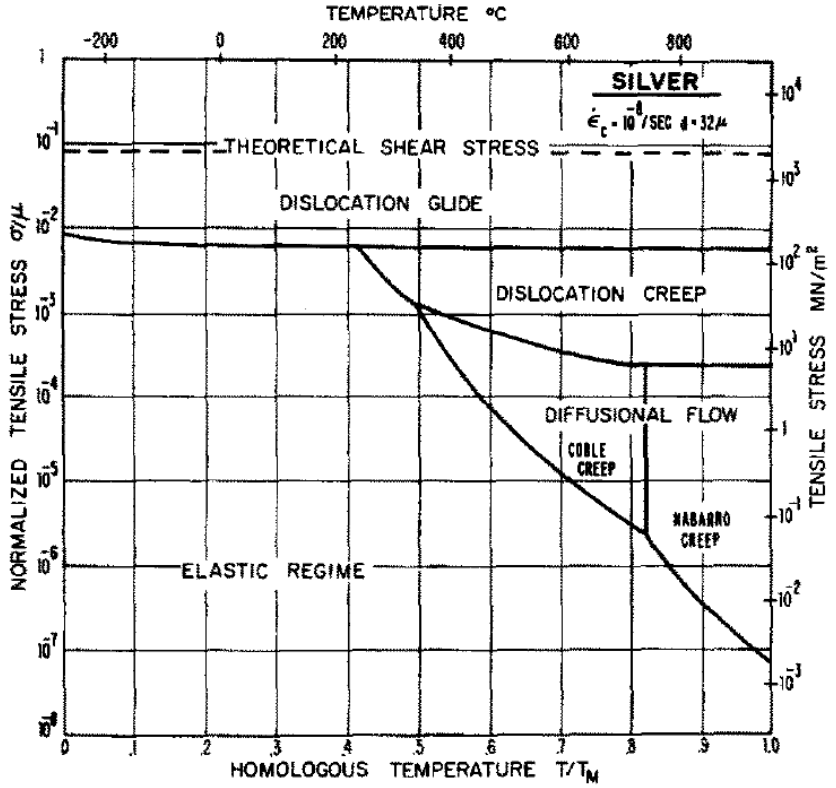

FIG. 1. A deformation–mechanism map for pure silver, of grain size 32 μ, and for a critical strain rate $\dot{\varepsilon}_c$ of 10^{-8}/sec.

Constitutive laws (rate equations) + Parameters from experimental data

Ashby, Acta Metull. 20 (1972) 887.

"Deformation map" for metallic glasses

representing the deformation mode depending on extrinsic factors
since the plastic deformation of MG is governed by a single mechanism
(an elementary plastic unit of shear transformation)

Spaepen, Acta Metall. (1977)

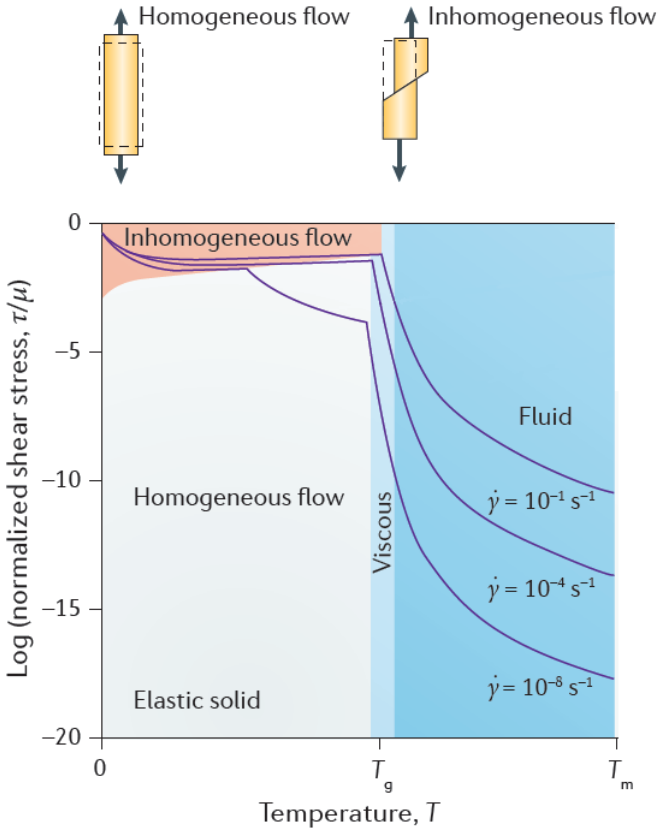

Schuh et al., Acta Mater. (2007)

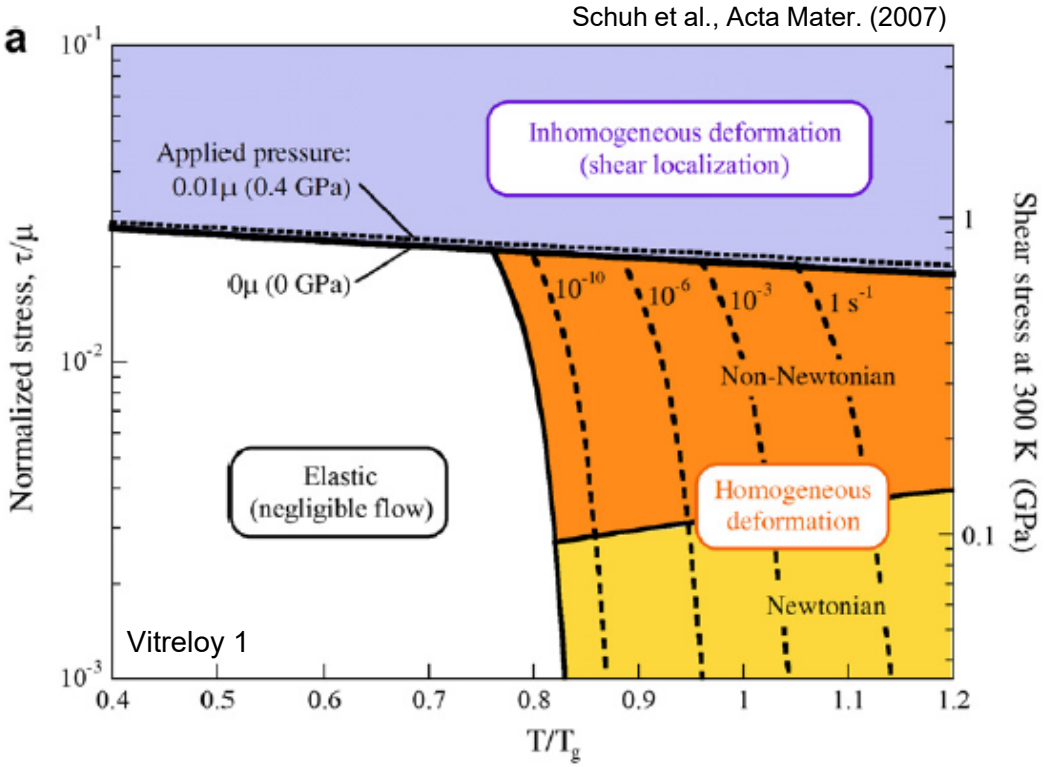

"Deformation map" for nanoscale metallic glasses

Based on Shear transformation zone (STZ) model as a constitutive equation,

1) Transition boundary between **Newtonian and non-Newtonian flow behavior**

2) **Iso-viscosity contours** representing stress and temperature effect on viscosity

3) **Critical stress curves for shear banding** reflecting **the sample size effects**

Constitutive equation for metallic glass : Shear Transformation Zone (STZ) model

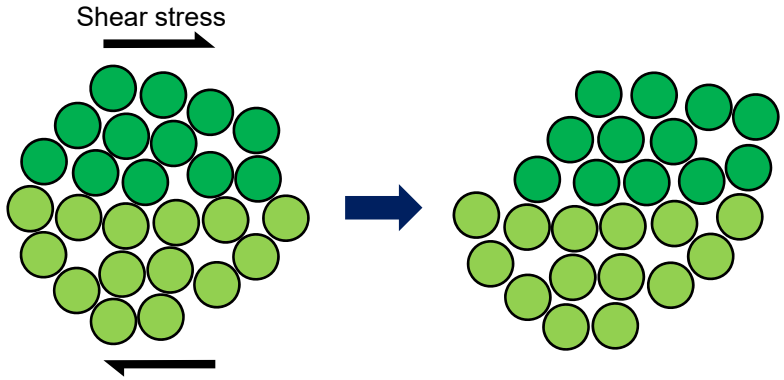

In a steady-state flow condition,

$$\dot{\gamma} = \underbrace{\alpha_0 \nu_0 \gamma_0}_{(1)} \underbrace{\exp\left(-\frac{Q}{kT}\right)}_{(2)} \underbrace{\sinh\left(\frac{\tau V}{kT}\right)}_{(3)}$$

Activation energy

Activation volume

(1) Product of constants

(2) Related to **activation energy** of the process

(3) The **net rate** of forward & backward operations

α_0: numerical constant
ν_0: frequency of the fundamental mode vibration
γ_0: characteristic strain for operation of STZ
k : Boltzmann constant
$V = \gamma_0 \Omega_0$ where Ω_0 is the volume of STZ

Argon, Acta Metull. 27 (1979) 47.
Schuh et al., Acta Mater. 55 (2007) 2067.

Determination of T range for high-T tensile creep test

From the melt-spun ribbon of the same composition with the nanoparticles

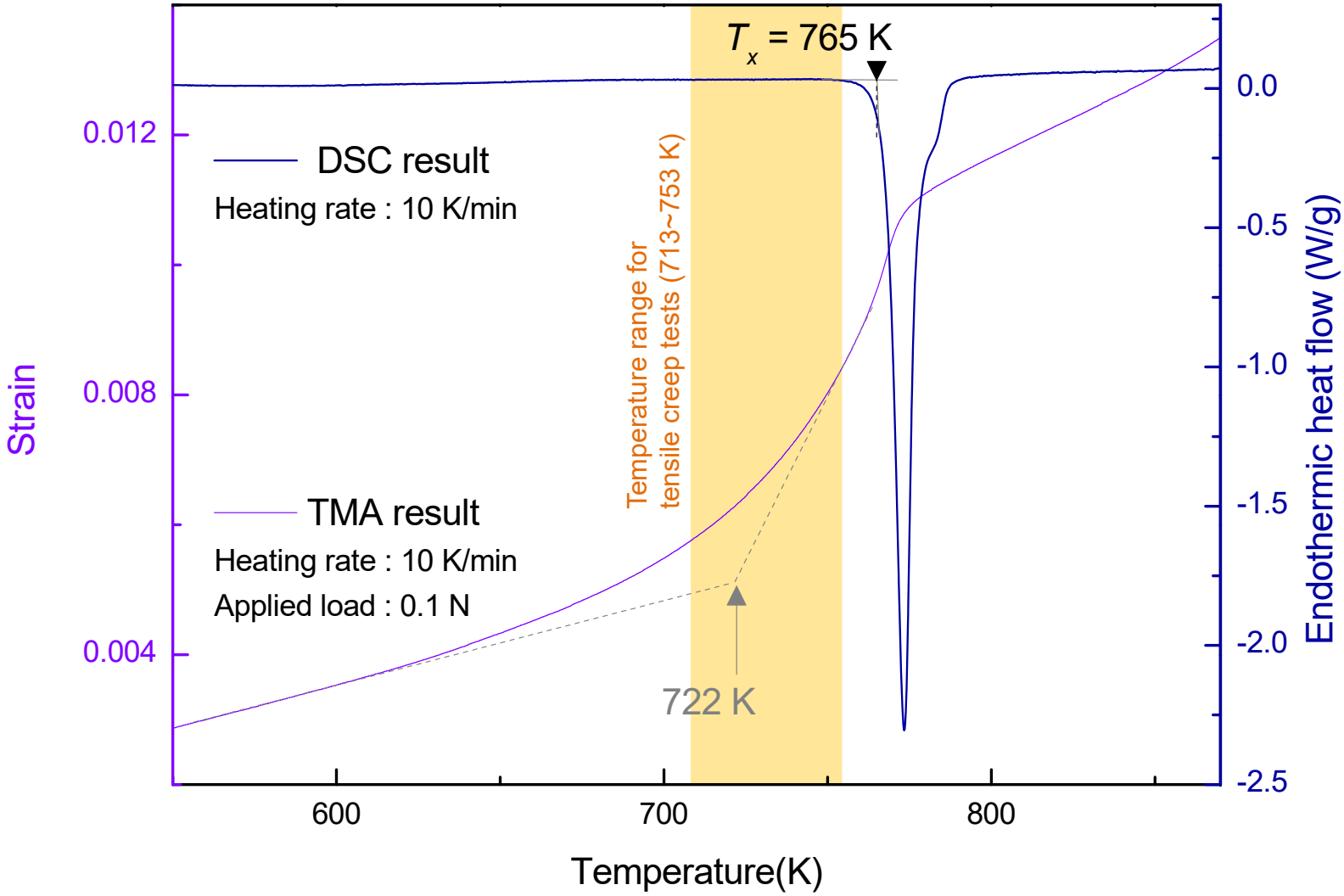

High-T tensile creep test of micro-ribbon samples

TMA tensile mode apparatus

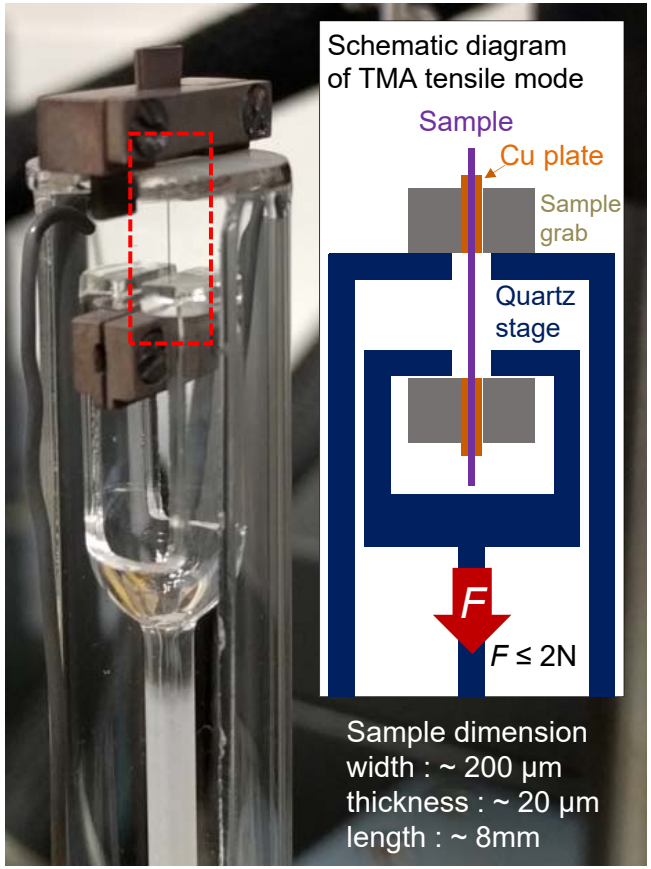

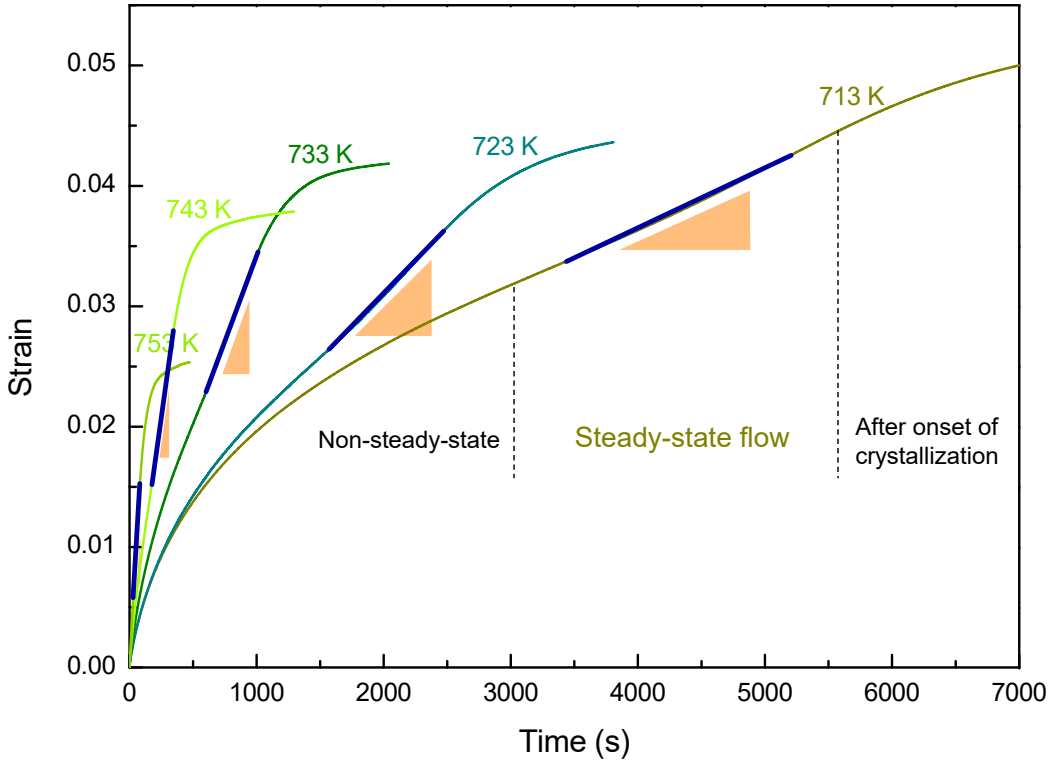

Steady-state flow region		
T (K)	Stress (MPa)	Strain rate (s^{-1})
713	250	5.20×10^{-6}
723	250	1.13×10^{-5}
733	250	2.95×10^{-5}
743	250	7.59×10^{-5}
753	250	1.84×10^{-4}

Strain rate - stress relation in steady-state homogeneous flow

For a uniaxial tensile mode,

$$\dot{\varepsilon} = \alpha'_0 \nu_0 \gamma_0 \exp\left(-\frac{Q}{kT}\right) \sinh\left(\frac{\sigma V}{\sqrt{3}kT}\right)$$

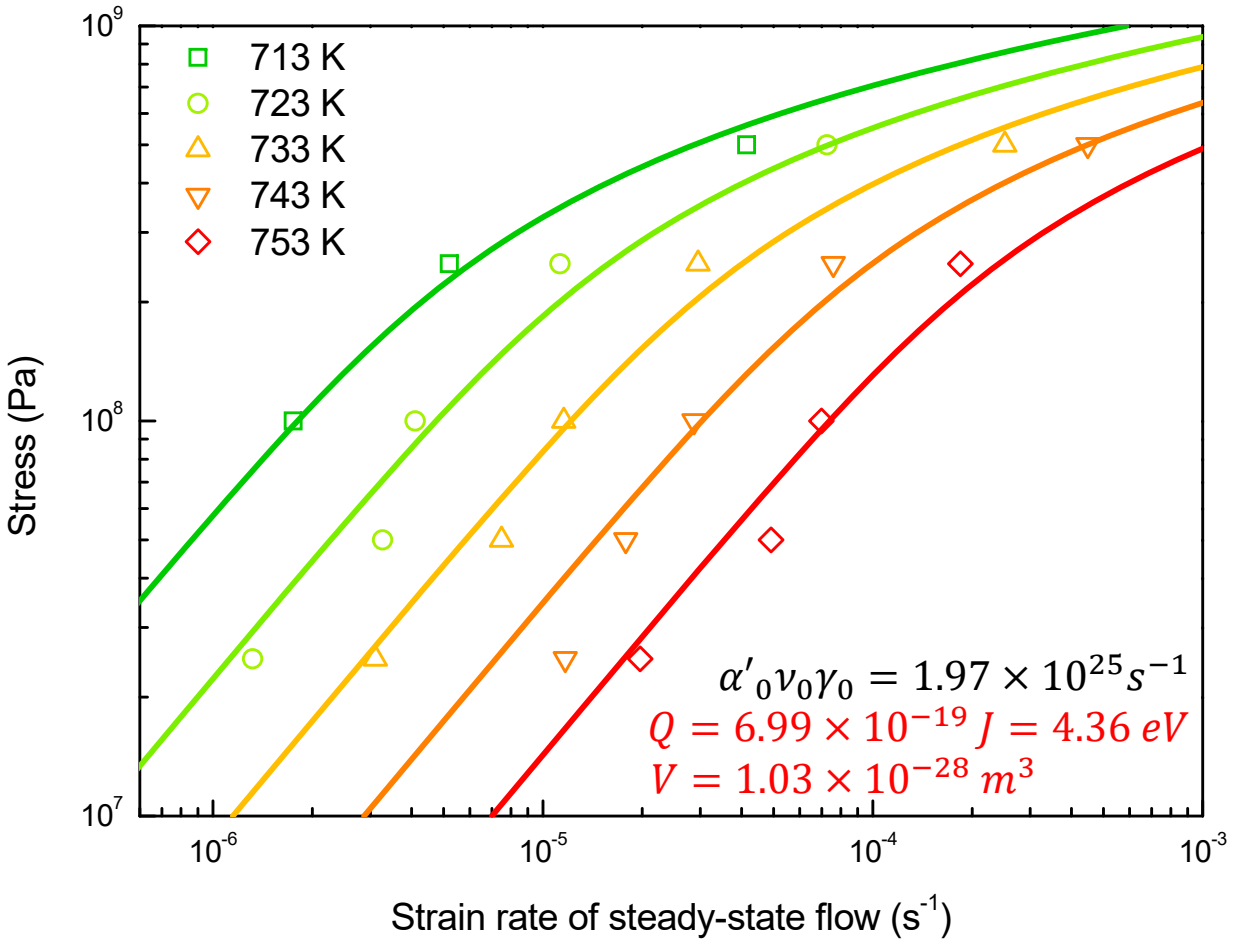

(1) Transition boundary of Newtonian-to-Non-Newtonian homogeneous flow

For a steady-state flow,

$$\dot{\gamma} = \alpha_0 \nu_0 \gamma_0 \exp\left(-\frac{Q}{kT}\right) \sinh\left(\frac{\tau V}{kT}\right)$$

$\tau \ll kT/V$

$$\dot{\gamma} = \frac{\alpha_0 \nu_0 \gamma_0 V}{kT} \exp\left(-\frac{Q}{kT}\right) \tau$$

➡ $\dot{\gamma} \propto \tau$ *at constant T*

Newtonian flow

$\tau \gg kT/V$

$$\dot{\gamma} = \frac{\alpha_0 \nu_0 \gamma_0}{2} \exp\left(-\frac{Q - \tau V}{kT}\right)$$

Non-Newtonian flow

Boundary : $\tau = kT/V$

(or $\sigma = \sqrt{3}kT/V$ for uniaxial case)

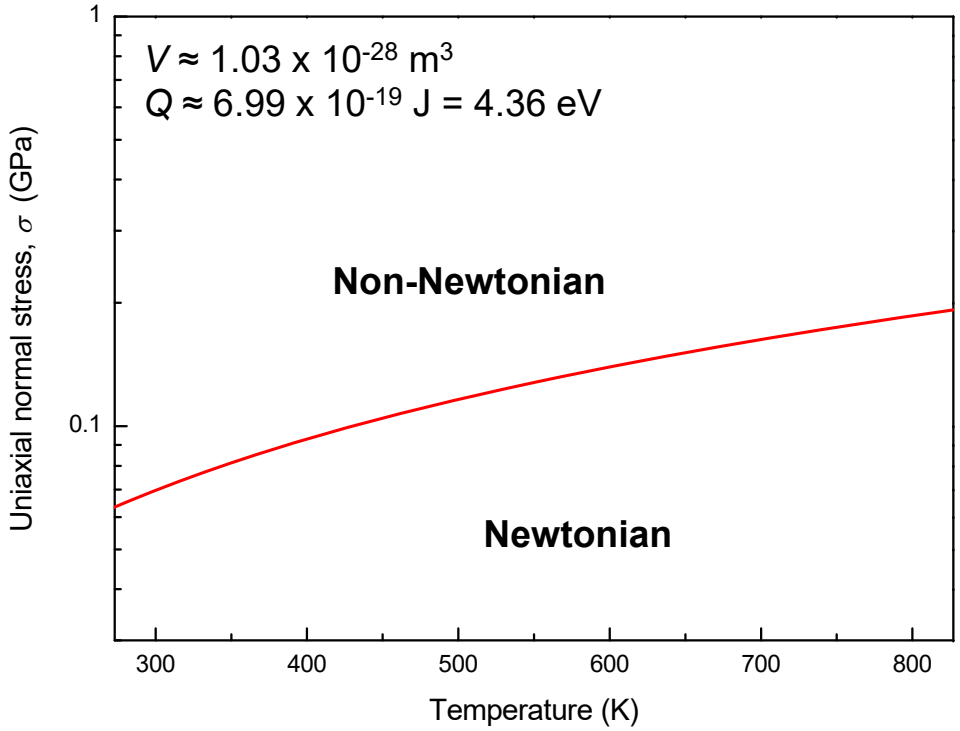

Mechanically induced viscosity drop in metallic glass

Temperature-stress scaling for constant viscosity

$$\frac{T}{T_0(\eta)} + \left(\frac{\sigma}{\sigma_0(\eta)}\right)^2 = 1$$

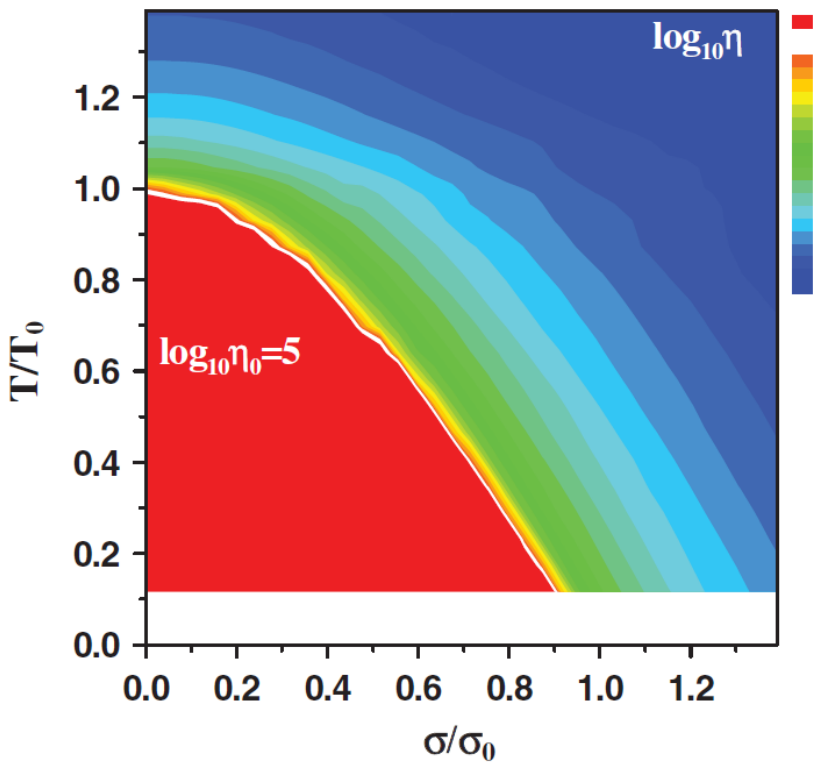

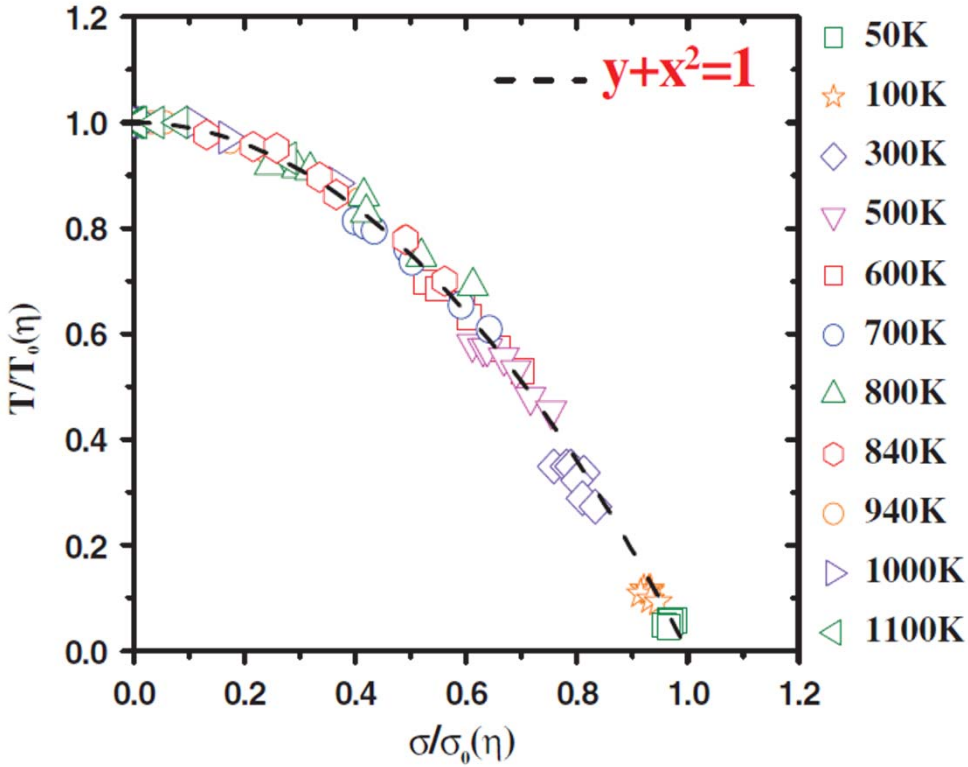

Applied shear stress has the equivalent effect as temperature in reducing the viscosity and inducing mechanical flow.

Guan et al., Phys. Rev. Lett. 104 (2010) 205701.

(2) Iso-viscosity contours in stress-temperature relation

$$\eta = \frac{\sigma}{3\dot{\varepsilon}} \quad (Trouton's\ law)$$

$$\dot{\varepsilon} = \alpha'_0 \nu_0 \gamma_0 \exp\left(-\frac{Q}{kT}\right) \sinh\left(\frac{\sigma V}{\sqrt{3}kT}\right)$$

$$\frac{T}{T_0(\eta)} + \left(\frac{\sigma}{\sigma_0(\eta)}\right) = 1$$

Stress-Temperature data point for specific viscosity value

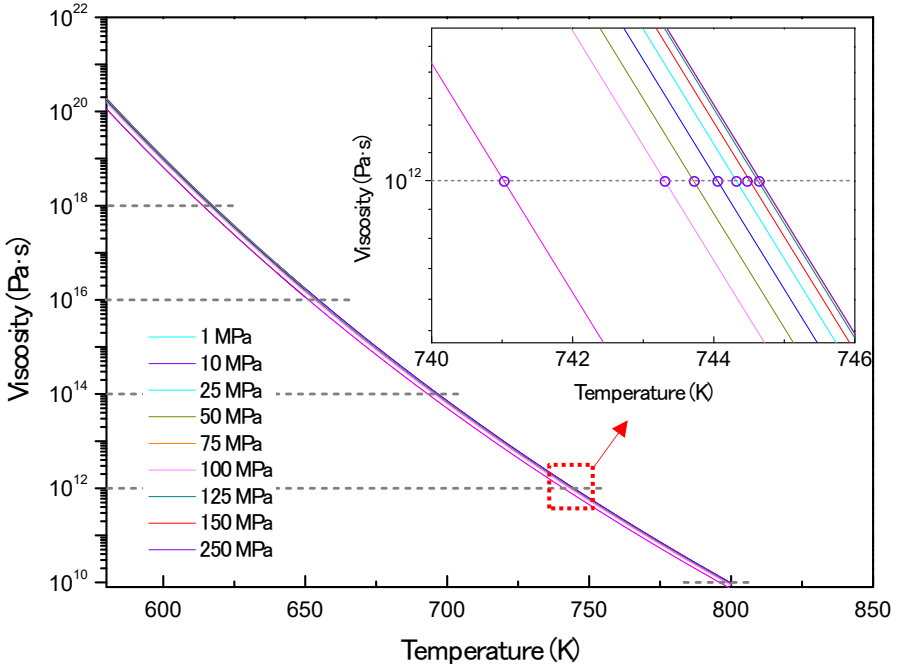

Iso-viscosity contours in stress-temperature plot

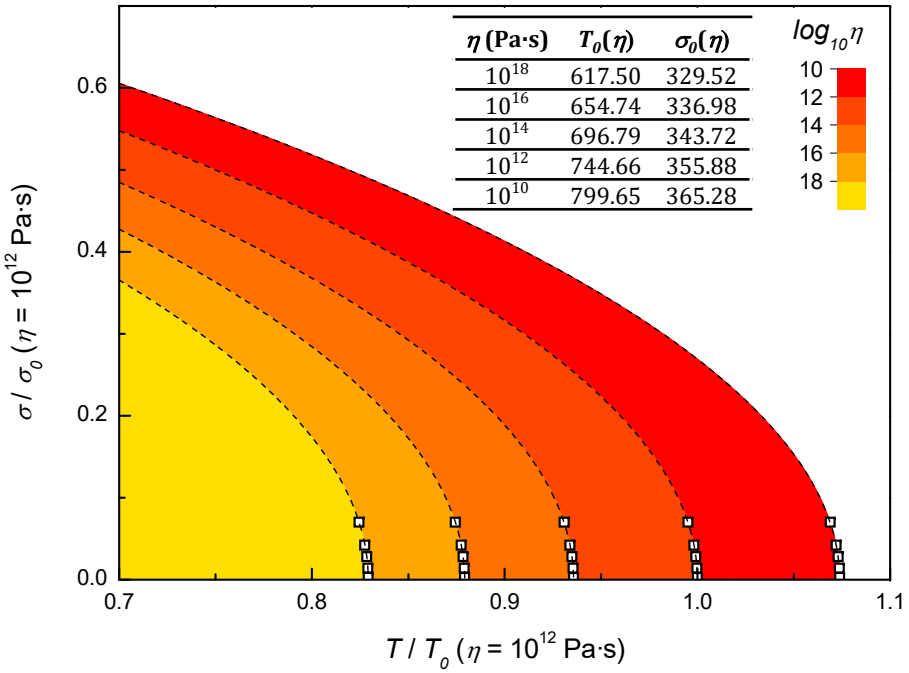

(3) Critical stress curves for shear localization

= Yield stress line when plastic deformation is governed by shear banding

- Universal relation for plastic yielding of metallic glass mediated by shear banding

$$\tau_y/\mu = \gamma_c\left(1 - \left[D \cdot \ln(\dot{\gamma}_s/\dot{\gamma}) \cdot \frac{T}{T_g}\right]^{0.5}\right.$$

- **Universal parameter**

$$\gamma_c \approx 0.037$$

$$D \cdot \ln\left(\frac{\dot{\gamma}_s}{\dot{\gamma}}\right) \approx 0.2$$

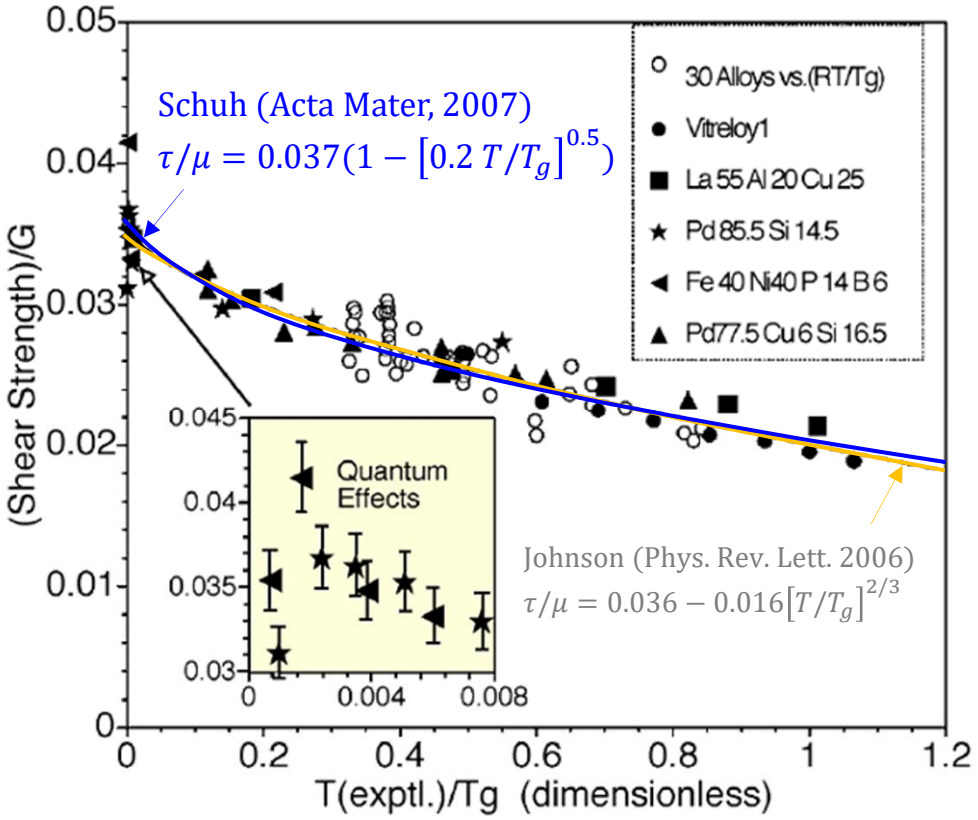

Johnson et al., Phys. Rev. Lett. 95 (2006) 195501.
Schuh et al., Acta Mater. 55 (2007) 2067.

(3) Critical stress curves for shear localization

Size effect on yield strength governed by shear banding

For metallic glass nanoparticles

$$\sigma_{SB} = \sqrt{{\sigma_0}^2 + \frac{3\boldsymbol{E}\Gamma}{2d}(\varepsilon')^2}$$

where bulk strength $\sigma_0 \approx \sqrt{3}\tau_y$

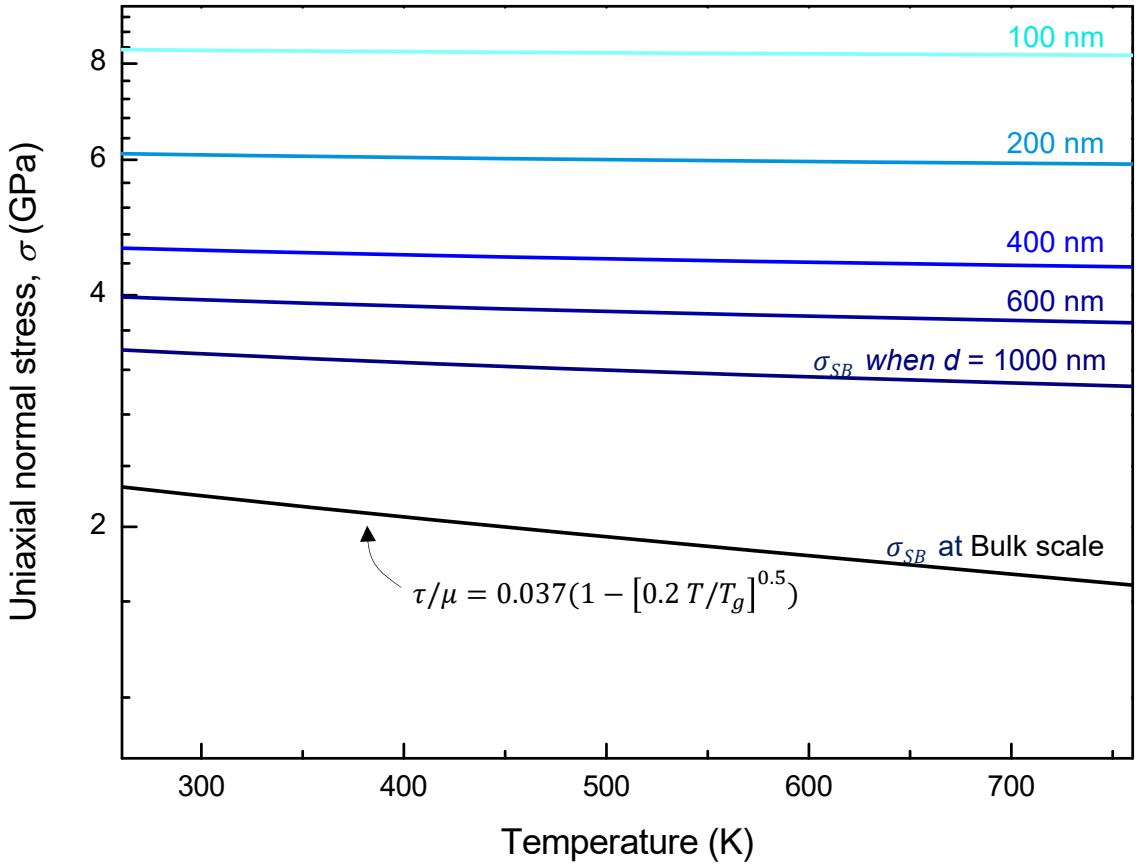

Shift of σ_{SB} curve by sample size reduction

III. Construction of deformation map of nanoscale metallic glasses

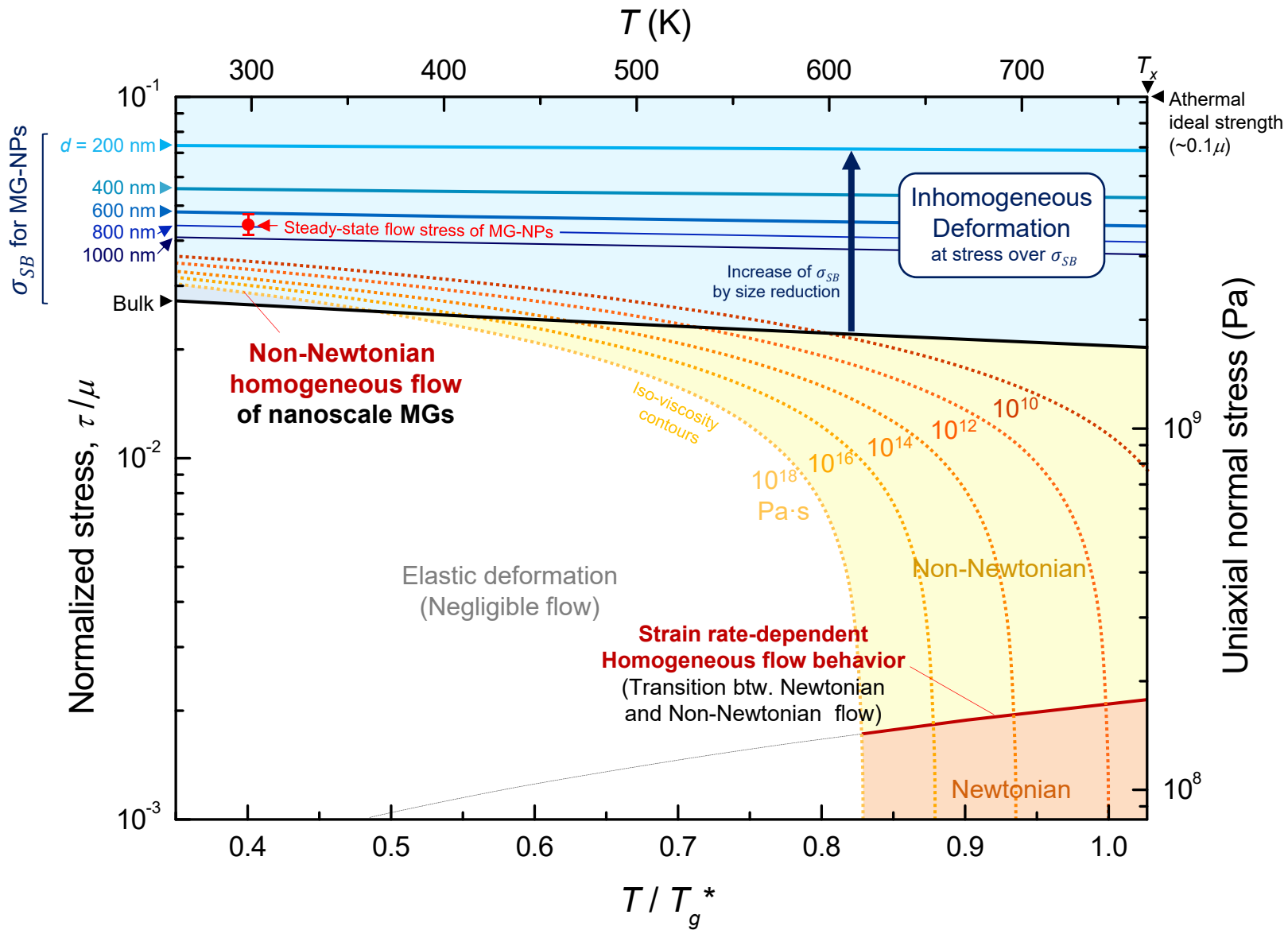

Critical boundaries of deformation map and tuning parameters

- **Critical stress curve for inhomogeneous deformation: Poisson's ratio**

From energy balance model

$$\sigma_{SB} = \sqrt{{\sigma_0}^2 + \frac{2\sqrt{2}E\Gamma}{ad}}$$

C.-C. Wang et al., Acta. Mater. 60 (2012).

σ_0 : Bulk yield strength
a : Aspect ratio
d : Pillar diameter
E : Young's modulus
Γ : Shear band energy per unit area
$\Gamma \approx t_{SB}\mu\gamma_c$, where t_{SB} = Shear band thickness
μ = Shear modulus
γ_c = Characteristic shear strain ~ 0.037

Normalization →

$$\frac{\tau}{\mu} = \frac{\sigma_{SB}}{\sqrt{3}\mu} = \sqrt{\left(\frac{\tau_0}{\mu}\right)^2 + \frac{a'(1+\nu)t_{SB}\gamma_c}{d}}$$

a' : Numerical constant determined by sample geometry

- **Iso-viscosity contours for homogeneous deformation: Activation energy and STZ volume**

$$\eta = \frac{\sigma}{3\dot{\varepsilon}} \qquad (Trouton's\ law)$$

$$\dot{\varepsilon} = \underbrace{A'}_{(1)} \underbrace{\exp\left(-\frac{Q}{kT}\right)}_{(2)} \underbrace{\sinh\left(\frac{\sigma\gamma_0\Omega}{\sqrt{3}kT}\right)}_{(3)}$$

(1) Product of constants ~ $\alpha_0'\nu_0\gamma_0$

(2) Related to **activation energy** of the process

(3) The **net rate** of forward & backward operations

α_0': Fraction of material available to deform via the activated process
ν_0: Frequency of the fundamental mode vibration
γ_0: Characteristic strain for operation of STZ ~ 0.1
k : Boltzmann constant
Q : Activation energy
Ω : STZ volume

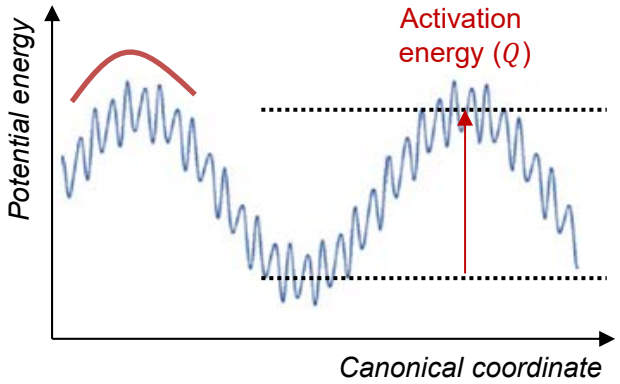

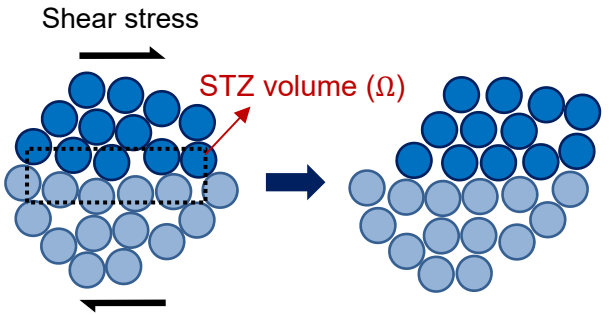

Argon, Acta Metull. 27 (1979).
Schuh et al., Acta Mater. 55 (2007).

Correlations among tuning parameters and intrinsic properties

Activation energy (Q)

$$Q \approx 1.4 m R T_g \ln(10)$$

m : Fragility
R : Gas constant
T_g: Glass transition temperature

Fragility (m) and Poisson's ratio (ν)

$$m \approx 10^{\frac{\nu+0.179}{0.312}}$$

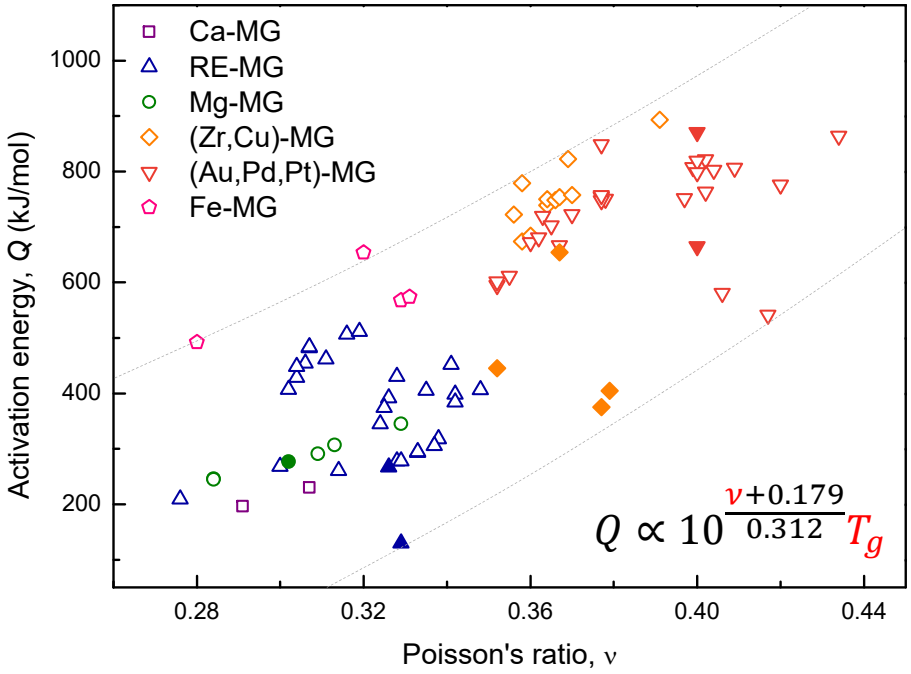

STZ volume (Ω)

$$\Omega = \pi^2 W_{STZ} / 8 \gamma_c^2 \mu \zeta$$

W_{STZ}: Potential energy barrier for a STZ
γ_c: Average elastic limit ~ 0.027
μ: Shear modulus
ζ : Correction factor due to matrix confinement~ 3

Potential energy barrier for a STZ (W_{STZ}) and glass transition temperature (T_g)

$$W_{STZ} \approx 26 R T_g$$

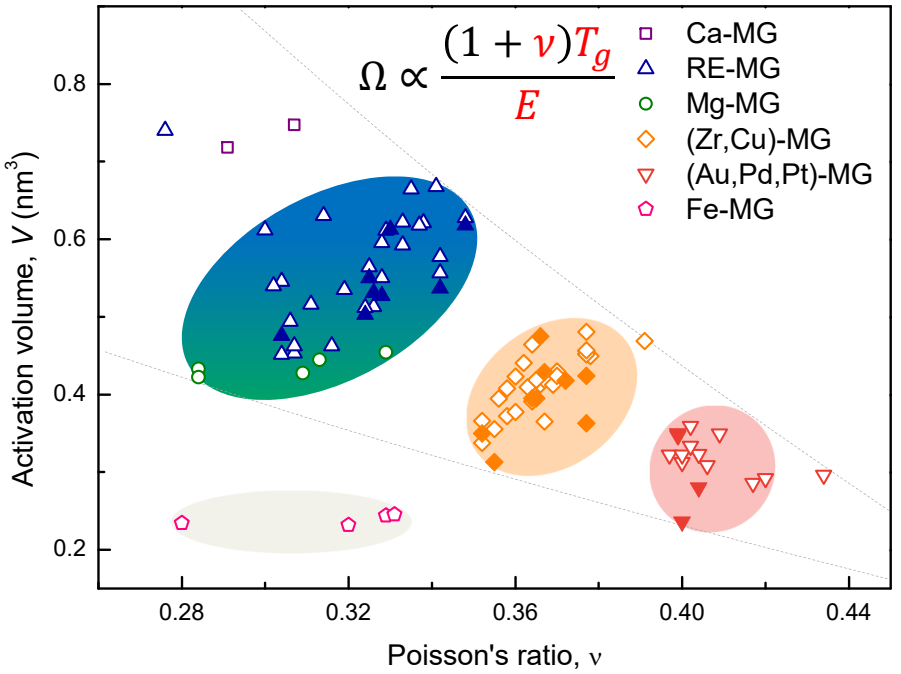

W.H. Wang, J. Appl. Phys. 110 (2011).
E.S. Park et al., Appl. Phys. Lett. 91 (2007).
W.L. Johnson et al., Phys. Rev. Lett. 95 (2005).

IV. Manipulation of tuning parameters and the shift of critical boundaries

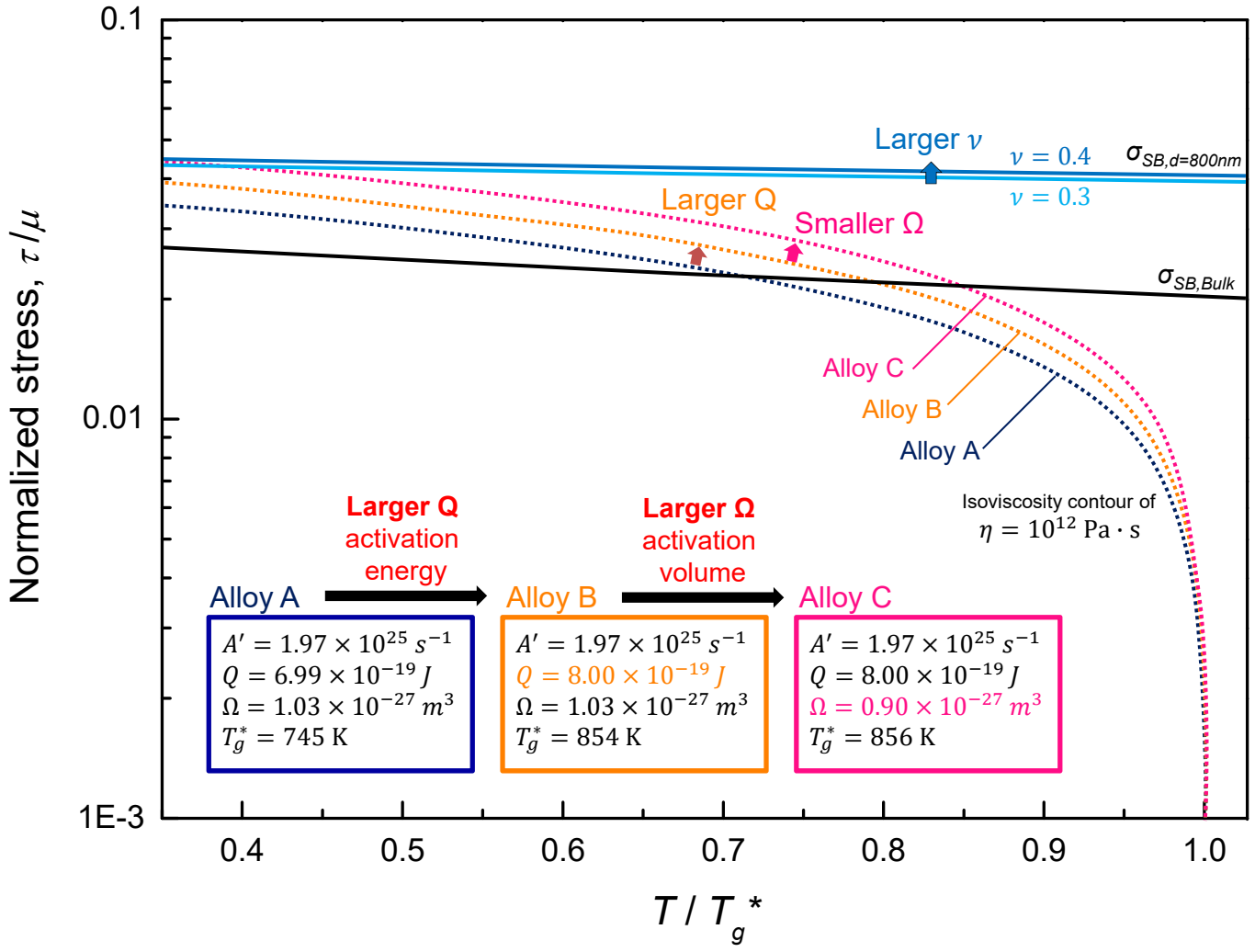

Counteractive effect of large ν (Plasticity indicator of bulk specimen)

- Greater dependence of normalized critical stress on sample size → **Higher σ_{SB}** = Effective suppression of inhomogeneous deformation
- Iso-viscosity contour at higher stress level → **Higher slope** of Iso-viscosity contour at lower T : Hindrance to deformation mode transition at a larger sample size

Selective dissolution of Y-rich phase in Y-Ti-Al-Co PS metallic glass

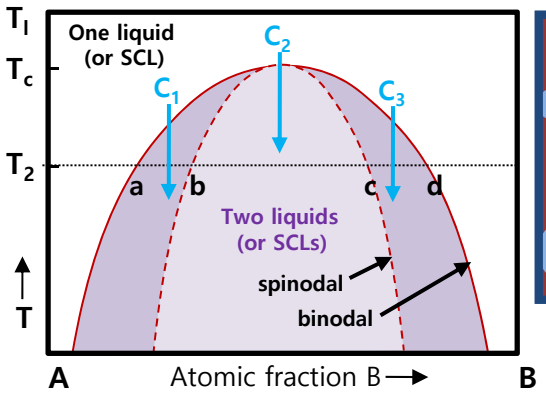

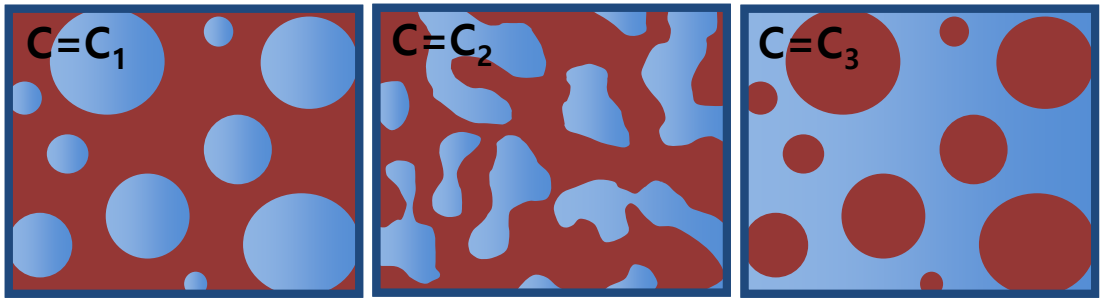

A-rich matrix
B-rich droplet

Interconnected
structure

B-rich matrix
A-rich droplet

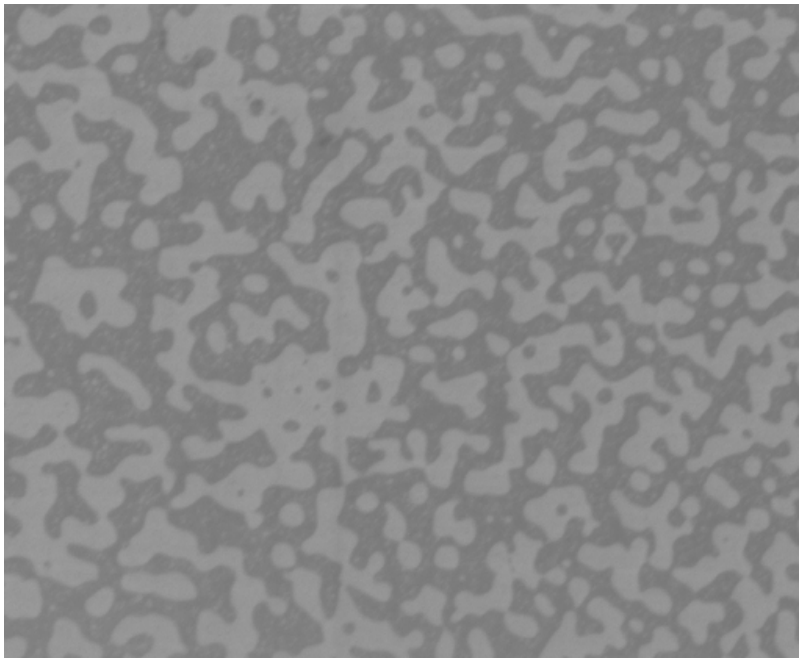

PS-MG precursor alloy

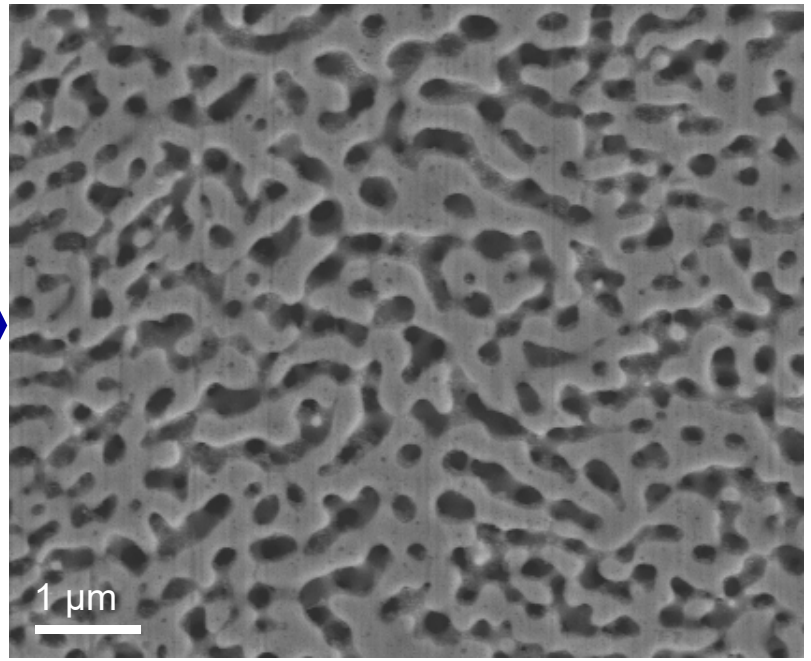

Ti-based amorphous nanofoam

V. Compressive deformation of metallic glass nanofoam

Ligament average size ~ **150 nm**

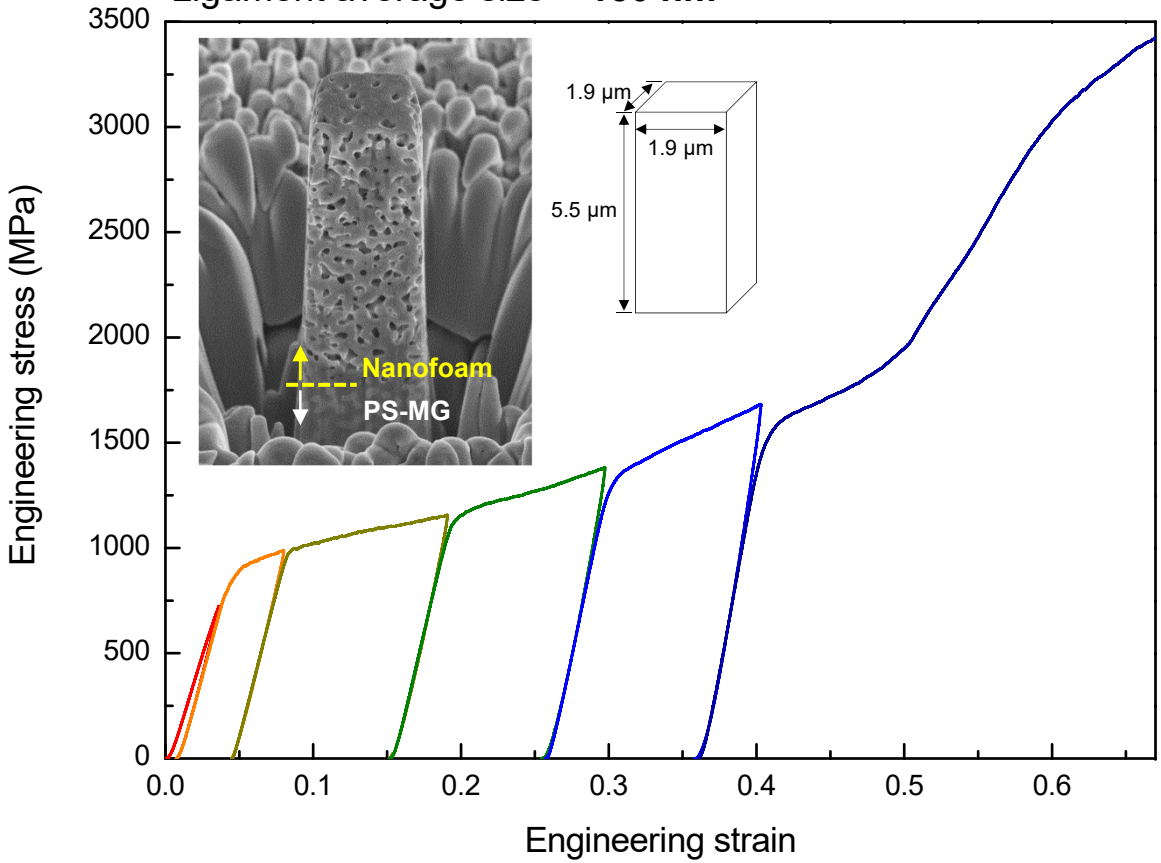

High strength (σ_{foam}~ 880 MPa)
with excellent compressive plasticity
(porosity ~ 42%)

For open-cell foams,

$$\frac{\sigma_{foam}}{\sigma_{ligament}} = 0.23\,\rho_{rel}^{1.5}(1+\rho_{rel}^{0.5})$$

where $\rho_{rel} = (1 - porosity) = \frac{\rho_{foam}}{\rho_{bulk}}$

Gibson & Ashby, *Cellular Solids : Structure and properties*, 2nd ed. (1997)

➡ $\sigma_{ligament}$~ 4.9 GPa

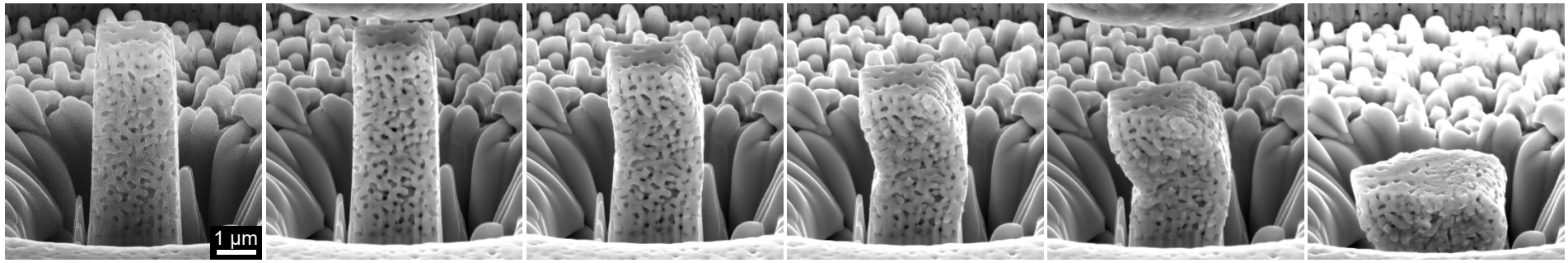

After cycle 1 | After cycle 2 | After cycle 3 | After cycle 4 | After cycle 5 | After cycle 6

Deformation map for nanoscale metallic glass : Cylindrical samples

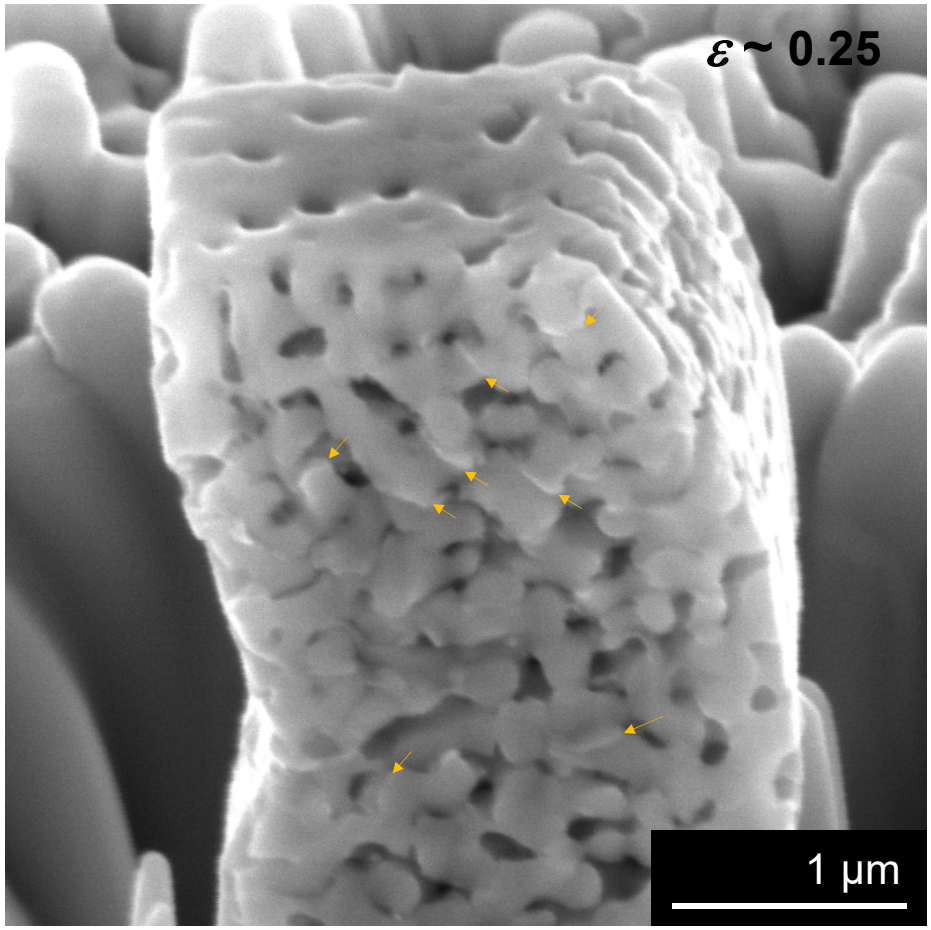

von Mises stress distributions in nanoporous Au metal (FEM)

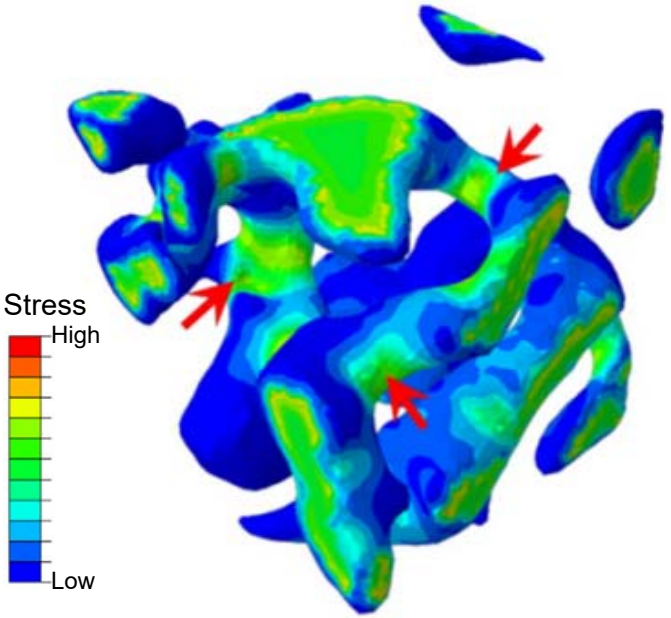

Only 3% of the elements exceed the yield strength at the onset of yielding

Cho et al., Scripta Mater 115 (2016) 96.

Deformation map for nanoscale metallic glass : Cylindrical samples

σ_{SB} for nano-pillars

$$\sigma_{SB} = \sqrt{\sigma_0^2 + 2^{3/2}\frac{E\Gamma}{aD}}$$

$V = \pi r^2 h$

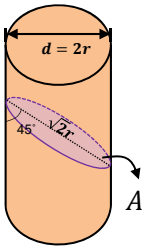

$A = \sqrt{2}\pi r^2$

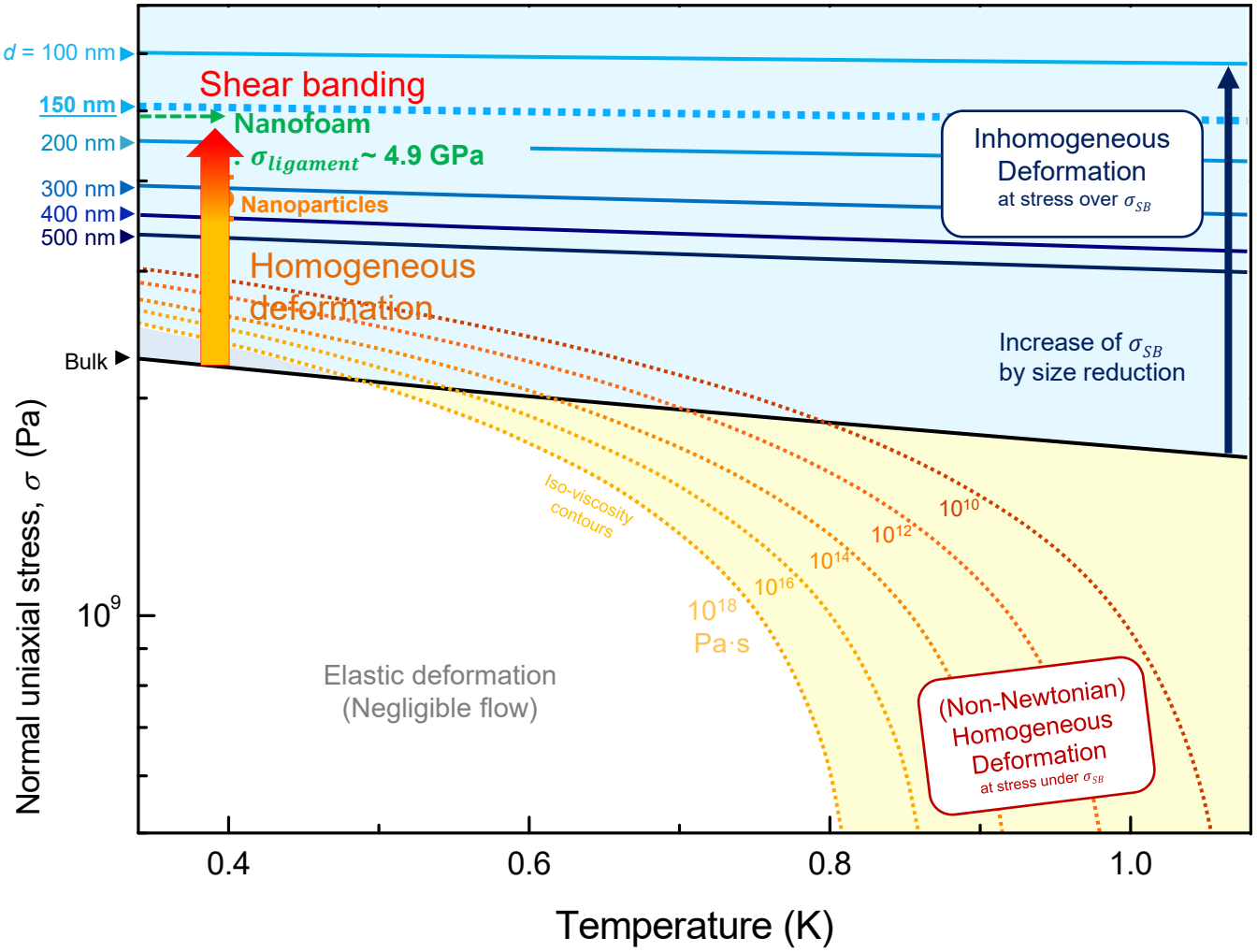

Conclusion : Mechanical response of nanoscale metallic glass

Supression of localized shear banding

mechanically-induced glass transition

Homogeneous deformation at room temperature

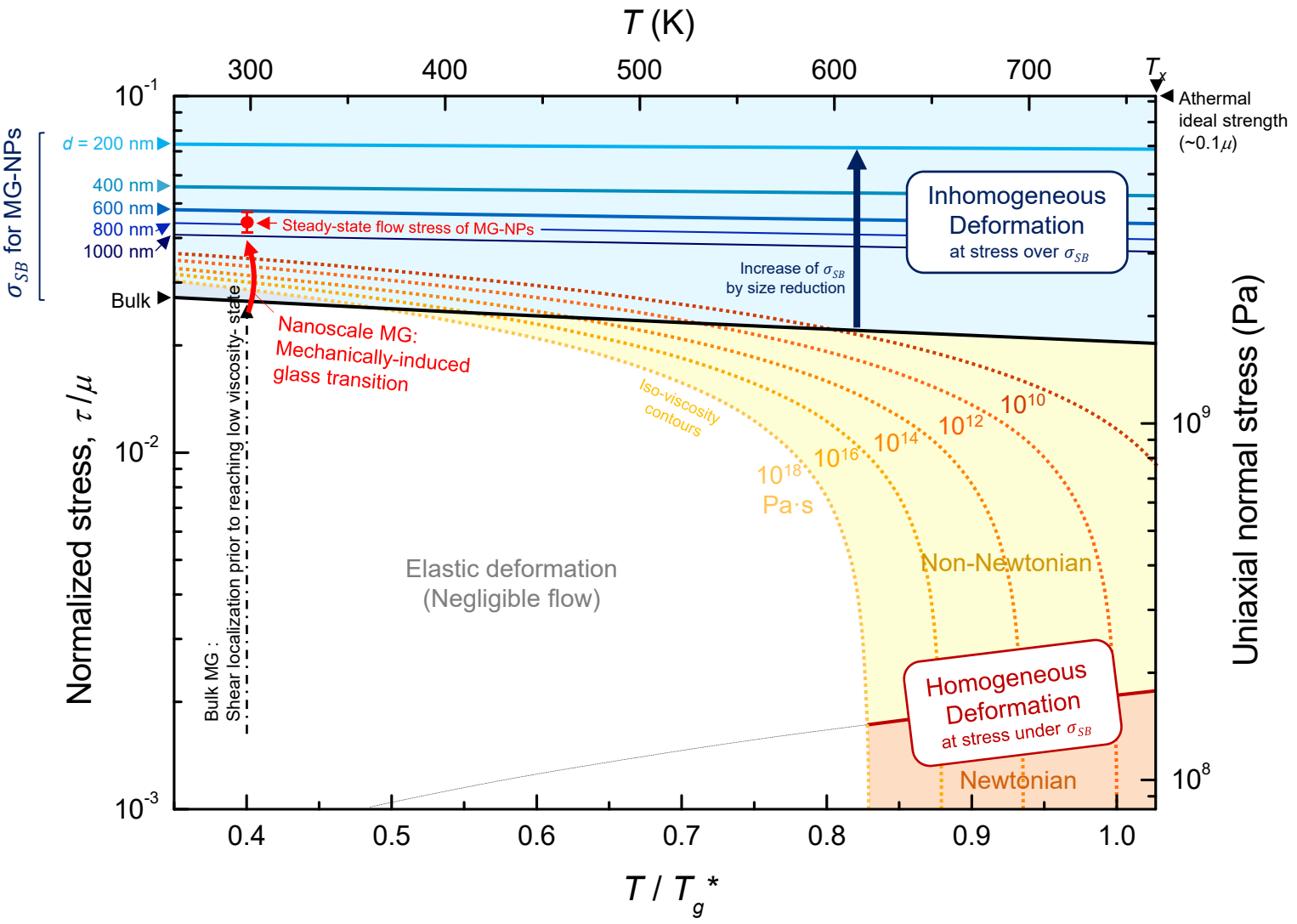

Provision of extended understanding on the mechanical behavior of metallic glasses